การประเมินเชิงปริมาณของความสัมพันธ์ระหว่างโครงสร้างกับสมบัติเชิงหน้าที่ของสตาร์ชข้าว

นางสาว ปิยรัตน์ หนูสุก

วิทยานิพนธ์นี้เป็นส่วนหนึ่งของการศึกษาตามหลักสูตรปริญญาวิทยาศาสตรดุษฎีบัณฑิต
สาขาวิชาเทคโนโลยีทางอาหาร ภาควิชาเทคโนโลยีทางอาหาร
คณะวิทยาศาสตร์ จุฬาลงกรณ์มหาวิทยาลัย
ปีการศึกษา 2546

ISBN 974-17-3993-1

THE ASSESSMENT OF THE RELATIONSHIP BETWEEN STRUCTURE AND FUNCTIONAL PROPERTY OF RICE STARCH

Miss Piyarat Noosuk

A Dissertation Submitted in Partial Fulfillment of the Requirements
for the Degree of Doctor of Philosophy in Food Technology
Department of Food Technology
Faculty of Science
Chulalongkorn University
Academic Year 2003
ISBN 974-17-3993-1

Thesis Title	The assessment of the relationship between structure and functional property of rice starch
By	Piyarat Noosuk
Field of Study	Food Technology
Thesis Advisor	Assistant Professor Pasawadee Pradipasena, Sc.D.
Thesis Co-advisor	Professor John R. Mitchell, Ph.D.

Accepted by the Faculty of Science, Chulalongkorn University in Partial Fulfillment of the Requirements for the Doctor's Degree

…….Dean of Faculty of Science
(Professor Piamsak Menasveta, Ph.D.)

THESIS COMMITTEE

……Chairman
(Associate Professor Vanna Tulyathan, Ph.D.)

……Thesis Advisor
(Assistant Professor Pasawadee Pradipasena, Sc.D.)

……..…Thesis Co-Advisor
(Professor John R. Mitchell, Ph.D.)

…….Member
(Associate Professor Kalaya Laohasongkram, Ph.D.)

…….Member
(Associate Professor Saiwarun Chaiwanichsiri, Ph.D.)

…….Member
(Associate Professor Klanarong Sriroth, Ph.D.)

ปิยรัตน์ หนูสุก : **การประเมินเชิงปริมาณของความสัมพันธ์ระหว่างโครงสร้างกับสมบัติเชิงหน้าที่ของสตาร์ชข้าว** (THE ASSESSMENT OF THE RELATIONSHIP BETWEEN STRUCTURE AND FUNCTIONAL PROPERTY OF RICE STARCH) **อ. ที่ปรึกษา** : **ผศ.ดร. พาสวดี ประทีปะเสน อ. ที่ปรึกษาร่วม:** Prof. John R. Mitchell, Ph.D. 183 หน้า ISBN 974-17-3993-1

งานวิจัยนี้ศึกษาความสัมพันธ์ระหว่างโครงสร้างและสมบัติของสตาร์ชข้าวไทย โดยการตรวจวิเคราะห์องค์ประกอบทางเคมี โครงสร้าง และสมบัติเชิงหน้าที่ สตาร์ชข้าวที่ศึกษาสามารถแบ่งออกได้เป็น 3 กลุ่ม ตามปริมาณอะมิโลส ดังนี้ กลุ่มที่ 1 คือ สตาร์ชข้าวที่มีปริมาณอะมิโลสต่ำ (1-3 %) ได้แก่สตาร์ชจากข้าวพันธุ์กข6 และสตาร์ชข้าวเหนียวทางการค้า กลุ่มที่ 2 คือ สตาร์ชข้าวที่มีปริมาณอะมิโลสปานกลาง (14-15 %) ได้แก่สตาร์ชจากข้าวพันธุ์ดอกมะลิ 105 และ กลุ่มที่ 3 คือ สตาร์ชข้าวที่มีปริมาณอะมิโลสสูง (21-23%) ได้แก่สตาร์ชจากข้าวพันธุ์สุพรรณบุรี 1 และสตาร์ชข้าวเจ้าทางการค้า สตาร์ชข้าวที่มีปริมาณอะมิโลสต่ำและปานกลางมีสัดส่วนของสายอะมิโลเพคติน (amylopectin chain ratio, ACR) เท่ากับ 0.25 (อะมิโลเพคตินเป็นชนิด “S”) ส่วนสตาร์ชข้าวที่มีปริมาณอะมิโลสสูงมี ACR เท่ากับ 0.19 (อะมิโลเพคตินเป็นชนิด “L”) เส้นผ่านศูนย์กลางเฉลี่ย (4-6 μm) และรูปร่างของเม็ดสตาร์ชจากข้าวต่างสายพันธุ์ไม่มีความแตกต่างอย่างมีนัยสำคัญ น้ำหนักโมเลกุลเฉลี่ยโดยน้ำหนักของอะมิโลสของสตาร์ชข้าวที่มีปริมาณอะมิโลสปานกลางและปริมาณอะมิโลสสูงมีค่าอยู่ในช่วง 1.8 ถึง 2.9 x 10^5 ปริมาณผลึกของสตาร์ชข้าวที่วัดด้วย x-ray diffraction มีค่าลดลงจาก 34.62% เป็น 23.00% และสัดส่วนของ short-range molecular order ต่อ amorphous ที่วัดด้วย infrared spectroscopy มีค่าลดลงจาก 0.91 เป็น 0.72 เมื่อปริมาณอะมิโลสเพิ่มขึ้นจาก 1.70% เป็น 22.70%

ปริมาณอะมิโลสในสตาร์ชข้าวเป็นปัจจัยหลักที่มีอิทธิพลต่อสมบัติเชิงหน้าที่ซึ่งได้แก่ กำลังการพองตัว ดัชนีการละลายน้ำ ลักษณะการเกิดแป้งเปียก intrinsic viscosity ([η]), consistency index (k) และ storage modulus (G′) โดยพบว่าเมื่อปริมาณอะมิโลสในสตาร์ชข้าวเพิ่มขึ้นทำให้ดัชนีการละลายน้ำเพิ่มขึ้น (แบบเชิงเส้น จาก 6.01% เป็น 26.60%) setback viscosity เพิ่มขึ้น (แบบเอกซ์โปเนนเทียล จาก 300 เป็น 2526 mPa.s) และ G′ เพิ่มขึ้น (แบบเอกซ์โปเนนเทียล จาก 47 เป็น 478 Pa สำหรับ สตาร์ชข้าวเข้มข้น 12% โดยน้ำหนัก วัดที่ 1 Hz และ 60 ^{0}C) ขณะที่กำลังการพองตัวลดลง (แบบเชิงเส้นจาก 34.92 เป็น 14.17 g swollen/g dry starch) [η] ลดลง (จาก 192 เป็น 156 ml/g) และค่า k ลดลง (จาก 6.32 เป็น 0.29 Pa.s^n สำหรับสตาร์ชข้าวเข้มข้น 5% โดยน้ำหนัก วัดที่ 60 ^{0}C และ 50-1000 sec^{-1}) แต่ breakdown viscosity และอุณหภูมิเริ่มต้นที่ความหนืดเพิ่มขึ้นและเกิดเจลาติไนเซชันของสตาร์ชข้าวมีความสัมพันธ์กับ ACR โดยสตาร์ชข้าวที่มีอะมิโลเพคตินชนิด “L” มี breakdown viscosity ต่ำกว่า แต่มีอุณหภูมิเริ่มต้นที่ความหนืดเพิ่มขึ้นและเกิดเจลาติไนเซชันสูงกว่าสตาร์ชข้าวที่มีอะมิโลเพคตินชนิด “S”

ความเข้มข้นเริ่มต้น (c_0) ที่เม็ดสตาร์ชเริ่มเกิดอันตรกริยาต่อกันสำหรับสตาร์ชข้าวที่มีปริมาณอะมิโลสสูง ปริมาณอะมิโลสปานกลาง และปริมาณอะมิโลสต่ำ มีค่าเท่ากับ 2.5%, 1.5% และ 1.10% ตามลำดับ แต่เมื่อเปรียบเทียบสตาร์ชข้าวที่มีปริมาณอะมิโลสเท่ากันพบว่าสตาร์ชข้าวที่มีการสูญเสีย short-range molecular order ระหว่างการเกิดเจลาติไนเซชันที่สูงกว่ามี c_0 ต่ำกว่า

จากการศึกษาเจลสตาร์ชข้าวที่ความเข้มข้น 6% ถึง 15% โดยน้ำหนัก ความถี่ 0.1 ถึง 10 Hz และอุณหภูมิ 25 ^{0}C กับ 60 ^{0}C พบว่าเจลสตาร์ชข้าวทั้งหมด มีค่า G′ สูงกว่า loss modulus (G″) แสดงว่ามีการเกิดอันตรกริยาระหว่างองค์ประกอบหรือระหว่างเฟสในสารละลายสตาร์ช เจลจากสตาร์ชข้าวที่มีปริมาณอะมิโลสสูงและปริมาณอะมิโลสปานกลางมีลักษณะคล้ายยาง (rubber-like gel) ส่วนเจลจากสตาร์ชข้าวที่มีปริมาณอะมิโลสต่ำมีลักษณะที่เปราะ (weak gel) นอกจากนี้ยังพบว่าสตาร์ชข้าวที่มีปริมาณอะมิโลสสูงเท่านั้นมีค่า G′ เพิ่มขึ้นเมื่ออุณหภูมิของเจลลดลง เจลของสตาร์ชข้าวแสดงสมบัติแบบวีสโคอีลาสติก (viscoelastic property) ที่สามารถอธิบายได้ด้วยแบบจำลองของ Burger (4-element Burger model) ยกเว้นเจลของสตาร์ชจากข้าว RD6 ที่ความเข้มข้น 6% โดยน้ำหนัก เท่านั้นที่แสดงสมบัติของของเหลวเพียงอย่างเดียว

การเกิดรีโทรเกรเดชันของเจลสตาร์ชข้าวที่ความเข้มข้น 30% โดยน้ำหนัก ในช่วงเก็บรักษาเป็นเวลา 100 ชั่วโมง ที่ 25 ^{0}C พบว่าเจลสตาร์ชของข้าวที่มีปริมาณอะมิโลสสูงเท่านั้นที่เกิดรีโทรเกรเดชัน โดยในช่วงแรกของการเกิดรีโทรเกรเดชัน G′ และสัดส่วน short-range molecular order ต่อ amorphous มีค่าเพิ่มขึ้นอย่างรวดเร็วในอัตรา 0.44-0.57 kPa/h และ 0.001-0.002 h^{-1} ตามลำดับ ผลการวิจัยบ่งชี้ว่าสตาร์ชที่มีอะมิโลเพคตินชนิด “S” ช่วยป้องกันการเกิดรีโทรเกรเดชัน

ภาควิชาเทคโนโลยีทางอาหาร	ลายมือชื่อนิสิต.....…….....……
สาขาวิชาเทคโนโลยีทางอาหาร	ลายมือชื่ออาจารย์ที่ปรึกษา.....…….....……
ปีการศึกษา 2546	ลายมือชื่ออาจารย์ที่ปรึกษาร่วม.....…….....……

4373825923: MAJOR FOOD TECHNOLOGY

KEYWORD: RICE STARCH/ PASTE VISCOSITY/ GRANULE STRUCTURE/ VISCOELASTICITY/ RETROGRADATION/ RICE AGING

PIYARAT NOOSUK: THE ASSESSMENT OF THE RELATIONSHIP BETWEEN STRUCTURE AND FUNCTIONAL PROPERTY OF RICE STARCH. THESIS ADVISOR: ASST. PROF. PASAWADEE PRADIPASENA, Sc.D., THESIS CO-ADVISOR: PROF. JOHN R. MITCHELL, Ph.D., 183 pp. ISBN 974-17-3993-1

In order to establish the relationships between structure and properties, the chemical composition, structural properties and functional properties of five Thai rice starches were determined. These starches were classified into 3 groups according to the true amylose content: low amylose content (1-3%, RD6 and a commercial waxy rice starch), medium amylose content (14-15%, Jasmine rice starch) and high amylose content (21-23%, Supanburi 1 and a commercial rice starch). The rice starches with low amylose and medium amylose content had an amylopectin chain ratio (ACR) of 0.25 (S-type amylopectin), while the rice starches with high amylose content had an ACR of 0.19 (L-type amylopectin). There were no significant differences in granule size (average size of 4-6 μm) and shape among these rice starches. For the medium and high amylose starch, the weight average molecular weights of amylose were in the range of 1.8 to 2.9 x 10^5. The crystallinity (measured by x-ray diffraction) and ratio of short-range molecular order to amorphous (measured by infrared spectroscopy) decreased from 34.62% to 23.00% and from 0.91 to 0.72, respectively, with increasing amylose content from 1.70% to 22.70%.

The functional properties, namely swelling power, water solubility index, pasting characteristics, intrinsic viscosity ([η]), consistency index (k), and storage modulus (G′) were related to the true amylose content. An increase in amylose content (from 1.70% to 22.70%) increased water solubility index (linearly from 6.01% to 26.60%), setback viscosity (exponentially from 300 to 2526 mPa.s), and G′(exponentially from 47 to 478 Pa, for 12%, w/w, measured at 1 Hz and 60 °C). Furthermore, an increase in amylose content decreased the swelling power (linearly from 34.92 to 14.17 g swollen/g dry starch), [η] (from 192 to 156 ml/g), and k (from 6.32 to 0.29 $Pa.s^n$, for 5%, w/w, measured at 60 °C and 50-1000 sec^{-1}). However, the breakdown viscosity, onset of pasting temperature and gelatinization temperature related to the ACR values. L-type amylopectin resulted in a lower breakdown viscosity but higher onset of pasting temperature and gelatinization temperature than S-type amylopectin.

The onset concentrations (c_0), when the granule-granule interactions occur, were 2.5%, 1.5% and 1.10% for the rice starch with high amylose, medium amylose and low amylose content, respectively. For the same amylose content, a higher loss in the short-range molecular order on gelatinisation decreased this onset concentration.

In the concentration range from 6% to 15% (w/w), G′ was higher than loss modulus (G″) at 0.1-10 Hz, 25 °C and 60 °C for all rice starches, which indicates strong interactions between the components or phases. The rice starches with high amylose and medium amylose content had rubber-like gel property, while rice starch with a low amylose content was a weak gel. For the rice starches with high amylose content, G′ of the starch gel increased upon cooling, except for the RD6 starch at the lowest concentration measured (6%), which exhibited only the flow component, all others exhibited the combination of ideal elastic, retard elastic and flow components, which could be represented by the 4-element Burger model.

Retrogradation was followed during storage for 100 hours at 25 °C on gels (30%, w/w) and was found to occur for the high amylose starch only. For the initial stage of retrogradation, G′ and the ratio of short-range molecular order to amorphous increased rapidly at a rate of 0.44-0.57 kPa/h and 0.001-0.002 h^{-1}, respectively. It was suggested that the high propotion of amylopectin chains with DP ≤ 10 prevented retrogradation in the low and medium amylose starches.

Department.....Food Technology..... Student's signature .....

Field of study....Food Technology..... Advisor's signature .....

Academic year..2003..... Co-advisor's signature.....

ACKNOWLEDGMENTS

I would like to express my deepest gratitude to my advisor, Asst. Prof. Pasawadee Pradipasena, and my co-advisor, Prof. John R. Mitchell and Dr. Sandra E. Hill, for their excellent supervision, encouragement, support and valuable guidance throughout the PhD. I also wish to thank my examining committee, Assoc. Prof. Vanna Tulyathan, Assoc. Prof. Kalaya Laohasongkram, Assoc. Prof. Saiwarun Chaiwanichsiri, and Assoc. Prof. Klanarong Sriroth, for their valuable suggestions.

I would like to thank to staff (Mr. Phil Glover, Mr. Mike Chapman, and Val Street) and friends (Helen Copeland, Linda Lopez, Marie-Astrid Ottenhof, Matt Boy, and Giuseppina Barra) at Food Sciences Department, the University of Nottingham, UK., for their help, guidance and technical support throughout my thesis.

I wish to thank all friends at the Department of Food Technology, Chulalongkorn University and my colleagues at the faculty of Agro-Industry, Prince of Songkla University for their help and encouragement. I would like to extend my gratefulness to all my friends who have helps me in so many ways throughout my stay in Sutton Boington, UK.

I would particularly like to acknowledge the Royal Thai Government and Faculty of Agro-Industry, Prince of Songkla Univeristy for providing the opportunity and scholarship.

Finally, I would like to forward my special thanks to my parents, brother, grandmother, and my best friend for their love, encouragement, and emotional support. Without them, I would not have been able achieve this degree.

TABLE OF CONTENTS

Page

TABLE OF CONTENTS (cont.)

Page

TABLE OF CONTENTS (cont.)

Page

TABLE OF CONTENTS (cont.)

Page

TABLE OF CONTENTS (cont.)

Page

TABLE OF CONTENTS (cont.)

Page

LIST OF TABLES

LIST OF TABLES (cont.)

LIST OF FIGURES

LIST OF FIGURES (cont.)

LIST OF FIGURES (cont.)

LIST OF FIGURES (cont.)

LIST OF FIGURES (cont.)

LIST OF FIGURES (cont.)

LIST OF FIGURES (cont.)

LIST OF FIGURES (cont.)

LIST OF FIGURES (cont.)

FIGURE Page

CHAPTER I

INTRODUCTION

Starch is composed of the two glucose polymers: amylose and amylopectin, organized into a radially anisotropic, semi-crystalline structure in the granule (Champagne, 1996). Among cereal starches, rice starch has the smallest granules (Biliaderis and Juliano, 1993). In addition, the amylose content of rice starches varies broadly between different varieties. It is well recognised that on storage rice changes in eating quality. Several different mechanisms have been implicated in this change (Ramesh *et al*., 2000, and Zhou *et al*., 2002)

In many applications, starches will be used generally in the gelatinised form where starch is heated in excess water. A combination of heat and water, however, causes starch granules to undergo unique and irreversible changes, the most dramatic of which are the disruption of the crystalline structure and swelling size. On cooling and storage a starch paste of sufficient concentration, the molecules of gelatinized starch begin to reassociate leading to a more ordered structure that may develop into a crystalline form. These changes are related significantly to pasting behavior and rheological properties of starches and they are governed by the structural properties of starches.

This research project developed because rice is one of the main exported agricultural commodities of Thailand in the form of both rice and rice starch. Functional properties of rice starch are thickening, emulsifying, gelation, binding, coating, glazing, and sizing. Therefore, rice starch can be used for various applications including food, textile, paper, cosmetic, and pharmaceutical. However,

the development of value-added products from rice starch depends on a thorough knowledge of the structure and functional properties of rice starch which can be done through physico-chemical characterization.

1.1 Objectives

The main objectives of this research were

1. to establish the relationship between structure and functional properties of starch, with the aim of developing for predicting functional behavior from structure,

2. to determine the effect of rice aging on change in structure and functional properties.

CHAPTER II

LITERATURE REVIEW

2.1 Rice

Rice is a semiaquatic, annual grass, which can be grown under a broad range of climatic conditions. The genetic relationships among common cereal grains (Figure 2.1) indicated that rice has properties more similar to oats than to other cereals (Bietz, 1982). There are two cultivated species of rice, *Oryza sativa L*. and *O. glaberrima Steud*. The former rice is distributed throughout the tropical and sub-tropical regions of Asia, Africa, Australia, Central and South America, while the later is endemic to western tropical Africa.

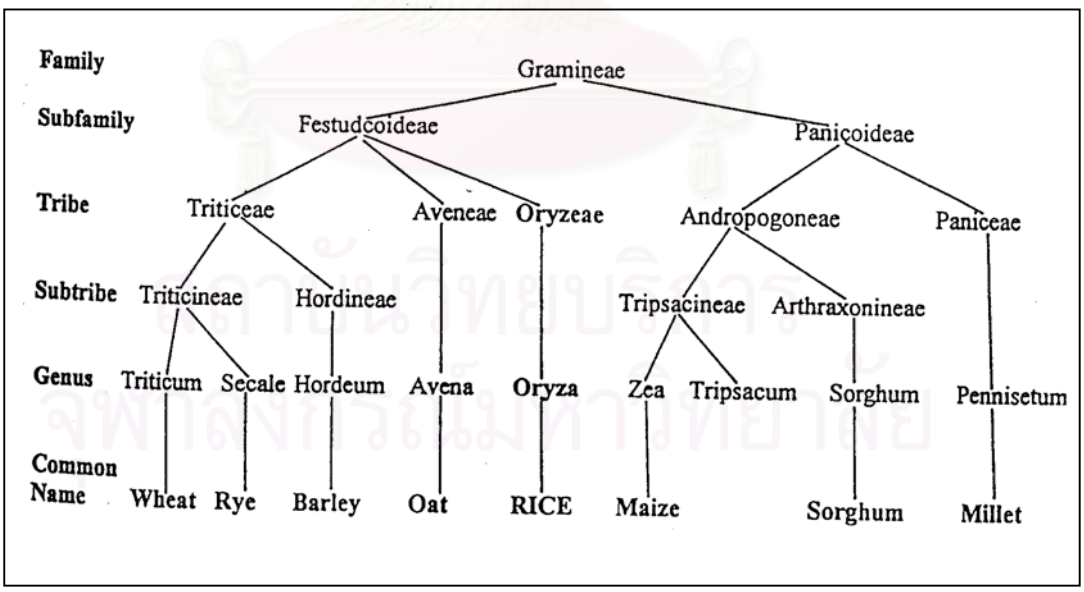

Figure 2.1 Genetic relationships among common cereal grains (Bietz, 1982).

Oryza sativa L. has undergone considerable diversification and improvement during dissemination to different cultural and climatic regions worldwide. The rice spread from India to Egypt and later to Europe, Africa, America and Australia. From China, it spread to Korea and Japan (Ganashan, 1974; and Huke, 1976). The *Oryza sativa L.* is the predominant species, which can be divided into three sub-species according to evolution and geographical origin: temperate race, (i.e. Japonica), tropical race (i.e. Indica) and the third sub-species of rice called Javanica, which does not conform to either Indica or Japonica (Chang, 1976). The evolution and the geographical spread of the sub-species of *Oryza sativa L.* from the regions of primary domestication i.e Northern India, Indo-China and Southern China as shown in Figure 2.2.

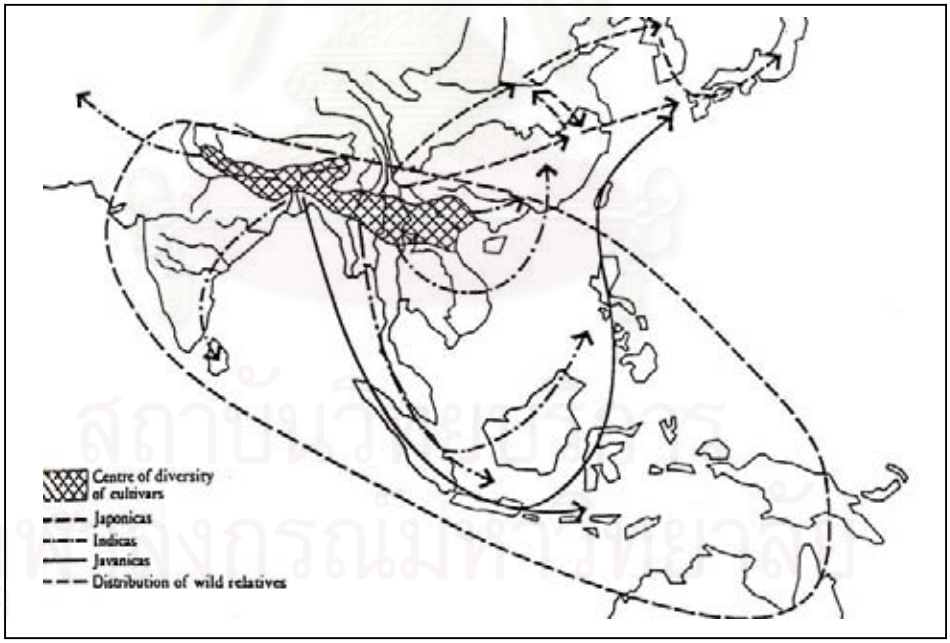

Figure 2.2 Evolution and spread of the geographical races of *Oryza sativa L.* rice (Chang, 1976)

Oryza sativa L. has been consumed by humans for almost 5000 years. It has adapted to diverse environments and currently sustains two-thirds of the world's population. Today China and India are first and second, respectively, in world rice production (Juliano, 1985a; and USDA, 1992) but the top rice-exporting countries are the United States and Thailand. The increased rice production especially in Asia has primarily resulted from the successful IRRI breeding programs in the 1960-1970s that developed semi-dwarf plants which gave a higher yield and better grain quality.

Rice has also been traditionally grouped into waxy (glutinous rice) and non-waxy (non-glutinous) rice depending on the presence of amylose. The waxy rice contains virtually none to less than 1-4 % of amylose (Juliano, 1985a). The waxy rice gives a very sticky texture, which has prompted the belief that the stickiness of rice is predominantly attributed to the amylopectin component in starch. The non-waxy rice can be subdivided into three groups i.e. low (10-20 %), intermediate (20-25 %) and high (25-33 %) amylose contents, as determined by iodine colorimetry (Juliano, 1982).

Another group of rice varieties which falls outside the traditional rice is predominantly derived from the aromatic (scented, fragrant) rice (Sharp, 1990). The major selected varieties include Jasmine from Thailand (Efferson, 1985), Della from America, Basmati from Pakistan and India (Sharp, 1990) and Hieri from Japan (Tsugita, 1986). Volatile aroma compounds generally play a role in consumer acceptability of rice (Bergman et al., 2000) and the popcorn-like smell of aromatic rice, stemming primarily from its 2-acetyl-1-pyrroline content (Bhattacharjee *et al*., 2002), is considered desirable by many consumers. Despite the higher cost, aromatic rice is favoured in Asian and is increasingly being accepted in Europe.

2.2 Rice starch

Rice has one of the smallest starch granules of the cereal starches, varying in size from 3 to 10 μm in the nature grain. Mean granule size varies from 4 to 6 μm (Juliano, 1984a). Starch granules of rice are compound, and they are polyhedral or pentagonal dodecahedron. Compound granules having diameter up to 150 μm form as clusters containing between 20 and 60 individual granule (Juliano, 1985b) and fill most of the central space within the endosperm cells. However, in waxy varieties the endosperm is opaque because of air spaces between the starch granules. Rice starch, as other starches, is composed of two polymer forms of glucose: amylose and amylopectin. These two molecules are organized into a radially anisotropic, semi-crystalline structure in the starch granule (Nikuni, 1978; and Lineback, 1984). The main variation in composition of rice starch is caused by the relative proportions of amylose and amylopectin in the starch granules and this, together with the chain length distribution and the frequency and spacing of branch points within the amylopectin molecule (Lu *et al*., 1997), has a profound influence on the physicochemical properties of starch (Jane *et al*., 1999).

2.2.1 The structure of amylose

Amylose is defined as a linear molecule of α-(1,4)–linked D-glucopyranosyl units. However, it is now accepted that amylose is slightly branched, having occasional α-(1,6) branch points. Simplified models for the structure of amylose are shown in Figure 2.3. There are 9-20 branch points per molecule. The side chains range in chain length from 4 to over 100 glucosyl units

(Hizukuri *et al*., 1981; and Takeda *et al*., 1987). The extent of branching has been shown to increase with the molecule size of amylose (Greenwood and Thomson, 1959).

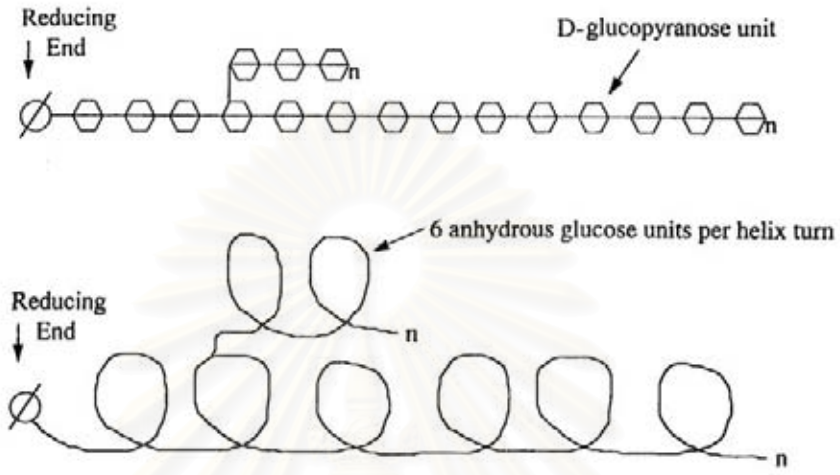

Figure 2.3 Amylose models. Amylose can be depicted as either a straight chain or a helix (Thomas and Atwell, 1997).

The amylose chains displayed a natural twist giving a helical conformation with six anhydroglucose units per turn (Zobel, 1988; and Morrison, 1995). Hydroxyl groups of glucosyl residues were located on the outer surface of the helix, while the internal cavity is a hydrophobic tube. Therefore, hydrophobic complexing agents (fatty acids, iodine, and some alcohols) can lie within the amylose helix stabilized by van der Waals contacts with adjacent C-H groups in amylose (Godet *et al*., 1993). The formation a helical complex between amylose and iodine gives rise to the typical deep blue color (λ_{max} = 640 nm) of starch dispersions stained with iodine and forms the basis for quantitative determination of amylose content. The ability to form inclusion compounds with a variety of materials gives rise to iodine affinity, which is about 20% by mass for rice amyloses. This is high compared

with the iodine affinity of rice amylopectin, which is 0.4-0.9% in low- and intermediate-amylose rice but 2-3% in high-amylose rice. This iodine binding allows a distribution to be made between amylose and amylopectin and permits the determination of the amylose content of native starch. Most starches contain between 20 and 25% w/w amylose although some waxy starches contain very little.

2.2.1.1 Rice amylose

Rice amylose has a β-amylolysis limit of 73-81%, indicating that is a slightly branched molecules with three to four chains on average (Takeda et al., 1986, 1989; and Hizukuri et al., 1989). This β-amylolysis limit is considerably higher than that of amylopectin (55-60%). Rice amylose has degree of polymerization (DP) values of 1,000-1,100 and average chain-lengths of 250-320 (Hizukuri *et al.*, 1989). These structural properties of amylose from rice are similar to those of wheat and maize, as indicated in Table 2.1 (Hizukuri, 1988).

Table 2.1 Structural properties of amylose

Source	β-Amylolysis limit (%)	Avg. Degree of Polymerization	Avg. Number Chains	Avg. Chain Length	Branched Molecules (%)
Wheat	88	1,300	4.8	270	27
Maize	82	930	2.7	340	44
Rice					
Indica	73	1,000	4.0	250	49
Japonica	81	1,100	3.4	320	31
Tapioca	75	2,600	7.6	340	42
Potato	80	4,900	9.5	240	

(Hizukuri, 1988)

Tongdang (2001) had previously determined the molecular weight of enzymatically debranched rice starches using Size Exclusion Chromatography Coupled to Multi-angle Laser-Light-Scattering detector and Differential Refractometer (SEC-MALLS-RI). The molecular weight of amylose for rice starches fell within the range of number average molecular weight, M_n, (1.9-4.1) $x10^5$ Da,, which are similar to those of some Indian rice starch, (0.2-3.8)$x10^5$ Da, (Ramesh *et al*., 1999). In addition, the M_w for these rice starches were (2.4-5.8)$x10^5$, which are similar to those of some Japonica rice, e.g. (3.3-6.1)$x10^5$ Da, (Asaoka *et al*., 1987). The polydispersities (M_n/M_w) for all rice starches were between 1.2-1.4, which are also within the same range reported by Ramesh *et al*. (1999). However, Ong (1994) reported higher weight average molecular weight, M_w, (0.9-3.7)$x10^6$ Da, and polydispersities, 2.6-6.9, for the amylose fraction of different rice starches. A possible reason for this is that in Ong's study the hydrolysis time was much shorter (2.5 h) compared to the others study resulting in the presence of partially debranched or undebranched amylopectin components that might have eluted along with the amylose (Ramesh, 1999).

The amylose content of starch granule varies with the botanical source of the starch and is affected by climatic and soil conditions during grain development. High temperatures decrease the amylose content of rice, whereas cool temperatures have the opposite effect. Amylose content of rice is specified as waxy, 0-2%, very low, 5-12%, low, 12-20%, intermediate 20-25%, and high, 25-33% (Juliano, 1992).

Amylose is quantitatively determined by several methods, and variable results have been reported. The iodine binding has been most commonly used for this purpose because it is specific, sensitive, and easy to determine

qualitatively and quantitatively by a spectrophotometer. However, these methods are subject to uncertainties. Amylopectin-iodine complexes also form. These reduce the concentration of free iodine measured by the non-colorimetric methods and may absorb at similar wavelengths to amylose-iodine complexes in colorimetric methods. These lead to an overestimation of amylose, requiring corrections to be applied. Inaccuracies also arise with the use of calibration curves employing amylose only, which do not account for absorption by amylopectin-iodine complexes, and with the finding that commercial sources of amylose for calibration curves vary in their iodine binding capacity. Additionally, the wavelength of maximum absorbance of amylose-iodine complexes increases with increasing degrees of polymerisation. Thus, methods based on the formation of amylose-iodine complexes, while rapid and convenient, are not readily applied to starches from various botanical origins (Gibson *et al*., 1997). Many researchers (Shanthy *et al*., 1980; Bhattacharya *et al*.; 1982, Ramesh *et al*., 1999) estimated the amylose of rice from the hot water soluble amylose, which agree well with the true amylose content of rice starch. Bhattacharya *et al*. (1972 and 1982) showed that the hot water (96 ^{0}C) solubility of amylose differed among varieties. These authors thus derived a new parameter called “hot water insoluble amylose” obtained from total amylose (amylose equivalent) minus water soluble amylose. An alternative method to using iodine binding is to separate the amylose by size exclusion chromatography. Amylose content determination can be carried out on either debranched or undebranched starches. The high pressure SEC using TSK gel columns has not provided good resolution between amylose and amylopectin for undebranced starch but it worked well with debranched material (Ong *et al*., 1994; Ramesh *et al*., 1999; and Tongdang *et al*., 1999). The specific formation of amylopectin complexes with the lectin concanavalin A (Con A) offers an alternative

approach to amylose measurement in starches that is not subject to these uncertainties (Matheson and Welsh, 1988; and Matheson, 1990). Under defined conditions of pH, temperature and ionic strength, Con A specifically complexes branched polysaccharides based on α-D-glucopyranosyl or α-D-mannopyranosyl units at multiple non-reducing end groups (Colonna *et al*., 1985; and Yun and Matheson, 1990) with the formation of a precipitate. This method has been utilized for both analytical and preparative purposes and gave values of amylose content comparable to those by iodine methods on potato, waxy rice, and rice starches (Hizukuri, 1996).

2.2.2 The fine structure of amylopectin

Amylopectin is the highly branched component of starch: it is formed through chains of α-D-glucopyranosyl residues linked together mainly by (1, 4) linkages but with 5-6 % of (1, 6) bonds at the branch points. The currently accepted structural models are derived from the cluster models proposed by Nikuni (1969); French (1973); Robin *et al*., (1974); and Manners and Matheson (1981) (Figure 2.4). The cluster structure model indicates the branch points are arranged in clusters and not ramdomly distributed through the macromolecule (Manner, 1985). This model was further revised by Hizukuri (1986) based on the polymodal distribution of chain profiles obtained from the fraction of potato and waxy rice amylopectin by gel permeation HPLC (Figure 2.5). According to his model, four types of B-chains (*i.e*. B1, B2, B3, and B4) were proposed. The A-chains, are unbranched and are linked to the molecule through their reducing end-group, the B-chians (B1-B4) which are jointed to the molecule in the same way but carry one or more A-chains, and the C-chain, which has the reducing end-group of the molecule.

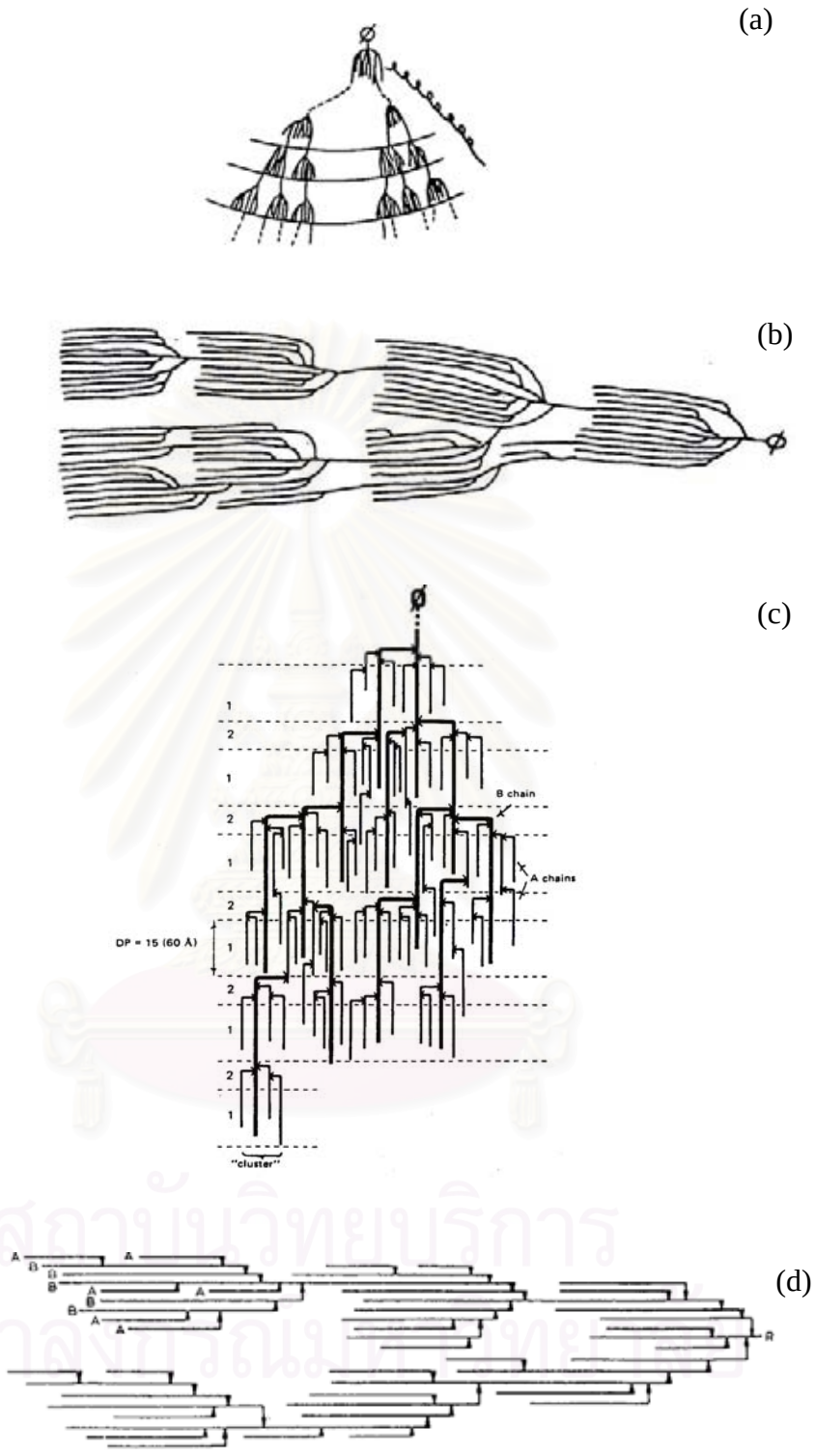

Figure 2.4 The cluster models for amylopectin structure proposed by Nikuni, 1969 (a); French, 1973 (b); Robin et al., 1974 (c); and Manners and Matheson, 1981 (d).

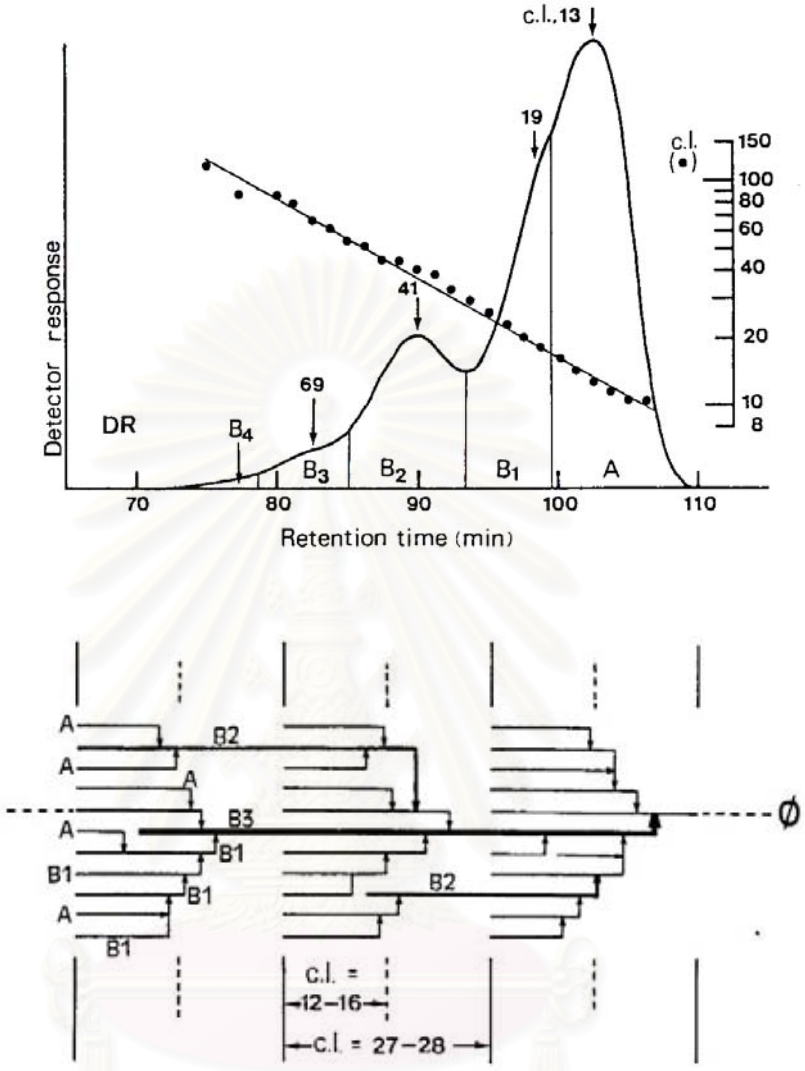

Figure 2.5 The cluster model for amylopectin structure proposed by Hizukuri (1986) resulting from the chromatogram of debranched waxy rice amylopectin (top Figure).

The chain length of A and B1 chains and that of B2-B4 are 14-18 and 45-55, respectively. The molar ratio of short to long chains is influenced by the starch source and varies between 3:1 and 2:1 (Hizukuri, 1985). Cereal starches generally have shorter chains in both the long- and short-chain fractions and larger amounts of short-chain fraction, compared with those of tuber starches (Hizukuri, 1985; and 1986). The reported weight average molecular weight ($\bar{M}_w$) of amylopectin from various sources falls within the range 4-5x10^8 (Banks and Greenwood, 1975).

The structural properties of amylopectins, as with amylose, vary depending on source (Table 2.2) (Hizukuri, 1988). The β-amylolysis limit of amylopectin is 55-60%, which is less than that of amylose. Furthermore, iodine does not form a stable complex with amylopectin due to short length of the unit chains, so only small amounts of iodine are bound (<0.6%), a red-brown complex is formed with iodine ($\lambda_{max} \approx$ 530-540 nm). As the external chian length increases, the λ_{max} of iodine-amylopectin complex also increases (Banks and Greenwood, 1975).

Table 2.2 Structural properties of amylopectin

Source	Avg. Degree of Polymerization	Avg. Chain Length	Avg. Number Chains	Avg. External Chain Length	Avg. Internal Chain Length
Wheat	4,800	19	250	13	5
Maize	8,200	22	370	15	6
Rice					
Indica	4,700	21	220	14	6
Japonica	12,800	19	670	13	5
Tapioca	18,500	18	1,000	12	5
Potato	9,800	24	410	15	8

(Hizukuri, 1988)

2.2.2.1 Rice amylopectin

Rice amylopectins have β-amylolysis limits of 56-59% and widely different DPs and linear chain distribution values (Hizukuri *et al*., 1989; and Takeda *et al*., 1987). Low average DP values are observed for indica (4,700), as compared to those for Japonica rice (12,800) and waxy rice (18,500) amylopectin. The iodine affinity (i.a.) and intrinsic viscosity, [η], of rice amylopectin were both dependent on the longest chain component, which were abundant in some normal Indica rice but lacking in waxy rice (Takeda *et al*., 1987 and 1989). Takeda *et al* (1987 and 1989) demonstrated that i.a. of amylopectin was directly proportional to long-B chains and inversely related to the short chains. The [η] of rice amylopectin is in the range 134-137 and 150-170 for Japonica and Indica rice, respectively (Takeda *et al*., 1987; Hizukuri *et al*., 1989; and Takeda *et al*., 1989). The [η] is dependent on molecular shape, chain-length distribution, and the amount of the ionized groups, in addition to molecular weight (Hizukuri *et al*., 1996).

The chain length distribution of rice amylopectin is analyzed by conventional GPC, SEC-MALLS-RI or high-performance-anion-exchange chromatography system equipped with pulsed amperometric detection after enzymatic branching. Reddy *et al*. (1993) reported that the debranched amylopectin contained three fractions with on average chain length DP_n in the range of 55-75, 42-55 and 10-25 anhydroglucose units, respectively. The debranched amylopectin of Taiwanese rice varieties were reported to have two main fractions, long chain (40-44) and short chains (10-15) (Lu *et al*., 1997). Ong (1994) analysed the chain length of debranched rice amylopectin by SEC-MALLS-RI. It was found that the main distinctions among the samples are the differences between the longest (DP 92-98) and the shorter amylopectin chains (ca. DP 22-25, 18, 14-16 and 10-11), whilst the intermediate chain

lengths of DP 67-68 and 43-45 were similar for all the rice. Tongdang (2001) found that the debranched amylopectin profile for all varieties had a small fraction of extra-long chain (F1) and 2 main fractions, a long chain (F2) and a short chain (F3). These results are similar to a previous finding for rice amylopectin (Ong, 1994). The F1 fraction of amylopectin of non-waxy rice varieties tell in the range of DP_n 58-88 and the highest was found in waxy rice (DP_n 118). The F2 and F3 had chain lengths within the range of 24-41 and 5-9, respectively.

The defined multiple-cluster structure of Asian rice amylopectin was analyzed by measuring the molar distribution of α-1,4-chain lengths from amylopectin isoamylolysates using capillary electrophoresis (Nakamura *et al*., 2002). The results clearly showed that Taichung 65 amylopectin had more short chain of DP ≤ 11 than the Co 13 amylopectin,but the former contained fewer intermediate-size chains of 12 ≤ DP ≤ 24 than the latter. However, chians of DP ≥ 25 and the chain of DP 11 were included in both amylopectins to a similar extent. Based on these results, the ratio of the short chains of DP ≤ 24 was calculated and the value (the amylopectin chain ratio, ACR value) used to characterize the amylopectin fine structure of rice. They found that amylopectin could be distinctly classified into two groups having ACR values in the range 0.159-0.200 and 0.240-0.287 although the amylopectin from #215 Khauk Yoe showed an intermediate ACR value of 0.220. The amylopectin having more long cluster-chains was designated as an L-type amylopectin and that with more short cluster-chains in the latter group as an S-type amylopectin. The amylopectin of #215 Khauk Yoe was called an M-type amylopectin. The difference in structure between L-type and S-type amylopectins was attributed to difference in the lengths of A and B1 chains constituting the unit cluster of the amylopectin molecule, but there was no difference in the proportion of long chains, i. e. B2 and

longer chains. It is reasonable to conceive that the varietal difference in amylopectin structure is found only in the relative numbers of short and intermediate α-1,4 chians with a single cluster, and that there is no difference in the modes of α-1,6 branches, i. e. the total number of α-1,6 branches and their location within the cluster. The idea is schematically illustrated in Figure 2.6. The α-1,6 branches are seperately localized in two regions of amylopectin cluster, i.e. amorphous lamellae and crystalline lamellae (Hizukuri, 1996; Jane *et al*., 1997; and Bertoft and Koch, 2000). In rice amylopectin, branching point of most B1 chains are located in the amorphous lamellae and those to which many A-chains attach are in the crystal lamellae.

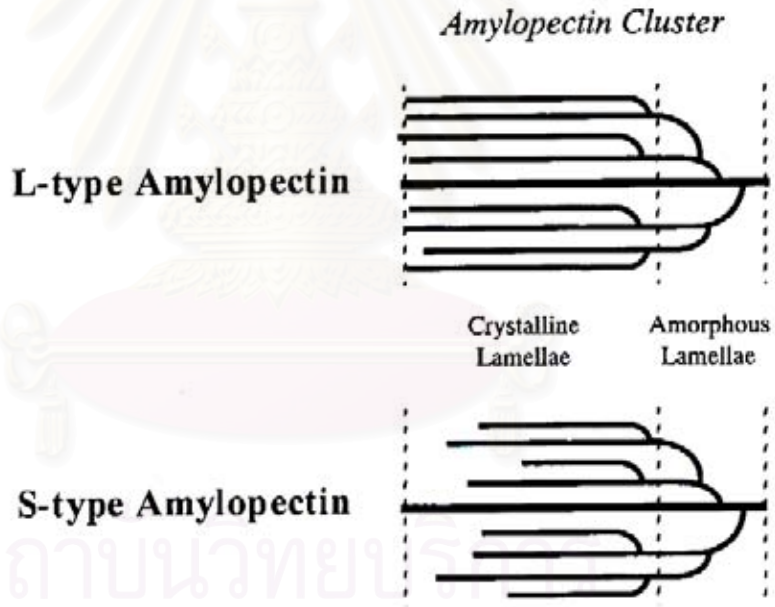

Figure 2.6 Schematic representation of cluster structure of L-type and S-type amylopectin (Nakamura *et al*., 2002).

2.2.3 Crystalline structure

The crystallinity is produced by the ordering of the amylopectin chains. The clustered branches of amylopectin occur as packed double helices. These double helical structures form the many small crystalline regions in the dense layers of the starch granules. The crystalline structure exhibited distinct X-ray diffraction patterns that can be classified into three categories: A, B and C type crystal (Figure 2.7). Most cereal starches (e.g. wheat, rice, corn) exhibited the A type crystal. Tuber starches (e.g. potato, canna) and high amylose starches show the B type crystal. Several rhizome and bean starches belong to the C type crystal. The C type crystal is believed to be a superposition of the A and B types crystal.

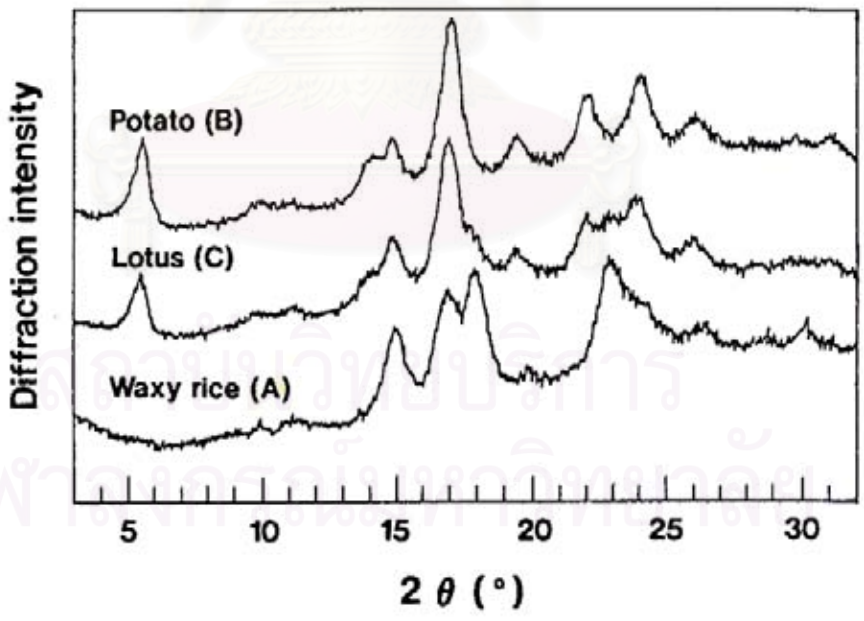

Figure 2.7 X-ray diffraction pattern of A, B, and C type (Hizukuri, 1996).

The double helices of the A type crystal form crystallized in a monoclinic lattice (unit cell parameter a = 2.14 nm, b = 1.172 nm, c = 1.069 nm, and $\alpha = \beta = 90^0$, $\gamma = 123.5^0$) having the maltotriose as a repeating unit and four water molecules (3.6%) per unit cell (Figure 2.8). The B-type crystal forms a the hexagonal lattice (unit cell parameter a = b = 1.85 nm, c = 1.04 nm, and $\alpha = \beta = 90^0$, $\gamma = 120^0$) having a more "open" packing of double helices, a maltose moiety as a repeating unit, and 36 water molecules per unit cell (Figure 2.8). In both crystal types, there is 1.1 nm between the axes of the two double helices. Calculated densities for the crystalline region of the A and B type crystal are 1.48 and 1.14, respectively (Imberty *et al*., 1988; and Imberty and Perez, 1988/). The A type crystal (the most thermodynamically stable form) is favored under conditions of shorter α-D-glucan chain length, higher crystallization temperatures, higher polymer concentration, slower crystallization conditions, and the presence of alcohol. The reverse is true for the B type crystal (kinetically preferred form), which crystallize readily from pure water (Gildley and Bulpin, 1987; and Gidley, 1987). Imberty (1991) reported a model of the solid-state transition from B type crystal to A (Figure 2.9). The pair of double helices are preserved while the water is removed and the helices rearranged to fill the void left by removal of the water. On the other hand, it appears that the reverse transition could not take place without a gelatinized intermediate that would disrupt the crystalline architecture of the dense A form.

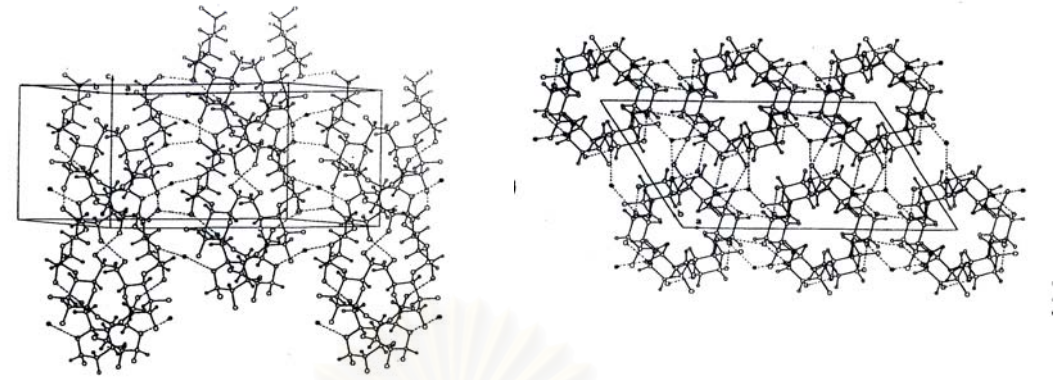

A type crystal

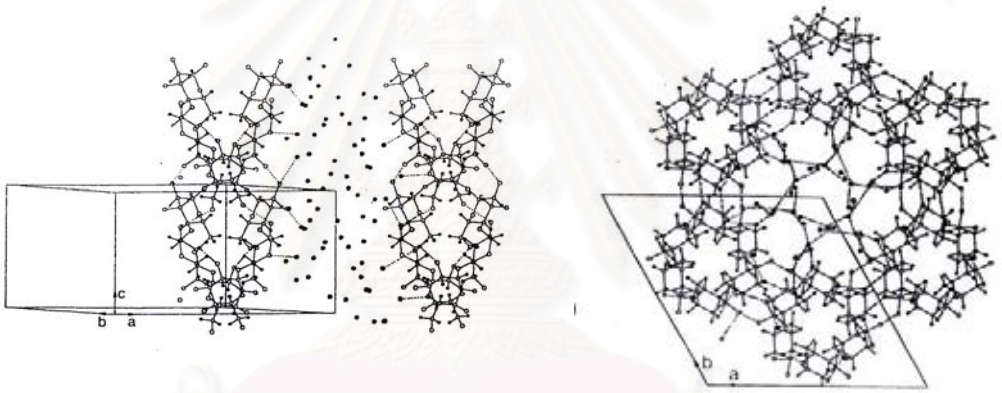

B type crystal

Figure 2.8 The crystalline structure of the A and B type crystal. (Left) Three-dimensional representation along the fiber axis (c direction), (Right) Projection of the structure onto the (a, b) plane. Dashed lines are the hydrogen bonds between the two strands of double helices, (•) indicate water molecules (Imberty *et al*., 1991).

Figure 2.9 Model of the polymorphic transition from the B to the A type crystal, in the solid state. The parallel double-helices which form the duplex are labelled 0 and ½ (this indicates their relative translation along the C axis). The water molecules are shown as dots (•)(Imberty *et al*., 1991).

2.2.4 Granule structure

The starch granule organization is very complicated and depends strongly on the botanical origin. Native starches are semi-crystalline structures composed of stacks of alternating growth rings of crystalline and amorphous lamellae of the granlues with the size of one amorphous and one crystalline lamellae ranging from 9 to 10 nm (Figure 2.10). The crystalline structure consists of a radial arrangement of clusters of amylopectin. Each cluster contains a region high in branch points and amylose (the amorphous lamellae) and a region where short chain segments of amylopectin have formed double helices (the crystalline lamellae). Molecular order in native starch is evident from the optical birefringence pattern ("Maltese cross") shown by granules when viewed under polarized light.

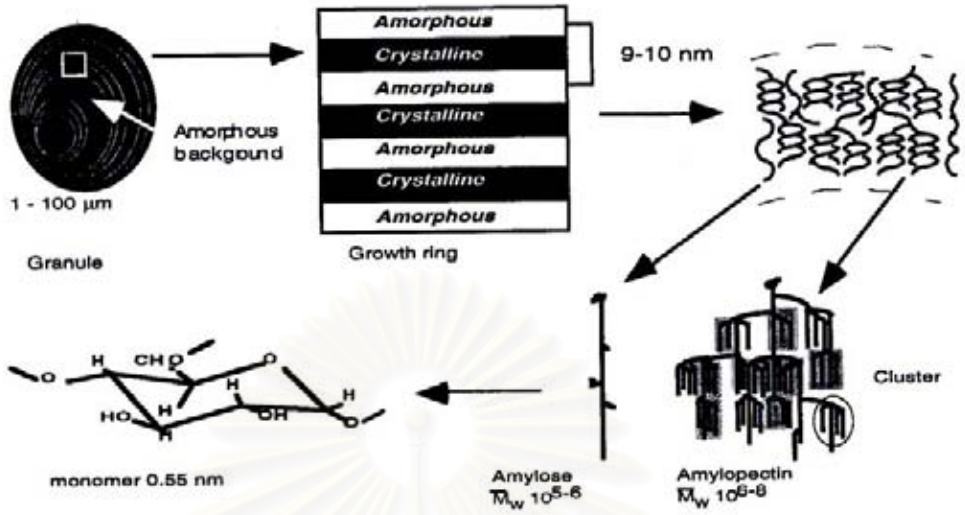

Figure 2.10 Schematic representation of the different structural levels of the starch granule and the involvement of amylose and amylopectin (Buleon *et al*., 1998).

According to Zobel (1988), crystallinity values for granular starches range from 15% to 45%, with the A type crystal showing values between 33% and 45%. Waxy starches give good X-ray diffraction patterns, while high amylose starches show low crystallinity, 15-22% (Zobel, 1988; and Gernat *et al*., 1993). These observations support the view that amylopectin is the principal crystalline component of native starches. A variety of techniques (e.g. acid hydrolysis, X-ray diffracton, and NMR) have been used to determined the absolute crystallinity of native starch but the values obtained are very dependent on the technique used (Table 2.3).

Table 2.3 Degree of crystallinity (%) of different starches determined by acid hydrolysis, X-ray diffraction and solid-state NMR

Starch	Acid hydrolysis	X-ray diffraction	C-NMR
A type crystal			
Normal maize	18.1-27.0	38-43	42-43
Waxy maize	19.7-28	38-48	48.53
High amylose maize	18.1	25	38
Wheat	20.0-27.4	36-39	39
Rice		38-39	49
B type crystal			
Potato	18.1-24.0	25-40	40-50
Cassava	24.0	24	44

(Robin *et al*., 1974; Gidley and Bociek, 1985; and Cooke and Gidley, 1992)

2.3 Starch gelatinization

Gelatinization refers to the disruption of molecular order within starch granules as they are heated in the presence of water. When an aqueous suspension of starch is heated above the gelatinization onset temperature (T_0), the granules absorb large amounts of water and swell considerably to impart a substantial increase to the viscosity of the suspension (Eliasson, 1986; Eliasson, 1996; Okechukwu and Rao, 1998; and Thomas and Atwell, 1999). Continued heating of starch granules in excess water results in further granule swelling and additional leaching of soluble components (primary amylose). Swelling of granules attains a maximum value at elevated temperatures and is subsequently followed by granular disruption and exudation of the granule contents into the suspension matrix (Eliasson, 1986) as shown in Figure 2.11. Thus gelatinized starch suspension may be regard as a composite material consisting of swollen granules and granular fragments dispersed in a continuous biopolymer matrix (Evans and Haiman, 1979; Eliasson, 1986; Morris, 1990; and Noel *et al*., 1993). It is logical that the rheological properties of such a material depends on three important component, the dispersed phase, the continuous phase, and interactions between the components (Table 2.4).

Table 2.4 Factors that might influence the rheological behavior of a starch pastes and gels

Dispersed phase = swollen starch granules
Concentration
Granule size and size distribution
Shape of granules
Swelling pattern of starch
Granule rigidity (e.g. crystallinity) and deformability
Continuous phase
Viscoelasticity of the phase
Amount and type of amylose/amylopectin that has leached from the granules
Entanglements
Interactions between the components
Granule-granule contact
Granule-amylose/amylopectin interactions
Granule-amylose/amylopectin-granule interactions
The surface of the starch granules

(Eliasson, 1986)

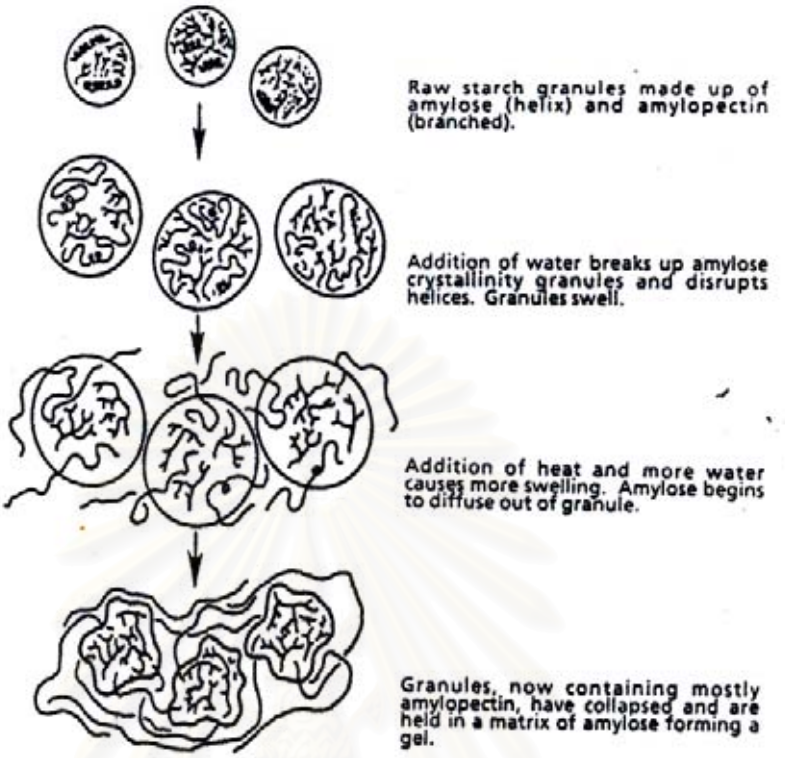

Figure 2. 11 Scheme of starch gelatinization (Remsen and Clark, 1978).

2.3.1 Starch changes during gelatinization

2.3.1.1 Loss of birefringence

In polarized light ungelatinized starch granules show birefringence, resulting in the “maltese cross” pattern (Fitt and Snyder, 1984). When T_0 is reached the birefringence begins to disappear. One of the most common methods for determining the gelatinization temperature range is to follow the loss of birefringence in excess water (Moss, 1976). The loss of birefringence occurs over a broader temperature interval when the water content is decreased.

2.3.1.2 Loss of crystallinity

The loss of crystalline order during heating is observed by X-ray diffraction. The diffraction pattern disappears, and eventually a pattern indicative of a completely amorphous material is obtained (Zobel *et al*., 1988). The temperature range during which the crystallinity is lost, and the rate with which it is lost depend on the water content and on the type of starch (Liu *et al*., 1991; and Svensson and Eliasson, 1995). The temperature range increases with decreasing water content, and at a water content below 50% the temperature for complete loss of crystallinity approaches 100 ^{0}C. The loss of crystallinity seems to occur in two steps: at first the loss occurs at a very low rate, but then at a temperature typical of the starch the rate increases dramatically (Svensson and Eliasson, 1995).

2.3.1.3 Endothermic transitions

The starch gelatinization is an endothermic process with enthalpy values in the range 10-20 J/g . During the last 10-15 years DSC has become the most important tool for studying starch gelatinization (Donaovan, 1979; Eliasson, 1980; and Atwell *et al*., 1988). DSC measures the gelatinization transition temperature and the enthalpy of gelatinization (ΔH). These DSC parameters are influenced by the molecular architechture of the crystalline region (Noda *et al*., 1996). Tester and Morrison (1990) have postulated that ΔH reflects the overall crystallinity (quality and amount of starch crystallines) of amylopectin. The amount of double-helical order in native starches should be strongly correlated to the amylopectin content, and granule crystallinity increases with amylopectin content.

2.3.1.4 Morphological changes

The swelling of starch granules and the solubilisation of macromolecules are the overall effects of the gelatinisation process. The process can be characterized by the swelling index and the solubility index. The high swelling power can be related to the sharp consistency increase observed on viscograms in the same temperature range. Simultaneously, a large amount of soluble material is recovered in the supernatant indicating a high solubilisation of starch granules. Using light microscopy and scanning electron microscopy several authors observed the morphological changes occurring at the different temperatures.

2.3.2 Viscous properties

2.3.2.1 Intrinsic viscosity

In dilute solutions, the polymer chains are separated, and the intrinsic viscosity, [η], of a polymer in solution depends only on the dimensions of the polymer chain. The [η] indicates the hydrodynamic volume of polymer molecule and it depends primarily on molecular weight, molecular shape, chain rigidity (conformation), chain-length distribution, the amount of the ionized groups and solvent quality (Launay *et al*., 1986; and Takeda *et al*., 1987). When the polymer is dissolved at a concentration, c (w/v), in a solvent, the solution viscosity (η) is increased from that of the solvent (η_s)at a given temperature. The ratio of (η) to (η_s) is called the relative viscosity (η_r), which equals to the ratio of the flow time (t) of the solution to the solvent (t_s), in the capillary viscometer. The parameters involved in the determination of [η] are as follows:

$$\text{Relative viscosity, } \eta_r = \frac{\eta}{\eta_s} = \frac{t}{t_s} \quad (2.1)$$

$$\text{Specific viscosity, } \eta_{sp} = \eta_r - 1 = \frac{\eta - \eta_s}{\eta_s} \approx \frac{t - t_s}{t_s} \quad (2.2)$$

$$\text{Reduced viscosity, } \eta_{red} = \frac{\eta_{sp}}{c} \quad (2.3)$$

The [η] is defined as Equation (2.4) which can be obtained from the zero extrapolation of the plot of η_{red} against concentration c or the slope of plot of η_r and c (Harding, 1997; and Tanglertpaibul and Rao, 1987).

$$[\eta] = \lim_{c \to 0} \frac{\eta_{sp}}{c} \quad (2.4)$$

The concentrations of polymers used should be such that the relative viscosities of the dispersions are from about 1.2-2.0 to ensure good accuracy and linearity of extrapolation to zero concentation (Morris and Ross-Murphy, 1981; Lopes da Silva and Rao, 1992).

The [η] can be converted to the viscosity average molecular weight (M) via the Mark-Houwink equation:

$$[\eta] = KM^a \quad (2.5)$$

where a and K are the constants for a particular polymer-solvent system. The exponent “a” is related to the shape of polymer molecule in solution.

The [η] of amylose, amylopectin, and starches obtained from difference sources are given in Table 2.5 (Hizukuri, 1989 and 1993; and Paterson *et al*., 1996).

Table 2.5 The intrinsic viscosity [η] and number average degree of polymerization (DP_n) of amylose, amylopectin and starches obtained from different sources

Source	[η] (ml/g)	DP_n
Japonica rice		
- amylose	216	1110
- amylopectin	134	13000
Indica rice		
• IR48		
- amylose	243	9300
- amylopectin	157	9000
• IR64		
- amylose	249	1000
- amylopectin	152	15000
• IR32		
- amylose	180	1000
- amylopectin	150	4700
Wheat starch	137	
Potato starch	224	

(Hizukuri, 1989 and 1993, and Paterson *et al*., 1996)

2.3.2.2 Flow behavior

At sufficiently high starch concentrations, most shear-thinning biopolymer solutions exhibit a similar three-stage viscous response when sheared over a wide shear rate range (Figure 2.12). At low shear rate, they show Newtonian properties, with a constant zero shear viscosity (η_0) over a limited initial shear range followed by a shear-thinning range where solution viscosity decreases in accordance with the power law relationship (Equation 2.6) to a limiting infinite shear-viscosity (η_∞) and a constant η_∞ range. Gelatinized starch exhibit yield stresses at low shear rates (Evan and Haisman, 1979; Doublier, 1981; Colas, 1986; and Giboreau *et al*., 1994). At high shear rates, the shear responses follows the power law relations prompting the use of the power law model (Equation 2.6) for the analysis the rheological behavior of gelatinized starch.

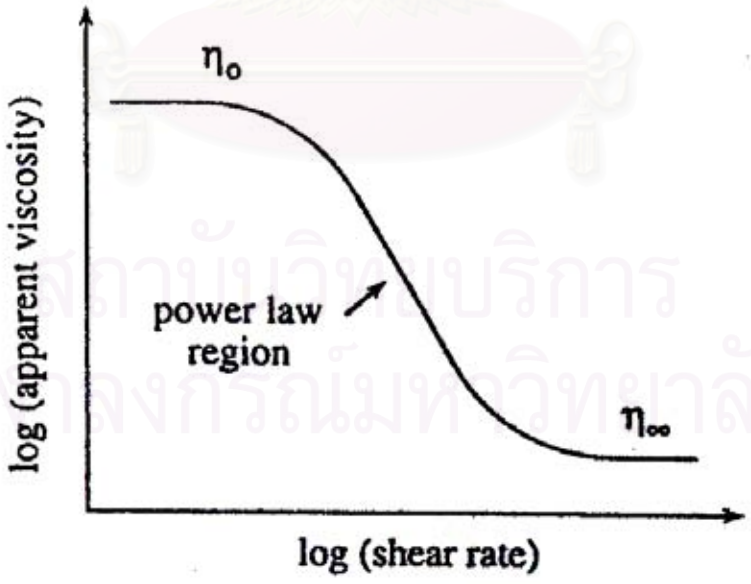

Figure 2.12 Plot of shear rate versus apparent viscosity for shear-thinning food, identifying three separate regions (Okechukwu and Rao, 1998).

$$\sigma = k\dot{\gamma}^{n} \quad (2.6)$$

where σ = shear stress

γ = shear rate

k = consistency index

n = flow behavior index (n = 1 for a Newtonian flow, < 1 for shear thinning flow, and > 1 for shear thickening flow)

At low starch concentration, most authors have used the simple power law model without a yield stress for describing shear responses over a wide range of shear (Okechukwu and Rao, 1998). The flow behavior index, n, and the consistency index, k, are useful parameters for describing the flow behavior of starch suspensions. Gelatinized starch pastes preheated to a temperature of about 90 ^{0}C are generally reported to be shear-thinning (pseudoplastic) fluids with values of n considerably less than 1.0 (Evan and Haisman, 1979; Doublier, 1981; Colas, 1986; Ellis *et al*., 1989; Noel *et al*., 1993). Evans and Haisman (1979) showed that in suspensions of corn, potato, modified corn, and tapioca starches as well as wheat flour, the n decreased rapidly from unity and approached a constant value at high concentration. The rice flour pastes exhibited shear-thinning behavior without a yield stress at concentration of 2-6 % and temperature of 25-80 ^{0}C and their flow properties were represented by a power law model (Wang and Sun, 1999).

2.3.2.3 Factors effecting on viscous properties

A number of factors, which include concentrations, temperature, volume fraction of the swollen granules, the deformability of the granules, as well as the degree of molecular entanglement, have all been reported to affect the viscosity of starch pastes (Doublier, 1990; and Okechukwu and Rao, 1998).

2.3.2.3.1 Starch notional volume fraction

The viscosity of starch pastes has often been interpreted in terms of the parameter cQ where c is a concentration and Q is the mass of water adsorbed per mass of dry starch. This starch granule mass fraction (cQ), which has been referred to as the "notional volume fraction" (Evans and Lips, 1992), plays an important role in determining the rheological properties of starch dispersions (Evans and Haisman, 1979). At low cQ, the granules are sufficiently far apart and do not affect viscosity substantially. However, as cQ increases the intergranular interactions become greater and this is accompanied by a large increase in dispersion viscosity (Okechukwu and Rao, 1995).

Rao and Tattiyakul (1999) reported that the relative viscosity (η_r) of 2.6% for tapioca starch dispersions strongly depended on their notional volume fraction is predicted by the model of Quemada *et al.*(1985) (Equation 2.7) with the structural parameter (k) = 1.80. Because heated starch granules are deformable, the k of red blood cells was selected for estimating the η_r values of tapioca starch dispersions.

$$\eta_r = \left(1 - \frac{1}{2}k\,(cQ)\right)^{-2} \qquad (2.7)$$

2.3.2.3.2 Starch concentration

Evans and Haisman (1979) reported that the apparent viscosity at any shear rate, η_γ, raised to power 0.4 was linearly correlated with concentration for potato, tapioca, and corn starch within the shear rate 10^1 to 10^3 s^{-1}:

$$(\eta_{\gamma})^{0.4} = K^{11}(c - c_0) \qquad (2.8)$$

where c_0 is the concentration at which the viscosity extrapolated to zero and K^{11} is a proportionality constant. Thus at various shear rates, it is possible to construct linear plots relating apparent viscosity with starch concentration. Plot of apparent viscosity as a function of starch concentration were later shown by Bagley and Christianson (1982) to be greatly affected by the pasting temperature and time. Power law relations have been used to describe the influence of starch concentration on the viscosity of gelatinized wheat starch suspensions over the shear rate range 20 to 200 s^{-1} (Doublier, 1981).

2.3.3 Viscoelastic properties

Viscoelastic materials are both elastic and viscous. Their rheological properties depend on the relative degrees of elastic and viscosity and are also dependent on the time-scale of the deformation. Many rheological measurements of viscoelastic materials are carried out in the “linear viscoelastic range”. This is generally defined to be where the material response (e.g. strain) at any time is directly proportional to the value of the applied force (e.g. stress). This simple definition follows from the superposition principle from which the material theory of linear viscoelasticity is based. In the linear region (Figure 2.13), rheological properties are

not strain or stress dependent. Strong gels may remain in the linear viscoelastic region over greater strains than weak gels (Steffe, 1996). Viscoelastic measurements of materials are usually classified as static or dynamic. Static measurements are made under steady shear or with a step change or sudden application of strain or stress. Dynamic measurements involve the application of a harmonically varying strain or stress.

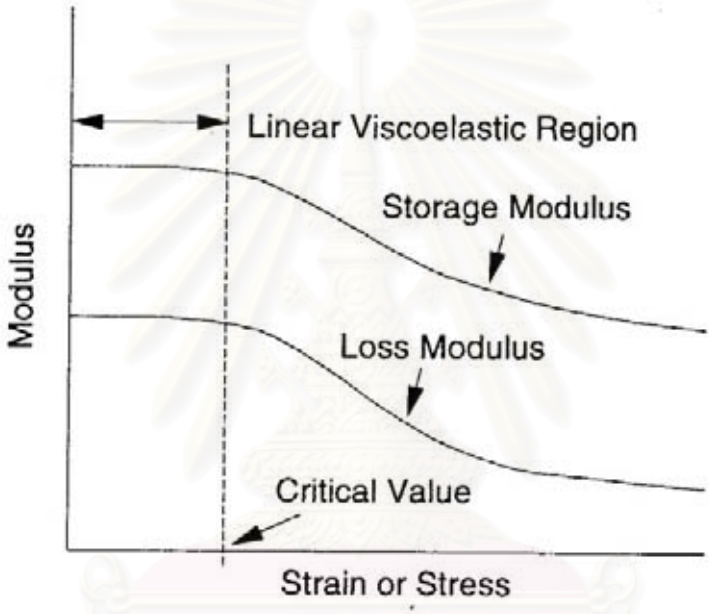

Figure 2.13 Typical response to a strain or stress sweep showing the linear viscoelastic region defined by the critical value of the sweep parameter (Steffe, 1996).

2.3.3.1 Dynamic viscoelastic

Dynamic experiments employing small-strain oscillatory shear are generally used in elucidating the viscoelastic properties of gelatinizing starch suspensions. In this studies, conducted at strain values within the linear viscoelastic range, the rheological response is resolved into elastic and viscous components that

provide bases for evaluating the storage modulus (G′), the loss modulus (G″), and the loss tangent (tan δ). The G′ expresses the magnitude of the stress that is stored in the material (or recoverable per cycle of deformation). G″ is a measure of the energy lost as viscous dissipation per cycle of deformation. It should be noted that if G′ is much greater than G″, the material will behave more like a solid, that is, the deformations will be essentially elastic or recoverable. However, if G″ is much greater than G′, the energy used to deform the material is dissipated viscously and the material's behavior is liquid-like. Figure 2.14 shows the variation of G′, G″ and tan δ with frequency for a polymer. At low frequencies the polymer is flow behavior and has a low modulus, which G″ increases with decreasing frequency. At high frequencies the polymer is glassy with a high G′, which is independent of frequency. At intermediate frequencies the polymer behaves as a rubbery (G′and G″ are independent of frequency) and viscoelastic solid (G′ increases with increasing frequency).

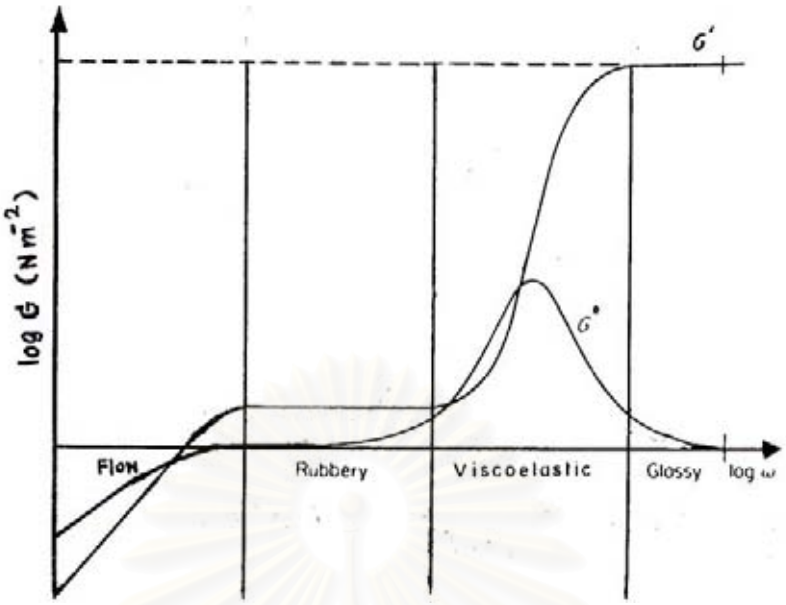

Figure 2.14 The mudulus as a function of frequency (ω) (adapt from Ward, 1990).

G' and G'' are influenced by concentration, temperature, frequency, strain (Okechukwu and Rao, 1998) and amylose content of starch (Biliaderis and Juliano, 1993; and Lii *et al*., 1996).

2.3.3.1.1 Effect of starch concentration

Results from studies on the gelation of starches from various botanical sources indicate that the elastic modulus increases with starch concentration. At lower concentration (e.g. <10%), most starch granules could swell under less restriction than could those in higher concentration (e.g., 25%). Therefore, the rigidity of the swollen granule was related to starch concentration. Starch granules were close-packed at low degrees of swelling with more rigid structure at the high starch concentration. Starch granules were not close-packed when the swollen

granule was less rigid in the low concentration system. In addition, the total available surface for the interaction among swollen granules in lower concentration systems could be smaller than in higher concentration systems. Consequently both G′ and G'_{max} of lower concentrations were lower than these of higher concentrations during heating (Tsai *et al.*, 1997).

Potato and pea starches have shown a linear dependence of G′ with concentration over the range 6-30% starch solids (Ring, 1985; Evans and Haisman, 1979), while corn starch exhibited a linear dependence of log G′ with concentration over the range 5-10% (Hansen *et al.*, 1990). Exponential relationships have also been used to describe the variation of G′ with concentration of wheat starch suspensions over the range 2-6% (Wong and Lelivre, 1981).

Lii *et al.* (1995) studied the effect of starch concentration over the range 5-30% on viscoelastic properties of three rice starches: KSS7, TNu67 and TCW70. The starch concentration effect was very important for producing a continuous matrix with embedded swollen granules. In the lower starch concentration (5%), the concentrations of the leached-out amylose and swollen granules were not high enough to interact to form a continuous matrix. The higher concentration (10-30%) gave sufficient interaction to enhance gel formation and display higher G′ value at 95 ^{0}C. Thus both G′ and tanδ are necessary to describe the rheological properties of a gel.

2.3.3.1.2 Effect of amylose content

Cereal starches, where amylose leaches out of the granule during gelatinization and largely contributes to the viscoelasticity of the continuous

phase, it is interesting to explore the relationship between amylose content and mechanical properties of starch gels. Different in gel strength have been reported for starches from rice with different amylose content. Rice starches, because of their uniform granules (shape, size, and size distributions) offer a unique model system in this respect. An inverse linear relationship between tanδ and amylose content of 25% gels of rice starches from 43 different varieties was observed (Biliaderis and Juliano, 1993). Also there was a general trend for increased G′ with amylose content.

Lii *et al*. (1996) studies effects of starch variety and amylose on the viscoelastic properties of rice starch during heating. The result indicated that the rice starch with higher amylose content gave the higher G′ than starch with lower amylose content. The result coincided with the fact that starch granules with low amylose content were less rigid and tended to disintegrate easily when swollen intensely and overcrowded (Sandharani and Bhattachya, 1989). The structure of the granule with high amylose content was highly strengthened and more rigid.

2.3.3.1.3 Effect of cooling temperature and aging time

As a hot gelatinized starch dispersion is cooled, G′ begins to rise at a temperature designated as the gel temperature. This temperature, which marks the onset of structure development in the hot paste, also coincides with the peak temperature on a tanδ-temperature plot (Hansen *et al*., 1990). When hot gelatinized dispersions of starch are rapidly quenched and aged isothermally, structure development, measured by oscillatory shear on a time scale, follows a biphasic pattern. The initial rise in G′ marks the beginning of the short-term development in

gel strength, attributable to amylose network formation and growth in the dispersion matrix. This view is supported by comparative studies on G′ development in dispersions of smooth pea starch and amylose in water quenched from 90 ^{0}C to 26 ^{0}C (Miles *et al*., 1985). In starches, such as that of potato, with a large swelling ability and hindered solubilization of amylose into the continuous matrix, the initial gel strength development is poor, due to low levels of amylose in the suspending matrix. The latter stage in gel strength is the contribution due to amylopectin recrystallization.

Lii *et al*. (1995) reported during cooling, the G′ of rice starch steadily increased. KSS7 (25.6% amylose) had a higher rate of increase in G′ than did TNu97 (14.80% amylose) at the same levels of starch concentration during cooling. Higher G′ during cooling might be explained by the interactions including hydrogen-bond formation favored at lower temperatures. Cooling was a process of starch retrogradation, mainly due to amylose retrogradation during the shot period (Biliaderis and Zawistowski, 1990). The cooled gel was more rigid than the hot gel (Biliaderis, 1992).

2.3.3.2 Mechanical models for viscoelastic

Mechanical models consisting of a spring and a dashpot can be used to simulate elastic and viscous components in a viscoelastic material subjected to shear or deformation in the linear viscoelastic range. The properties of the spring, which obeys Hook's law, and the dashpot's behaving as a Newtonian fluid permit a rational analysis of a viscoelastic response, provided the material is strained within its linear range. Springs and dashpots can be connected in various ways to portray the behavior of viscoelastic materials. The most common mechanical analogs of

rheological behavior are the Maxwell and Kelvin models depicted in Figure 2.15. Mechanical analogues provide a useful means of interpreting creep and stress relaxation data. These data may also be presented in terms of various compliance and modulus distribution functions as well as electrical models (Mohsenin, 1986; Sherman, 1970; Ferry, 1980; and Barnes *et al*., 1989).

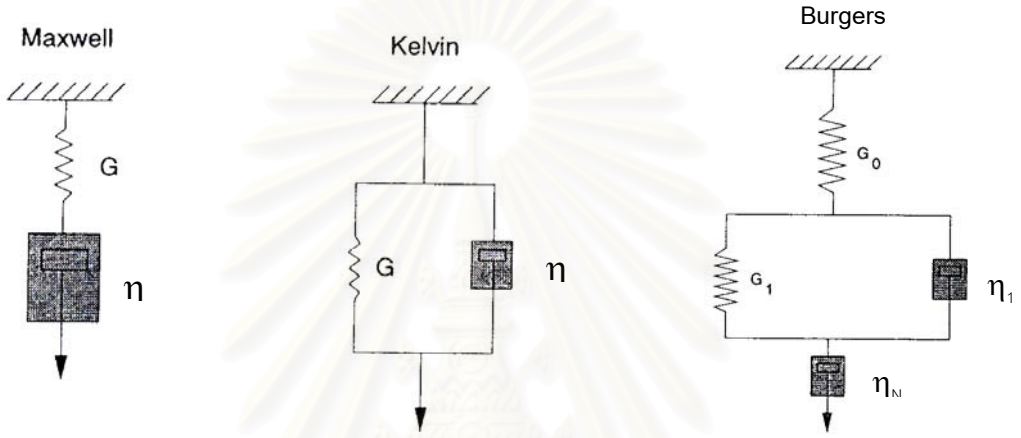

Figure 2.15 Maxwell, Kelvin, and four element Burgers models (Steffe, 1996)

2.3.3.2.1 Creep Compliance

In a creep test, an instantaneous stress is applied to the sample and the change in strain (called creep) is observed over time. When the stress is released, some recovery may be observed as the material attempts a return to the original shape. The Kelvin model shows excellent elastic retardation but is not general enough to model creep in many biological materials. The solution to this problem is to use a Burger model, which is a Kelvin and Maxwell model placed in

series. Figure 2.16 shows a typical creep compliance-time curve. It can be subdivided into three principal regions (Sherman, 1970), as described below:

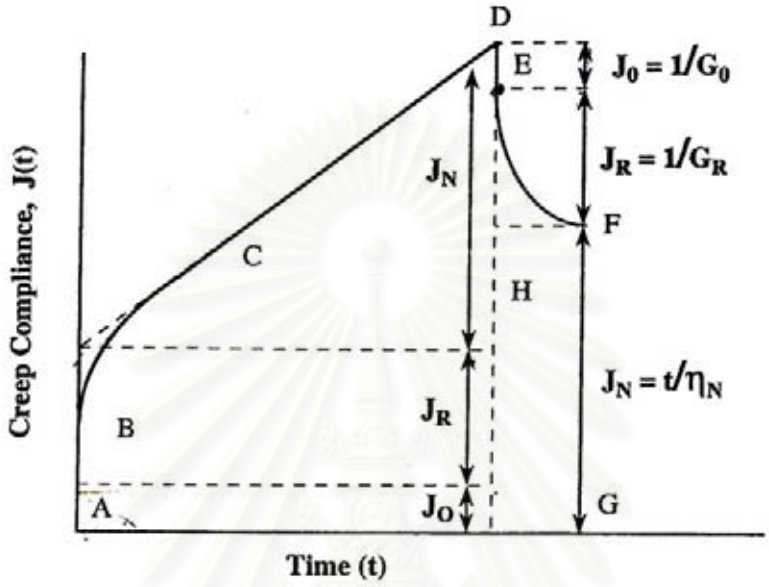

Figure 2.16 Illustration of a creep-compliance curve (Sherman, 1970)

(a) A region (A-B) of instantaneous compliance J_0 in which the bonds between the different structural units are stretched elastically. If the stress was removed at B then the sample would completely recover its original structure. The compliance is related to the corresponding modulus as following:

$$J_o = \frac{1}{G_0} \qquad (2.9)$$

where G_o is the instantaneous elastic modulus. The magnitudes of G_o and of G' at a low frequency (~ 1 Hz) were found to be of the same order of magnitude for a gel-like modified starch paste (Giboreau *et al*., 1994).

(b) Region B-C corresponds to a time dependent retarded elastic region with a compliance $J_{R.}$ In this region the bonds break and reform, but all of them do not break and reform at the same rate. The equation for this part, using mean values for the parameters, is

$$J_R = J_m[1 - \exp\frac{-t}{\tau_m}] \qquad (2.10)$$

where J_m is the mean compliance of all the bonds involved at any time t, and τ_m is the mean retardation time ($\tau_m = J_m\eta_m$, where η_m is the mean viscosity associated with the retarded elasticity).

(c) Region C-D is a linear region of Newtonian compliance in which the units as a result of rupture of the bonds flow past one another. The compliance J_N and the terminal viscosity (η_N) at compliance time (t) are related by

$$J_N = \frac{t}{\eta_N} \qquad (2.11)$$

When the stress is suddenly removed at D, the pattern consists of an elastic recovery (D-E) followed by a retarded elastic recovery (E-F). Since bonds between structural units were broken in the C-D region, a part of the structure is not recovered. This is represented by F-G, which is equivalent to D-H.

2.4 Starch Retrogradation

Starch granules when heated in excess water above their gelatinization temperature, undergo irreversible swelling resulting in amylose leaching into the solution. If a gelatinised starch is cooled to room temperature, the starch chain (amylose and amylopectin) reassociate, leading to the formation of a more ordered structure resulting in viscosity increase, gel firming, and textural staling (Eliasson, 1996; Okechukwu and Rao, 1998; and Thomas and Atwell, 1999).

2.4.1 Factors affecting starch retrogradation

2.4.1.1 Component of starch

Many investigation have been carried out to determined the respective role of amylopectin and amylose and their combined effects in the retrogradation of starch gels (Gudmundsson, 1994). The roles of amylose and amylopectin depend on the composite nature of the starch gels where swollen gelatinized starch granules are embedded within an amylose-gel matrix (Eliasson and Bohlin, 1982; Christianson and Bagley, 1983; and Steenken, 1989).

Goodfellow and Wilson (1990) studied the retrogradation of amylose using Fourier Transform Infrared (FT-IR). They found that helix formation must occur before the creation of crystallites; therefore double helix must form at the short or early on in the gelation process. Thus in summary, a model of gelation and retrogradation in which double helices form before or at the same time as phase separation, to create a gel network, with subsequent aggregation of these helices producing crystallinity would be consistent with the experimental data (Figure 2.17).

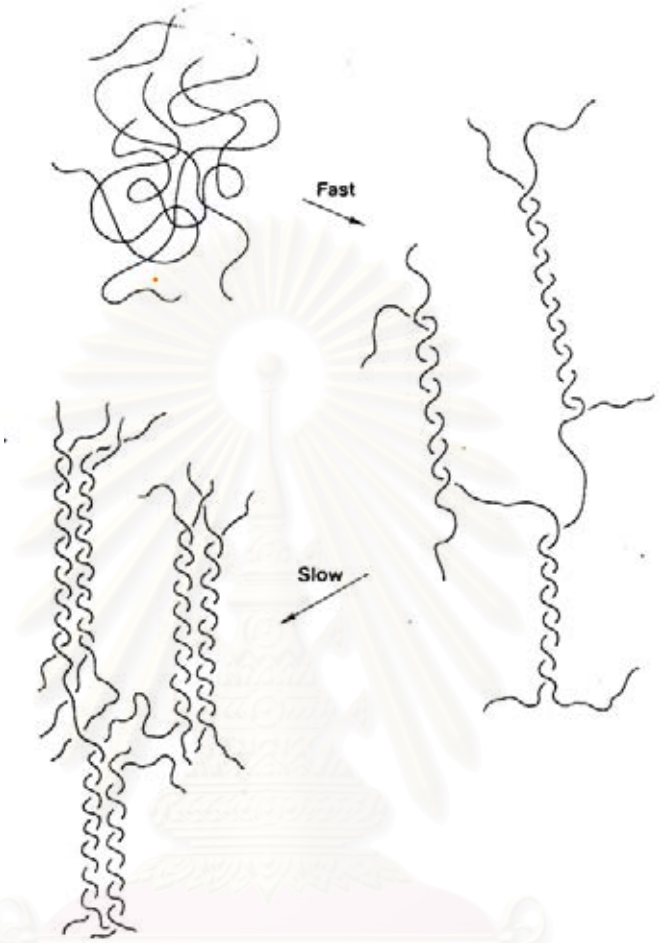

Figure 2.17 Schematic diagram showing the process occurring the gelation and retrogradation of amylose (Goodfellow and Wilson, 1990).

The IR results for amylopectin suggest an initial fast change followed by a much slow change. Previous IR work (Wilson et al., 1987) in which the spectra for amylopectin from 6 to 340 hour were obtained suggest that FT-IR and G′ monitor the same process-namely the crystallization of the amylopectin side chains followed by a slow aggregation of these helices to produce crystallinity (Figure 2.18).

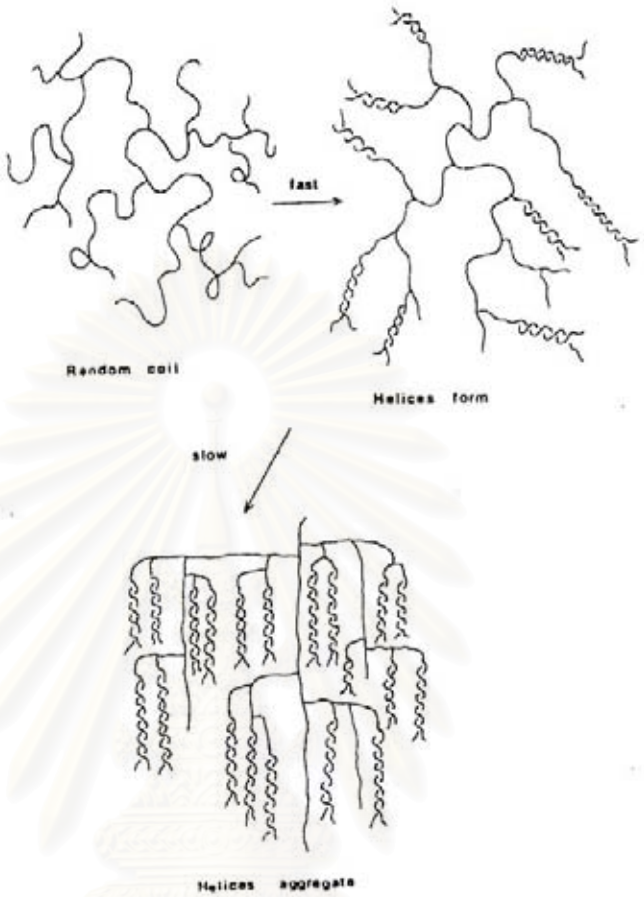

Figure 2.18 Schematic diagram showing the process occurring during the gelation and retrogradation of amylopectin (Goodfellow and Wilson, 1990).

This secondary aggregation is observed by FT-IR for amylopectin but not for amylose as a result of the branched nature of the amylopectin molecule. Once the helices have formed in the amylopectin side chains they are still connected to the main chain and the segments connecting the helical regions to the main chains will be large. However, when the helices aggregate, the range of bond energies for the main chain and connecting segments will be reduced. This short-range ordering has occurred that will be detected by FT-IR. This is in contrast to amylose, where the subsequent

aggregation of the polymer helices leave disordered amorphous regions connecting the aggregated sections. Thus the short-range order of this system is not affected. The initial fast change for amylopectin is not observed by X-ray diffraction or G′. The X-ray diffraction monitors crystallinity, so this fraction would not be picked up. The G′ experiment measures gel strength. The coil to helix transition within the side chains would not increase the development of the gel network to any extent as it is an intramolecular process. The subsequent crystallization of the helical side chains produces rigid sections within the molecule, increasing gel strength. In amylose, the coil to helix transition is an intermolecular process, which leads directly to the creation of a three-dimensional network.

Cereal amylose may form double-helical associations of 40-70 glucose units, whilst amylopectin forms shorter double helices (Miles *et al*., 1985; Goodfellow and Wilson, 1990; Leloup *et al*., 1992; Gudmundsson, 1994; and Liu *et al*., 1997). The latter can be attributed to restrictions imposed by the branching structure of the amylopectin molecules and the chain lengths of the branches. Thus, amylose, is responsible for short-term changes while amylopectin is responsible for the longer term rheological and structural changes of starch gel. Double helices may associate and organise into crystallites, most of which are related to association of the amylopectin chain which comprise the bulk of the starch component of rice. The retrogradation of maize amylopectins was proportional to the amount of short chains having a DP of 16-30 and inversely proporytional to the level of short chains with a DP of 6-11 Shi and Seib (1995).

Lu *et al*. (1997) studied the retrogradation of amylopectin from Taiwan rice varieties. They reported that the short chains of amylopectin with DP 10-15 glucose units would result in more retrograded crystalline building blocks. On

this basis as well, it would require more energy to disorder the greater number of double helical linkages of retrograded amylopectin. Thus, the plateau enthalpy would be higher (Sander *et al*., 1990). As Gidley and Bulpin (1987) suggested, a chain length of at least 10 units is required for crystallinity development and, by inference, for the formation of double helices. On the other hand, short chains with DP 6-9 glucose unit are known to inhibit retrogradation (Levine and Slade, 1986, and Shi and Seib, 1992). The retrogradation of waxy rice starches (rice, maize, barley) appears to be directly proportional to the mole fraction of unit chains of amylopectin with DP 14-24 and inversely proportional to mole fraction DP 6-9 (Shi and Seib, 1992).

The botanical source is of great importance for the retrogradation of starch gels (Orford *et al*., 1987; Gudmundsson and Eliasson, 1993; and Kalicheusky *et al*., 1990). This does not concern differences in amylose content, because it has even been observed in starches with very similar amylose content. This indicates that structural differences found in the amylopectin molecule may be the cause of differences in the recrystallization rate. Amylopectin from cereals has also been shown to retrograde to a lesser extent than pea, potato and canna amylopectin, which has been attributed to shorter average chain length in the cereal amylopectin (Orford *et al*., 1987; and Kalicheusky *et al*., 1990). The structural differences in cereal amylopectin as related to retrogradation can be related either to differences in the amorphous regions or to differences in the ratio of short to long chains and the ratio of A- to B- chains. A greater amount of short chains over 15 glucose units and increase ratio of A- to B-chains probably promote retrogradation. It has also been reported that very short chain (6-9 glucose units) can inhibit or retard retrogradation of starch gels (Levine and Slade, 1986).

2.4.1.2 Water concentration

Several studied have shown that the extent of retrogrdation is very sensitive to water content of starch gels (Gudmundsson, 1994). Longton and Legrys (1981) observed that crystallization during aging occurred only in gels with starch content between 10 and 80 % and maximum crystallization, measured with DSC, occurred in gel with 50-55 % starch. Eliasson (1983) and Zeleznak and Hoseney (1986) have confirmed that maximum crystallinity occurs in gels with 50-60 % starch.

The recrystallization process depends on the glass temperature (T_g) of amorphous gel because the mobility of the chains determines their amorphous gel. As a plasticizer, water controls the T_g of the amorphous gel. At very low water content, the T_g is above room temperature and the amorphous gel is in a highly viscous glassy state that effectively hinders molecular mobility. Recrystallization increases with increasing water content (depress of T_g below room temperature) up to 45-50 %, because of progressively more effective plasticization (increase molecular mobility); with further increase of water content up to 90 %, it decreases, apparently due to excess dilution (Slade and Levine, 1987).

Orford *et al*. (1987) examined the effect of starch concentration on retrogradation. They found that an increase in G′ with time to an apparent plateau value is concentration dependent. A linear relationship between starch concentration and G′ of cereal, tuber, and legume starch gels was observed. The increase in G′ was negligible at a concentration of 20 % (w/w). However, 30 % and 40 % (w/w) gels of these starches showed a marked increase in G′. The rate of G′ increases with increasing concentration. This suggests that there is an increase concentration of amylose in the material.

The effects of water content on the kinetics of the retrogradation of nonexpanded waxy maize starch extrudates were studied using NMR and Wide Angle X-ray Diffraction (Farhat *et al*., 2000). The rate of retrogradation depends strongly on the water content of the sample. The description of the dependence of the rate of retrogrdation at a constant storage temperature on the water content was attempted using the Lauritzen-Hoffman theory. The calculated lines described satisfactorily the experimental data for the isothermal recrystallization results obtained at 313, 329 and 353 K. It is interesting to point out the contrast between the effect of increasing the amount of water in the sample. Over the moisture content range of interest for this study (20-60 % db) at these storage temperatures: for example, at 40 ^{0}C the increase of water content enhanced the rate of retrogradation, which at 80 ^{0}C the opposite effect was observed.

2.4.1.3 Storage temperature

Retrogradation is greatly affected by storage temperature. Compared to storage at room temperature, storage of starch gels containing 45–50 % water at low temperature but still above the glass temperature ($T_g \approx 5.0$ ^{0}C) increases the retrogradation, especially during the first days of storage, compared to starch gels stored at room temperature (Gudmundsson, 1994). Storage temperature below T_g virtualy inhibits recrystallization. Higher temperatures (above 32-40 ^{0}C) effectively reduce retrogradation (Colwell, 1969; and Eliasson, 1985a).

Colwell *et al*. (1969) studied the effect of storage temperature (-1 to 43 ^{0}C) on concentrated starch gels by DSC. They found that the mechanism of starch crystallization (instantaneous nucleation followed by rod-like growth of crystals) is the same over the whole range of temperature. Moreover, at higher

storage temperatures, a more symmetrically perfect crystalline structure is found. The dynamic rheological properties of wheat starch pastes are influenced by storage temperature. G′ increased with decreasing storage temperature in the order $10^{0} > 15^{0} > 20^{0} > 30^{0}$C (Wong and Lelievre, 1982). The rate of nucleation increases exponentially as the temperature decreases to the T_g (Figure 2.19). However, the rate of propagation increases exponentially as the temperature increases to just below the melting point (T_m) of the crystallites. The overall rate of crystallization occurs at a point mid way between T_g and T_m (Slade and Levine, 1987). At low storage temperature (4-5 ^{0}C), the crystallites are less perfect having a lower T_m than those form at higher storage temperature (Gidley, 1987; and Slade and Levine, 1987).

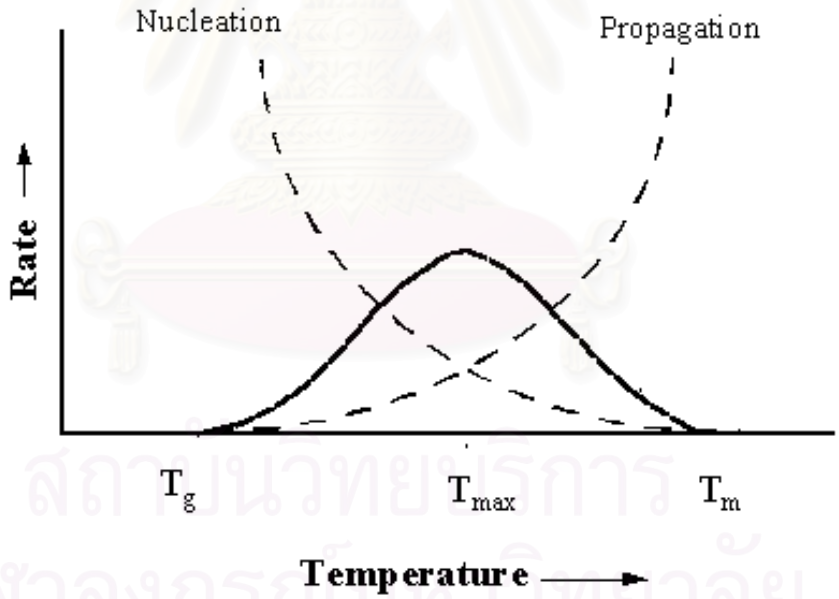

Figure 2.19 The effect of temperature on the crystallization kinetics of a partially-crystalline polymer (Slade and Levine, 1987).

The rate of retrogradation is expected to be at a maximum approximately mid way between the melting temperature of the crystallites, T_m and T_g. This reflects a balance between the effect of temperature on the driving force favoring crystallization, and the slowing of mobility as the glass transition is approached. Bell-shaped curves of extent of retrogradation versus temperature are observed supporting this suggestion (Farhat *et al*., 2000).

Biliaderis and Zawastowski (1990) studied the effect of temperature on rigidity of 5 % (w/w) amylose and 40 % (w/w) waxy maize starch gels. The rate of change in G′ of gels with respect to time decreased with increase in temperature, implying that gelation follows nucleation kinetics in a manner that is typical of crystallization in polymer-dilute mixture (Mandelkern, 1964). Moreover, the G′ of amylose gels was found to be less temperature sensitive than the waxy maize (amylopectin) gels. These observations further support the notion that amylose gelation mainly involves rapid formation of double helical junction zones upon cooling of amylose solutions, whereas a network-based structure for amylopectin is established mainly as a result of separation of partially crystalline structure (Ring, 1987).

2.4.2 Method used for estimating retrogradation

Retrogradation has been studied using an analysis varieties of different techniques, FTIR, X-ray diffraction, DSC, Raman spectroscopy and rheological techniques, (Eliasson, 1985; Russell, 1983; Zeleznak and Hoseney, 1986; and Kim et al., 1976).

2.4.2.1 Retrogradation monitored by FT-IR

Van Soest et al. (1994) studied the retrogradation kinetics of a potato starch (10 % w/w) by FT-IR. The spectra showed the C-C and C-O streching region (1300-800 cm^{-1}) to be sensitive to the retrogradation process. The spectrum of native potato starch showed three seperated bands in the region of 1100 to 900 cm^{-1} located at 1047 cm^{-1}, 1018 cm^{-1} and 994 cm^{-1}. This absorbance are related to the amount of crystalline starch and to the water content. Gelatinization of starch results in the convergence of these seperated bands to one intense broad band in this region with a maximum intensity at 1022 cm^{-1}. During retrogradation for several weeks, this broad line becomes resolved into three bands around 1053, 1022 and 1000 cm^{-1}. The most pronounces changes in the spectra occur at 1000 (peak), 1035 (valley) and 1053 (peak) cm^{-1}. Changes in the intensity of bands during storage reflects changes in specific aspects of starch conformation such as long range ordering and crystallinity, whereas, band narrowing reflects ordering of the polymer chains and retrogradation replacing the number of conformations. The multi-stage process was observed during the retrogradation of potato starch and characterized as the formation of short- and long-range order. The first stage was characterized as the formation of helices and the rapid formation of crystalline amylose regions. The second stage was described as the induction time for amylopectin helix aggregation. Stage three was described as the helix-helix aggregation and the crystallization of amylopectin. This crystallization has been confirmed by the appearance of diffraction in X-ray measurements for the gels over the 360 h of retrogradation.

2.4.2.2 Retrogradation monitored by rheological technique

The amylose and starch gels quickly attain a nearly constant value of rigidity; starch gels, however, show a slow rigidity increase with time. The gelation of amylopectin gels is very slow, taking several weeks to approach the limiting value (Ring *et al.*, 1987). Mita (1992) studied the effect of aging on the dynamic viscoelastics of potato starch pastes was investigated by measurement of dynamic viscoelasticity. The value of G′ increased rapidly with time for the first few hours, but attained equilibrium after a long period of aging. The author reported that the two processes occurred during the aging of starch pastes. The rapid increase in G′ at the early stage of aging will depend mainly on the chain entanglement of starch molecules in the amorphous regions, since the entanglements behave as crosslinks with short life-times. The slow increase in G′ over a long period of aging will be brought about by the increase in the rod-like growth of crystals which is attributable to the entanglement junction points developed on aging being replaced by micro-crystalline junction zones.

2.4.2.3 Retrogradation monitored by X-ray diffraction

Early X-ray diffraction studied on aged starch gels showed that the B-type diffraction pattern developed slowly (Zobel, 1973). Crystal growth, as detected by X-ray diffraction, is slower than formation of the gel network and has been proposed as occurring in the polymer-rich regions of the gel (Miles *et al*., 1985a, and Miles *et al*., 1985b). For both amylose and starch gel, the initial development of crystallinity occurred at similar rates. However, the crystallization of amylose effectively reached a limit after 2 days, where as the crystallinity of the starch gel

continued to increase (Miles *et al*., 1985b). The amylopectin gels show only a slow increase in crystallinity with time and approach a limiting value after 30–40 days (Ring *et al*., 1987). Isolated gelatinized starch granules that have been washed free from all exudated amylose gave no X-ray diffraction pattern immediately after cooling. After two weeks of storage, the B-type pattern is obtained.

Bulkin and Kwak (1987) analyzed the retrogradation of potato starch (52 % starch) by rapid Raman spectroscopy and X-ray diffraction. The Raman spectra revealed four stages in the retrogradation processes: (i) an initial rapid phase (representing conformational ordering involving the formation of double helices in amylopectin branches within a single polymer molecule; (ii) a plateau (represents the induction time for the onset of amylopectin helix aggregation and crystal growth; (iii) a slow process (represents the primary amylopectin aggregation and crystallization step); and (iv) a very slow process (represents crystalline phase propagation and perfection step). X-ray data from their work indicated that crystals do not begin to develop until stage (iii). Thus, any ordering that occurred in stage (i) must be short-range. Moreover, the X-ray data showed continued development of crystallinity in stage (iv). The authors have postulated that the role of amylose can be viewed as providing an acceleration by a template effect on amylopectin. Amylose itself retrogrades rapidly, forming an ordered (on the molecular level) matrix, which is not necessarily highly crystalline. These ordered chains may act as seed nuclei for regions of the amylopectin, accelerating all steps in the crystalline process.

2.4.3 Retrogradation kinetics

During retrogradation, crystal can grow from different nucleation centers and, therefore, the amount of crystallized material present at a given time is a combined function of crystal growth rate and the density of mucleation. During crystallization, the unconverted function at time (t), U(t), can be described by the Avrami equation (Avrami, 1941) as following:

$$U(t) = \exp(-kt^n) \quad (2.12)$$

where k is the crystal growth rate and n is the Avrami exponent depending on the type of nucleation.

$$U(t) = \frac{Y_\infty - Y_t}{Y_\infty - Y_0} \quad (2.13)$$

where Y(t) is any physical parameter describing the crystallization process (G′, the ratio of short range molecular order to amorphous, X-ray crystallinity index, etc.). Y_0 and Y_∞ are the initial value (at t = 0) and the plateau value (at t = ∞) of Y(t).

Combination Equation (2.12) and (2.13) leads to

$$Y(t) = Y_\infty - [Y_\infty - Y_0 \exp(-kt^n)] \quad (2.14)$$

The value of n and k are obtained from Equation 2.12 by plotting the linear relationship Log (ln [U(t)]) and Log(t) with Y_0 and Y_∞ being, respectively, the first and the last Y(t) values measured after gelatinization. Once the

value of k and n had been determined, the overall rate of retrogradation, G, can be calculated by the Equation 2.15.

$$G = k^{1/n} \quad (2.15)$$

The Avrami exponent (n) deals with the kinetics of phase changes during crystal growth around randomly distributed nuclei in term of the change in dynamic modulus (Sherman, 1970). The value of n is also a constant whose value lies between 1 and 4, depending on the nucleation mechanism (Mandalkern, 1964). It has been demonstrated that the basic mechanism of retrogradation of starch is instantaneous nucleation followed by rod-like growth of crystals (i.e. n= 1).

2.5 Rice aging

Rice aging is complicated. It involves changes both the in physical and chemical properties of the rice grain. The changes in aging properties of rice have been reported to depend on the storage conditions, temperature, light, and moisture content. The rate and extent of changes have been found to increase with the storage temperature and light (Vilareal *et al*., 1976; Swamy *et al*., 1978; Okabe, 1979; Chrastil, 1990 and 1992; Kumar and Ali, 1991) and to lesser extent with the moisture content of rice (Barber, 1972). The changes were relatively rapid at first, gradually slowing down later, but did not show signs of being halted even after 4 years, suggesting that aging of rice probably had no definite end-point (Sowbhagya and Bhattacharyat, 2001). Indudhara Swamy *et al*. (1978) and Bolling *et al*. (1978) studied the phenomenon for 5-7 years and noted that the changes continued until this time and perhaps beyond.

Moritaka and Yasumatsu (1972) proposed a mechanism of aging involving lipids and proteins. Lipids form free fatty acids, which can complex with amylose and carbonyl compounds and hydroperoxides, which can accelerate protein oxidation and condensation plus accumulation of volatile carbonyl compounds. Protein oxidation (formation of disulphide linkages from sulhydryl groups), together with an increase in the strength of micelle binding of starch, inhibits swelling of starch granules and affects cooked rice texture. Fat is hydrolysed (largely by lipase) to free fatty acids (FFA), which then complexs with amylose or long chains of amylopectin. Fat and FFA also undergo autoxidation to carbonyl compounds which, apart from causing on aroma change, interact with starch and protein. Mod *et al*. (1983) proposed that oxidation of ferulate esters of hemicellulose would contribute to cross-

linking and increased strength of cell walls during storage. A model for the aging process is presented in Figure 2.20.

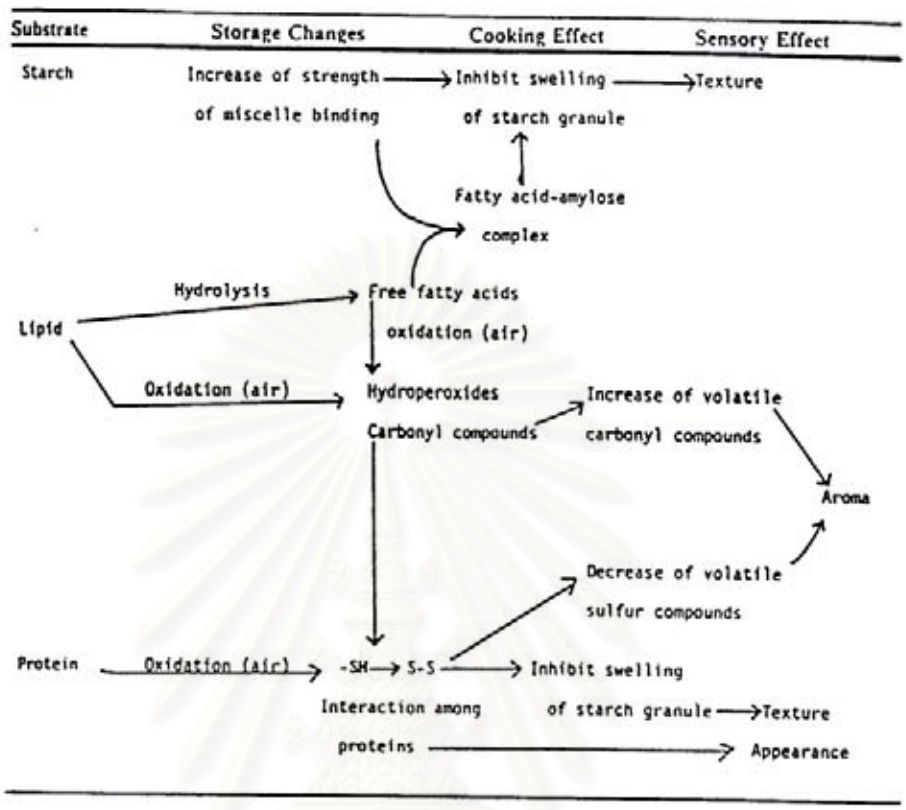

Figure 2.20 Schematic model of the aging process in rice (Moritaka and Yasumatsu, 1972).

Studies of the behaviour of different enzymes and the changes in the viscosities during storage of rice may suggest that enzymic activity may continue during the storage of rice. Dhaliwal *et al*. (1991) showed that the amylase activity was greater in freshly harvested rough rice, and the protease and lipase concentrations increased with storage. The higher amylase activities in the fresh rice sample correlated well with the lower peak viscosities of fresh rice that have been mentioned earlier.

The changes in the physicochemical properties of rice which had different amylose content were studied when 4 rice varieties were stored at 2 ^{0}C and 29 ^{0}C as rough rice, milled rice, defatted milled rice, and as starch for 6 months (Villareal *et al*., 1976). The hardness index increased with storage at both temperatures in all samples except for that of the waxy and defatted milled rice, which did not change with storage. The increase in water absorption and the decrease in extractable solids during cooking of milled rice were similar regardless of the form in which the rice was stored. The stickiness of non waxy rice decreased during storage, but that of waxy rice did not. Indudhara Swamy, *et al*. (1978) studied the changes in the physicochemical properties of rice with aging of seven varieties of rice as paddy and milled rice at 1-3 ^{0}C, room temperature (RT) and 37-40 ^{0}C in the dark and also in the light for 3.5 years. The aging process in rice appeared to be characterized by: (a) an increase in volume expansion and a steady decrease in solids loss upon cooking, (b) an initial increase followed by a steady decrease in the power of hydration, (c) probably a slow decrease in the solubility of the amylose and slow increase in the paste viscosity and setback, and (e) a sharply decreasing breakdown. The process was retarded by storage in the cold. Conversely, it was greatly hastened by storage at high temperature and to some extent by exposure to light. In addition, the process occurred much faster and/or to a greater extent in high-amylose rather than in low-amylose varieties, and to some extent in milled rice rather than in paddy. Kumar and Ali (1991) studied the properties of rice starch from paddy stored at 20-33 ^{0}C (designated "aged") and at 4-6 ^{0}C (designated "fresh") for 15 months. They found that the total amylose content was the same for the starches from both aged paddy. However, the hot water soluble amylose content was less in starches from "aged" paddy. The number average molecule weight as well as the swelling power and solubility of the

starches from aged paddy were also less indicating that the aging of rice could partly be associated with the changes in the physicochemical properties of its starch. Ong (1994) studied the effects of aging on rice stored at 18-21 ^{0}C for 20 weeks. The results showed that the pasting temperatures remained fairly constant with age, while the peak viscosity increased with time of storage. The setback appeared to decrease to a minimum after 10 weeks and increase thereafter. The higher adhesion force for the fresh cooked rice than the aged sample showed that the fresh rice was stickier than the aged sample. However, the temperatures and enthalpies of the gelatinization of starches were independent of the age. There was no detectable difference of granular structures and X-ray crystalline structure of starches between rice of various ages. Sowbhagya and Bhattacharya (2001) stored paddy of 15 varieties of rice at 26 ^{0}C for 51 months and found that the paste breakdown steadily decreased with time of storage, while the setback steadily increased.

CHAPTER III

MATERIALS AND METHODS

3.1 Materials

3.1.1 Starch extraction

3.1.1.1 Soaking

RD6 waxy rice (Rice Research Centre, Khonkhan, Thailand), aromatic Jasmine rice named Khao Dawk Mali 105 rice (Rice Research centre, Patumthani, Thailand) and Supanburi 1 rice (Rice Research centre, Patumthani, Thailand) were soaked in 0.3% NaCl solution (rice : 0.3% NaCl solution = 1: 5 by weight) at 33 ± 2 ^{0}C for 5 hours to soften the endosperm. After draining, the wet grains were fed into a grinding mill with 0.3% (w/v) NaOH solution, the weight ratio of wet grains to NaOH solution was 1: 5.

3.1.1.2 Deproteinization

The following alkaline method (Yamamoto *et al*., 1973 and Juliano, 1984b) was use for deproteinization. The obtained rice flour in NaOH was stirred for 9 hours at 33 ± 2 ^{0}C and allowed to settle overnight without stirring. After draining of the supernatant, the sediment was centrifuged at 1600g for 20 min. The supernatant was discarded and the sediment was added with water (sediment: water = 1:1 by weight) and centrifuged at 1600g for 15 min, this step was repeated to wash the

sediment. Then, the washed sediment was soaked in water (sediment : water = 1:1 by weight) and adjusted to pH 7 with 1 M HCl. The suspension was centrifuged immediately at 3000g for 15 minutes.

3.1.1.3 Drying

The final sediment from section 3.1.1.2 was dried in a hot air oven (Yeo Heng Co. Ltd., Bangkok, Thailand) at 50 ^{0}C for 20 hours. After dry milling with cross beater mill (Retsch Gmbh, Hann, Germany), the dried starch was sieved through wire mesh sieve (250 μm) and stored at 5 ^{0}C.

3.1.2 Ageing of rice

Fresh rices were stored at 33 ± 2 ^{0}C for a designated time of 0 and 5 months, then starches were extracted as described in 3.1.1.

3.2 Chemical composition analysis

Chemical composition, namely moisture, fat and protein content of the prepared rice starches and the commercial rice starches (Rice starch from Cho Heng Rice Vermicelle Factory, Co., LTD, Nakorn Prathom, Thailand; and waxy rice starch from Bangkok Interfood factory, Co., LTD., Thailand) were analysed using these following methods:

3.2.1 Protein, fat and moisture content

The moisture content and fat content were determined according to AOAC method (AOAC, 1995). Protein content was analysed by the Dumas method (AACC, 1999) using a nitrogen analyser (NA 2000, Fisons Instruments, Italy).

3.2.2 Amylose content

3.2.2.1 Iodine method

3.2.2.1.1 Amylose equivalent

Amylose equivalent (AE) was determined using the procedure as described by Sombhagya and Bhattacharya (1979). Rice starch of 100 mg was dissolved in solution containing 1 ml ethanol and 10 ml of 1 N NaOH, then heated at 100 ^{0}C for 5 min, and left overnight at 25 ± 2 ^{0}C. The starch solution was shaken thoroughly and diluted to 100 ml with distilled water. In 100 ml volumetric flask, 5 ml dilute solution was mixed with 50 ml distilled water and neutralized with 1 N HCl. After adding 2 ml of 0.2 % (w/v) iodine solution, the neutralized solution was made up to 100 ml with distilled water and left at 25 ± 2 ^{0}C for 20 min. The absorbance at 630 nm for each sample was read against the blank using a spectrophotometer (Ultrospec 4050, LKB Biochrom, UK). The standard amylose (Sigma Chemical Co, USA) was treated similarly to the starch sample, but used 1 ml of dilute solution instead of 5 ml to develop color. The total amylose content was calculated by Equation 3.1.

$$AE = \left(\frac{R}{A}\right) \times \left(\frac{a}{r}\right) \times 20 \qquad (3.1)$$

where	AE	=	amylose equivalent (%, db)
	R	=	absorbance of sample
	A	=	absorbance of standard amylose
	r	=	weight of sample (mg)
	a	=	weight of standard amylose (mg)

3.2.2.1.2 Soluble amylose

Soluble amylose was determined using the procedure as described by Shanthy *et al*. (1980). Rice starch (100 mg) was dissolved in solution containing 1 ml of ethanol and 50 ml of distilled water, then heated at 98 ^{o}C for 20 min with occasional shaking. The starch solution was cooled to 25 ± 2^{0}C and diluted to 100 ml total volume in a volumetric flask, then filtered through No.4 filter paper. 5 ml of the filtrate was used to develop color using the procedure as described in section 3.2.2.1.1. The soluble amylose content was also calculated using Equation 3.1.

3.2.2.2 Con A method

3.2.2.2.1 Determination of amylose

Amylose content was determined using a commercial assay kit from Megazyme (Ireland) according to the procedure described by Gibson *et al*., (1997). Rice starch of 20-25 mg was dissolved by heating at 100 ^{0}C for 15 min in 1 ml dimethyl sulphoxide (DMSO). Then starch was precipitated with 6 ml ethanol at 4 ^{0}C overnight. Prior to centrifuge at 2000g for 5 min the supernatant was discarded. The starch pellet was drained for 10 min, then recovered by adding 1 ml DMSO and

heated at 100 ^{0}C for 15 min with occasional mixing. The solution was mixed with 2 ml Con A solvent, then diluted to obtain 25 ml total volume in a volumetric flask. This final solution will be referred as Solution I. The mixture of 1 ml solution I and 0.5 ml Con A solution was made in a microfuge tube, allowed to stand for 60 min at 25 ± 2 ^{0}C after mixing, then centrifuged at 20000g for 10 min. To denature Con A, 1 ml supernatant was mixed with 3 ml of 100 mM of sodium acetate buffer and heated in boiling water bath for 5 min. The mixture was equilibrated at 40 ^{0}C for 5 min in water bath, then 0.1 ml of amyloglucosidase/α-amylase solution was added. The mixture was incubated at 40 ^{0}C for 30 min and centrifuged at 2000g for 5 min. The supernatant was mixed with 4 ml glucose oxidase/peroxidase (GOPOD) reagent and incubated at 40 ^{0}C for 20 min. The reagent blank (consisting of 1 ml of sodium acetate buffer and 4 ml of GOPOD reagent) and glucose controls (consisting of 0.1 ml glucose standard solution, 0.9 ml sodium acetate buffer and 4 ml GOPOD reagent were incubated concurrently. The absorbance at 510 nm for each sample and the glucose control were read against the reagent blank.

3.2.2.2.2 Determination of total starch

0.5 ml aliquot of solution I of was mixed with 4 ml of 100 mM of sodium acetate buffer and 0.1 ml amyloglucosidase/α-amylase solution. After incubation at 40 ^{0}C for 10 minutes, 1 ml mixture was mixed with the 4 ml of GOPOD reagent and incubated at 40 ^{0}C for 20 min. The reagent blank and glucose controls were incubated concurrently. The absorbance at 510 nm for each sample and the glucose control were read against the reagent blank.

3.2.2.2.3 Calculation of amylose content

The amylose content was measured as the ratio of glucose derived from the supernatant after treatment with Con A to the glucose derived from the total starch solution as described in Equation 3.2.

$$AM = \left(\frac{S}{T}\right) \times \left(\frac{\beta}{\lambda}\right) \times 100 \qquad (3.2)$$

where AM = amylose content (%)

S = absorbance of Con A supernatant

T = absorbance of total starch aliquot

β = dilution factor for Con A = 6.15

λ = dilution factor for total starch = 9.2

3.3 Structure characterization

Starch structure, namely crystallinity, granule size, short-range molecular order, molecular weight of the prepared rice starches and the commercial rice starches were analysed using these following methods:

3.3.1 Molecular structure

Prior to molecular structure determination, rice starch was defatted by Soxhlet extraction for 24 hours using 85% (v/v) methanol as the solvent. The extracted starch was then dried at 25 ± 2 ^{0}C.

3.3.1.1 Molecular weight of amylose

100 mg defatted starch was dispersed with 1 ml of ethanol and 10 ml of 1 N NaOH (Reddy *et al.*, 1993). The suspension was left at room temperature for 24 hours, then heated in a boiling water bath for 15 min. After cooling, the solution was neutralized with 1 N HCl. To debranch, 2 ml starch solution was treated with 20 μl isoamylase, ultracentrifugally and electrophoretically pure, from *Pseudomonas amylodermosa* (Hayashibara Biochemical Laboratories INC., Japan), dispersed in 1 ml of 30 mM acetate buffer having pH 3.5 and incubated in a water bath at 40 ^{0}C for 24 hours. The enzyme activity was terminated in a boiling water bath for 5 min. The debranched sample was cooled to 25 ± 2 ^{0}C, filtered through a 0.45 μm membrane (PVDF type, Whatman International Ltd., UK) and injected into the sample loop via a Rheodyne injector valve (rheodyne 7125) which was fixed on the column oven. The sample with eluent was pumped through a guard column (TSK GEL PWXL: 6x40 mm) and 5 analytical columns (one TSK GEL G4000 PWXL, two Asahipak GS-320H, one TSK G2500 PWXL, and one TSK G-Oligo PWXL). The eluent at pH 8.6 was composed of 0.1 M Na_2HPO_4, 0.05 M NaH_2PO_4 and 0.02% NaN_3 and filtered through a 0.2 μm nylon membrane and on line degassed online (DG-1200, HPLC Technology Co., UK) prior to entry into the Size Exclusion Chromatography coupled to Multi-angle Laser-Light-Scattering and a Differential Refractometer (SEC-MALLS-RI). The operating temperature was 30 ^{0}C. The pump flow rate was set at 0.5 ml/min. The eluate was detected by two in line detectors which were a MALLS (Wyatt Technology Inc., USA) with a He-Ne laser operating system at 632 nm equipped with 18 detectors at angles ranging from 3.3 to 158 ^{0} and a RI concentration detector (Optilab 903, Wyatt Technology Inc., USA). The refractive index increment value (*dn/dc*) for this solute-solvent system is

0.152 ml/g (Banks et al., 1969). The absolute weight average molecular weight values, M_w, the number average molecular weight, M_n, and polydispersity index (M_w/M_n) value of amylose were calculated using Zimm plot using ASTRA^{TM} software (Wyatt Technology Inc., USA).

3.3.1.2 Amylopectin chain length analysis

The distribution of degrees of polymerisation (DP) of amylopectin branch chain was determined by High Performance Anionic Exchange Chromatography (HPAEC) performed using a Dionex 100 system and equipped with Pulsed Amperometric Detector (PAD) as described by Blennow *et al*. (2000).

150 mg of defatted starch was dispersed in 20 ml of 5 mM sodium acetate, gelatinised in boiling water bath for 6 min, then cooled to 25 ± 2 ^{0}C. To debranch amylopectin, 15 μl isoamylase enzyme was added. The sample was incubated in a water bath at 37 ^{0}C for 4 hours and the enzyme was denatured by heating in a boiling water bath for 2 min. The sample was then cooled to 4 ^{0}C and centrifuged at 6000 rpm for 20 min. The supernatant was diluted five times before injection into the HPAEC system. The conditions for HPAEC system and gradient profile of the solvents are summarised in Table 3.1 and Table 3.2.

Table 3.1 The conditions for HPAEC system

Injection volume	5 – 50 μL
Column	Dionex PA 100
Detection	PAD – Integrated Amperometry
Flow rate	1.0 mL/ min
Solvents	1) 100 mM NaOH 2) 100 mM NaOH and 0.6 M Sodium Acetate

Table 3.2 Gradient profile of the solvents for HPAEC system

Time (min)	100 mM NaOH	100 mM NaOH and 0.6 M sodium acetate
0.00	100.00	0.00
1.00	100.00	0.00
2.00	100.00	0.00
30.00	0.00	100.00
30.10	100.00	0.00
35.00	100.00	0.00

3.3.2 Granule shape, surface features and birefringence

The starch granule shape and surface features were determined using Scanning Electron Microscope, SEM, (JSM-35, Tokyo, Japan) with a magnification of 2000X,while starch birefringence was observed under polarised light using an optical microscope (D-6330, Wild Leitz GmBH, Germany).

3.3.3 Granule size and size distribution

Size and size distribution of starch granules were determined using a Low-Angle Laser Light Scattering, LALLS, (Masterizer S, Malvern Instruments Ltd., UK). Water was used as the dispersant. A polydisperse mode of analysis was adopted for the analysis according to the Mie theory, which assumes particles are perfect spheres, using the Mastersizer S v2.19 software. The refractive index of the starch particle relative to the water was taken as 1.15, starch sample absorbance taken as 0.1 and the refractive index of water as 1.33. A He-Ne laser beam provided light at a wavelength of 630 nm. The 300 RF lens was selected, which encompasses a range of particle sizes within the 0.05 to 880 μm particle size range. A background reading was taken for 100 ml of disstilled water. Approximately 0.5 g starch sample was introduced into the distilled water, contained in small volume sample unit fitted with a stirrer. Sample dispersions were stirred for 5 min to break up any agglomerates, giving an obscuration value of 10-30%, before taking the measurement.

3.3.4 Crystallinity

Crystallinity of the starch granule was determined using the Wide-Angle X-Ray Diffraction (D5005, Seimens AXS, Germany), which the x-ray generator produces monochromatic copper K_α radiation with operating at 40 kV 50 mA and 0.154 nm wavelength. Starch powders were tightly packed into sample holder. The diffraction data were collected over an angular range from 4 to 30 ^{0} (2θ). The x-ray patterns were visually compared with the peak characteristics of theoretical diffractogram given by Zobel (1964). The % crystallinity was calculated as the ratio of area of the crystalline sharp peak over the total area (Figure 3.1) using a computer program based on the methods of Hermans and Weidinger (1948), and Nara *et al*., (1978).

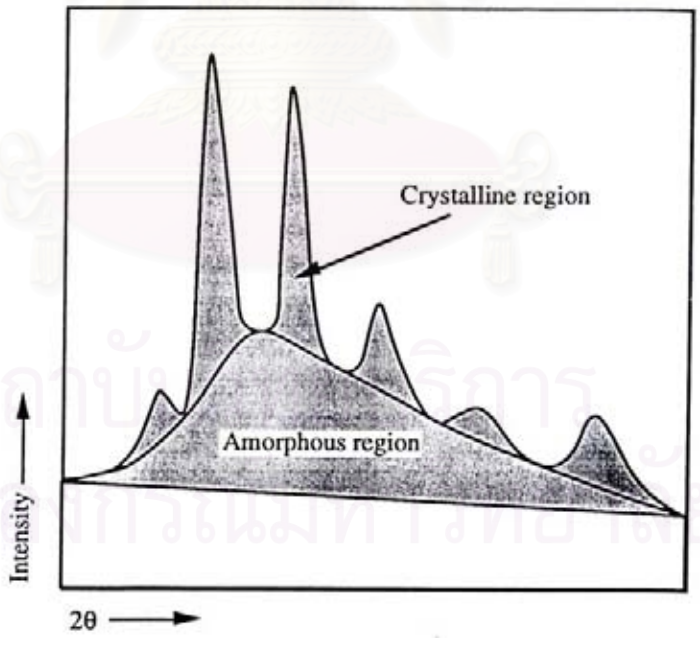

Figure 3.1 Wide angle X-ray scattering curve showing division of scattering areas into amorphous and crystalline regions (Jenkins, 1994).

3.3.5 The ratio of short-range molecular order to amorphous

The initial ratio of short-range order to amorphous (RSA) within the starch granule and the extent to which this was lost upon gelatinisation was obtained from Infrared spectra. The 4% (w/w) native starch dispersion and 4% (w/w) gelatinised starch prepared in the Rapid Visco Analyser (RVA) as described later in section 3.4.1 were used. The samples were poured into the attenuated total reflectance sample cell of the Fourier Transform Infrared (FTIR) spectrometer (IFS-48, Bruker, UK). Absorbance spectra were recorded at $25^{O}C$ at an angle of incidence beam of 45^{0}. The spectra obtained at a resolution of 4 cm^{-1} were averaged from 32 scans, recorded against an empty cell as background, and were subtracted from the spectrum for water. The ratio of absorbance at the wave number of 1047 to that at the wave number of 1022 were obtained from the deconvoluted spectra.

3.4 Functional properties determination

Functional properties of starches, namely pasting and gelatinisation properties, swelling power and solubility, viscosity, viscoelasticity and retrogradation of the prepared rice starches and the commercial rice starches were analysed using these following methods:

3.4.1 Pasting characteristics

The viscosity of rice starch was determined using a Rapid Visco Analyser (RVA series 4, Newport Scientific NSW, Australia). Rice starch of 3.5 g (corrected to the basis of 14% (db) of moisture content) was mixed with 25 g distilled water to give 10.6 % solid content of the mixture. The amount of added water was

adjusted according to the moisture content of starch. After pouring the starch and water into the sample holder, the paddle was inserted and jogged up and down through starch slurry to eliminate lumps. The slurry is initially rapidly stirred with a rotating paddle at 960 rpm for 10 sec to thoroughly disperse the sample in the solvent and then at constant speed of 160 rpm for the rest of the measurement, while being heated using the following temperature-time profile :

- heating at 50 ^{0}C for 1 min
- heating to 95 ^{0}C over a 3 min 42 sec period
- holding at 95 ^{0}C for 2 min 30 sec
- cooling to 50 ^{0}C over a 3 min 48 sec period
- holding at 50 ^{0}C for 2 min.

The parameters; peak, breakdown and setback viscosity, and pasting temperature calculated from viscosity and temperature profile were recorded.

3.4.2 Gelatinisation characteristics

11-13 mg of a slurry of 1: 4 weight ratio of rice starch to water (Lii *et al*., 1995) was hermetically sealed in a pre-weight aluminium pan at 25 ± 2 ^{0}C and reweighed in a microbalance. After sealing the pan and leaving to equilibrate for about 12 hours, the slurry was heated from 10-95 ^{0}C at 10 ^{0}C/min using a Differential Scanning Calorimetry (DSC-7, Perkin Elmer Inc., UK). An empty pan was used as reference. The temperatures of the characteristic transitions, onset (T_0), peak (T_p) and melting (T_m) were recorded and the gelatinization enthalpy (ΔH) of the transition was expressed as (J/g) on a dry weight basis.

3.4.3 Swelling power and water solubility index

The starch paste of 0.7% (w/w) was prepared in the RVA using the rmethod described in section 3.4.1 except for the cooling part which was stopped at 80 ^{0}C and held at this temperature for further 2 min. The hot solution was immediately centrifuged at 1000g for 15 min. The supernatant was removed by suction and the weight of residue was determined using Equation 3.3 (Schoch, 1964 and Eliasson, 1985b). 5 ml of supernatant of was dried at 100 ^{0}C overnight. The weight of residue solid was recorded, then the starch solubility was calculated using Equation 3.4.

$$Q = \frac{R}{W} \quad (3.3)$$

$$WSI = \left(\frac{D}{W}\right) \times 100 \quad (3.4)$$

where Q = swelling power

R = weight of residue (g)

W = dry weight of starch (g)

WSI = water solubility index (%)

D = weight of soluble starch (g)

3.4.4 Intrinsic viscosity

Samples were dispersed in 5 M KOH to obtain a 3% (w/v) concentration. The starch dispersion was heated at 95 ^{0}C for 10 minutes in a water bath. The samples were stirred overnight until a clear solution was visible. The

clear solution was filtered through glass wool using a suction pump. The filtrates were diluted to 5 concentrations ranging between 1 and 4 mg/ml. Measurements were made at 25 ± 0.05 ^{0}C using a 2 ml capacity Ostward type viscometer with an automated measuring unit (Schott Gerate, Germany) which gave a flow time for distilled water of 77.9 sec. For each concentration, 5 flow times of starch solution were recorded after 20 min of temperature equilibrium in the water bath. The relative viscosity was determined from the measured flow times, and the intrinsic viscosity was calculated from the slope of plot using Equation 3.5 (Tanglertpaibul and Rao, 1987), which is an extension of the Einstein's equation.

$$\eta_r = 1 + [\eta]c \qquad (3.5)$$

where η_r = relative viscosity = t / t_0

t = efflux time for starch solution (sec)

t_0 = efflux time for distilled water (sec)

$[\eta]$ = intrinsic viscosity (ml/g)

c = concentration (g/ml)

3.4.5 Viscosity

1-8% (w/w) starch pastes was prepared in the RVA using the method described in section 3.4.2. For samples measured in the rotational viscometer, the cooling cycle was stopped at 80 ^{0}C and held at this temperature for a further 2 min. While it was stopped at 60 ^{0}C during cooling for the RVA measurement. The paddle speed of RVA was maintained at 160 rpm and this corresponds to an average and maximum shear rate of 54 s^{-1} and 145 s^{-1} (Lai et al., 2000).

Viscosity values were determined using a rotational rheometer (VOR, Bohlin Instruments Ltd., UK) and the RVA. For the measurements using the rheometer, starch pastes were removed from RVA at 80 ^{0}C to loaded on coaxial cylinder geometry (C25) preheated to 60 ± 0.1^{0}C. Paraffin oil was used to cover paste surface to prevent moisture loss. The viscosity was determined by increasing the shear rate in the range 50-1000 s^{-1} at 60 ± 0.1^{0}C.

Viscosities were also determined for starch pastes within the RVA. The RVA viscosity values was taken at 60 ^{0}C during cooling.

3.4.6 Viscoelasticity

3.4.6.1 Paste preparation

Two sets of starch pastes, before and after cooling, were prepared as follows:

- the first set :

rice starch pastes of 6–15% (w/w) were prepared in the RVA using methods described in section 3.4.2 with the cooling part of the cycle stopped at 80 ^{0}C and held at this temperature for a further 2 min,

- the second set :

rice starch pastes obtained from the first set were poured immediately into moulds of (40 mm diameter x 5 mm height) for dynamic viscoelastic test and into moulds of (20 mm diameter x 2 mm height) for creep test. After cooling down to 25 ± 2 ^{0}C, the starch pastes were stored at 6 ^{0}C for 12 hours.

3.4.6.2 Dynamic viscoelastic

Dynamic viscoelastic of starch pastes before and after aging at 6 ^{0}C for 12 h. were determined using a rotational rheometer (CVO, Bohlin Instrumrnts Ltd., UK) equipped with cone and plate geometry (CP4/40). The measurement was performed in the linear viscoelastic range at 2% strain (Appendix A) and at frequency range of 0.1-10 Hz. The measurement temperatures were 60 ^{0}C and 25 ^{0}C for starch pastes and starch gels, respectively. The dynamic rheological parameters (storage modulus (G′) loss modulus (G″), complex modulus (G*), complex viscosity (η*) and loss tangent (tan δ) were recorded. Paraffin oil was used to cover paste and gel surface to prevent moisture loss.

3.4.6.3 Creep

Creep of starch pastes after aging at 6 ^{0}C for 12 h. were determined using a rotational CVO rotational rheometer equipped with parallel plate geometry (PP20). The creep test was performed at 25 ^{0}C in linear viscoelastic range at an applied stress of 10 Pa (Appendix A). The compliance was measured for 400 sec during application of the constant stress and a further 400 s after the stress was removed. Paraffin oil was used to cover the gel surface to prevent moisture loss. The curve fitting was performed by the graphical method of Inokuchi (Shama and Sherman, 1966; Sherman, 1966) as described in Appendix B.

3.4.7 Retrogradation

3.4.7.1 Rheology

Starch paste of 30% (w/w) prepared in RVA as described in section 3.4.6.1 was cooled immediately to 25 ^{0}C in CVO rotational rheometer equipped with cone and plate geometry (CP4/40). The measurement was performed in the linear viscoelastic range of 2% strain, frequency of 0.2 Hz and 25 ^{0}C. The dynamic rheological parameters as described in section 3.4.6.3 were recorded at hourly intervals up to 100 hours. Paraffin oil was used to cover paste surface to prevent moisture loss.

3.4.7.2 FT-IR

A starch paste of 20-40 % (w/w) prepared in the RVA as described in section 3.4.6.1 were cooled immediately to 25 ^{0}C into the attenuated total reflectance sample cell of the spectrometer (IFS-48, Bruker, UK). The measurment conditions were similar to that given in section 3.3.4. The spectra were run at hourly interval up to 100 hours. The ratio of absorbance intensities at the wave number 1047 to that at the wave number of 1022 was obtained from the deconvoluted spectra.

3.4.7.3 Wide-Angle X-ray Diffraction

The starch paste of 30 % (w/w) prepared in RVA as described in section 3.4.6.1 was cooled down immediately to 25 ^{0}C, covered and stored at 25 ^{0}C for a designated time of 0, 1, 2, 3, 4, 5 days. The crystallinity of each aged starch was determined using a Wide-Angle X-Ray Diffraction. The measurment conditions were similar to that given in section 3.3.3. The crystallinity index was obtained from the

shift corrected intensity of the peak at 17.2 ^{0} normalized to the intensity at 16 ^{0} using Equation 3.6.

$$CI = \left(\frac{I_{17.2} - I_{16.0}}{I_{16.0}} \right) \quad (3.6)$$

where CI = crystallinity index

$I_{17.2}$ = intensity at 2θ is 17.2

$I_{16.0}$ = Intensity at 2θ is 16.0

The retrogradation rate for all rice starch gels was calculated by Avrami equation as described in section 2.4.3. The relative extent of retrogradation (% retrogradation) for all rice starch gels was calculated using Equation 3.7.

$$\%\ retrograda\ tion = \left(\frac{Y_t - Y_0}{Y_{max} - Y_0} \right) \times 100 \quad (3.7)$$

where Y_t = any physical parameter describing the crystallization process

Y_0 = the initial value (at t = 0) of Y_t

Y_{max} = the plateau value (at t = ∞) of Y_t

3.5 Statistical Analysis

A factorial experiment with completely randomized design was used. Multiple correlation analysis was performed through SPSS program (Version10.0). Coefficient of determination (R^2) was assigned for values ranging from 0 to 1. The significant level was established as 99% ($P < 0.01$).

CHAPTER IV

RESULTS AND DISCUSSIONS

4.1 Composition and structure of rice starch

4.1.1 Amylose content and minor compositions

Table 4.1 shows that both protein and fat content in rice starches used in this study were less than 0.8%. The amount of protein and fat for both commercial rice starches were lower than the values obtained from the prepared rice starches due to the differences in the extraction process. The difference in rice varieties and rice ageing did not significant affect the protein and fat content of these rice starches. Due to the small amount of protein and fat presented in this rice starches as well as the small difference in these contents among the samples, the effect of these two components on the functional properties of these starches was considered negligible (Swinkels, 1985).

Table 4.1 Fat, protein and moisture contents in Thai rice starches

Starch source	Fat content* (%)	Protein content* (%)	Moisture content* (%)
1. RD6 rice			
- 0 month	0.66 ± 0.10	0.64 ± 0.00	8.20 ± 0.06
- 5 months	0.74 ± 0.07	0.77 ± 0.05	9.91 ± 0.08
2. Commercial waxy rice starch	0.35 ± 0.18	0.38 ± 0.01	9.76 ± 0.07
3. Jasmine rice			
- 0 month	0.67 ± 0.14	0.70 ± 0.01	6.85 ± 0.00
- 5 months	0.74 ± 0.12	0.78 ± 0.05	9.09 ± 0.16
4. Commercial rice starch	0.41 ± 0.07	0.56 ± 0.03	9.46 ± 0.07
5. Supanburi 1 rice			
- 0 month	0.67 ± 0.07	0.79 ± 0.05	6.74 ± 0.28
- 5 months	0.55 ± 0.16	0.78 ± 0.02	8.76 ± 0.23

* the dry basis values obtained from means of duplicates ± SD

Amylose and amylopectin are the main component of starch, affecting the physical properties of starch such as gelatinization, retrogradation, viscosity and viscoelasticity. It is common to determine the amylose content and infer amylopectin content by difference. In this study, true amylose content in rice starch was determined by the Con A method, which will not be influenced by amylopectin fine structure. Amylose equivalent (AE), commonly refers to the total amylose, and water-soluble amylose (AM) were determined by interaction with iodine. The difference between AE and AM was due to the binding of iodine to the long-B chains amylopectin, therefore represents the to amylose equivalent of the exterior long-B chains in amylopectin, AE_{LBCA}, (Reddy *et al.*, 1993). This AE_{LBCA} commonly

referred as water insoluble amylose (Bhattacharya *et al*., 1982; and Reddy *et al*., 1993). AM agreed well with true amylose. According to AM reported in Table 4.2, Thai rice starches were classified into 3 classes: low amylose content of 1-3% (RD6 and commercial waxy rice starch), medium amylose content of 14-15% (Jasmine rice starch), and high amylose content of 21-23% (Supanburi 1 and commercial rice starches). The results also indicated that aging of rice up to 5 months did not affect the amylose content.

Figure 4.1 shows that both AE and AE_{LBCA} increased exponentially with increasing AM ($R^2 = 0.99$, $p < 0.01$). This indicates that the higher the AM, the higher the exterior long-B chain amylopectin content. In contrast, both AE and AE_{LBCA} did not relate to AM for Indian rice having medium amylose content of AM of 9.4-18.2%(Bhattacharya *et al*., 1982; Sandhya Rani and Bhattacharya, 1985; Reddy *et al*., 1994; and Ramesh *et al*., 1999). Moreover for these Indian rice and rice flour paste, AE_{LBCA} had strong relationship to texture and other physicochemical parameters such as alkali score, starch-iodine blue value, and equilibrium moisture content on soaking in water, while AM did not (Bhattacharya *et al.*, 1972 and 1982; Sombhagya *et al*., 1987; Reddy *et al*., 1993 and 1994). However to consider in the broader range of amylose content (2-23% of AM), the data for Thai rice starch and Indian rice were combined and plotted in Figure 4.2. It shows that both AE and AE_{LBCA} trended to increase exponentially with increasing AM ($R^2 = 0.41$, $p < 0.01$). Since AM is one of the main components of starch and its absolute value can be determined directly, therefore in this study, AM will be used as the key parameter to relate the functional properties of rice starches instead of AE_{LBCA}.

Table 4.2 Amylose content of Thai rice starches

Starch source	Amylose content* (%, db)			
		Iodine method		
	Con A method	AE[a]	AM[b]	AE_{LBCA}[c]
1. RD6 rice				
- 0 month	2.08 ± 0.22	8.40 ± 0.27	2.56 ± 0.03	5.84 ± 0.22
- 5 months	1.70 ± 0.08	8.18 ± 0.33	2.21 ± 0.08	5.97 ± 0.03
2. Commercial waxy rice starch	2.39 ± 0.25	10.09 ± 0.23	3.78 ± 0.07	6.31 ± 0.12
3. Jasmine rice				
- 0 month	15.14 ± 0.21	25.62 ± 0.27	15.12 ± 0.13	10.50 ± 0.33
- 5 months	14.80 ± 0.02	26.29 ± 0.13	15.52 ± 0.05	10.77 ± 0.13
4. Commercial rice	21.21 ± 0.19	39.48 ± 0.20	21.97 ± 0.27	17.51 ± 0.18
5. Supanburi 1 rice				
- 0 month	22.43 ± 0.15	40.73 ± 0.33	23.08 ± 0.04	17.65 ± 0.34
- 5 months	22.70 ± 0.24	40.91 ± 0.20	22.65 ± 0.04	18.26 ± 0.28

* the values obtained from mean of triplicate ± SD

[a] amylose equivalent

[b] water-soluble amylose

[c] amylose equivalent of long-B chain amylopectin

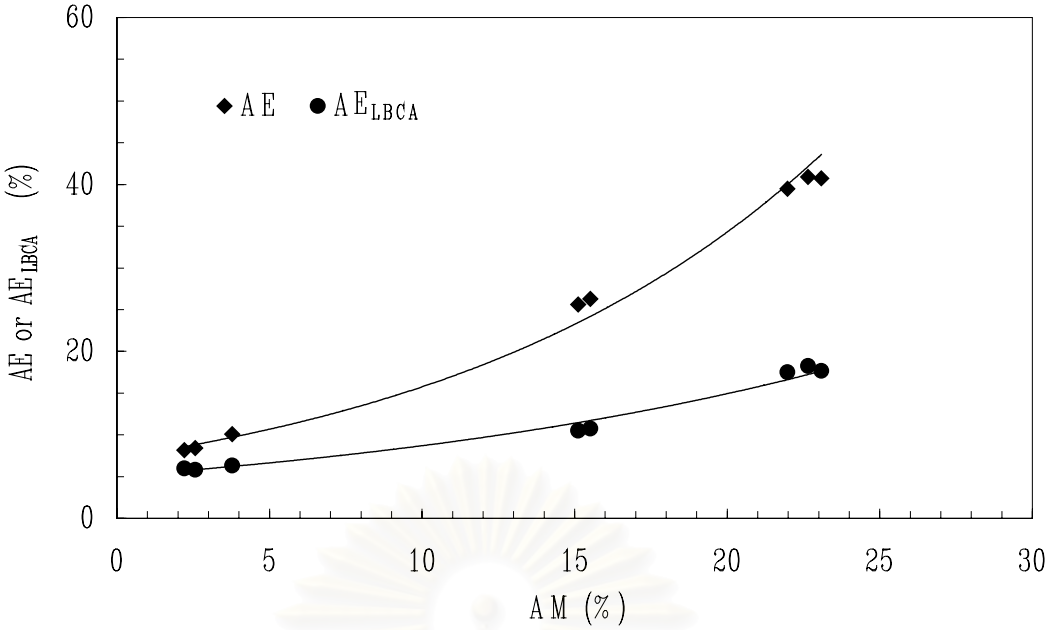

Figure 4.1 Relationship of both amylose equivalent (AE) and amylose equivalent of long-B chain amylopectin (AE_{LBCA}) to water-soluble amylose (AM) for Thai rice starches.

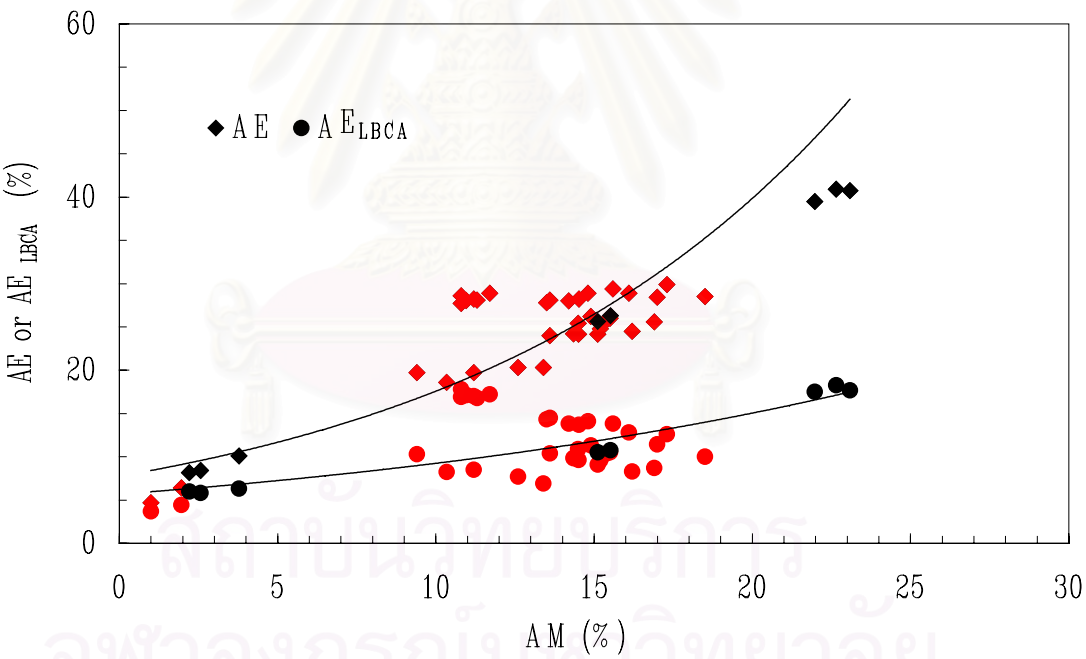

Figure 4.2 Relationship of both amylose equivalent (AE) and amylose equivalent of long-B chain amylopectin (AE_{LBCA}) to water soluble amylose (AM) for Thai rice starches (black symbol) and Indian rice (red symbol). Data for Indian rice were obtained from Bhattacharya *et al.*, 1982, Sandhya Rani and Bhattacharya, 1985, Reddy *et al.*, 1994, and Ramesh *et al.*, 1999.

4.1.2 Average molecular weight of amylose

The weight average molecular weight of AM was determined since it is one of the most fundamental parameters characterizing starch. It influences the functional properties such as viscosity, gelatinization, and also pasting properties of starch (Ong, 1994; Juliano *et al*., 1987; and Hizukuri, 1996).

Table 4.3 shows that the weight average molecular weight ($\bar{M}_w$) and the number average molecular weight ($\bar{M}_n$) of amylose obtained from isoamylase debranched rice starches had the same magnitude order of 10^5. However, the high amylose rice starches gave higher average molecular weights. Figure 4.3 shows that the average molecular weight of low amylose rice starch (< 3% of AM) can not be determined since the concentration of AM was lower than the limit of the instrument. In comparison to the other debranched rice starches, 6-15 % of AM (Ramesh *et al*., 1999; and Tongdang, 2001), the $\bar{M}_w/\ \bar{M}_n$ obtained, 1.2 - 1.4, were within the same range. However, the $\bar{M}_w$ ($3.6 – 5.2 \times 10^5$) and $\bar{M}_n$ ($2.6 – 3.8 \times 10^5$) of rice AM from these previous studied were about 3 times higher than those used in our work. In comparison to undebranched starches with pre-seperation of AM and amylopectin ,AP, (Takeda and Hizukuri, 1986; Takeda *et al*., 1989; and Hizukuri *et al*., 1989), the $\bar{M}_w$ ($4.4 – 5.6 \times 10^5$) are also about 3 times higher than those of our study, although the $\bar{M}_n$ ($1.5 – 1.8 \times 10^5$) are within the same range. The polydispersity indices from these studied (2.6 – 3.7) were also therefore higher values. These differences may suggest that the measurement of branched and linear AM obtained from undebranched starch with pre-separation of AM and AP may increase the polydispersity index.

Since the polydispersity index of amylose was similar between rice varieties, it can be assumed that the relationship of this parameter to functional properties of rice starches was negligible. On the other hand, the average molecular weight of amylose was apparently difference between rice varieties, and this may be one of the factors causing differences in functional properties.

Table 4.3 Average molecular weight of amylose for Thai rice starches

Starch source	Amylose Content (%)	$\bar{M}_w$[b] ($x10^5$)	$\bar{M}_n$[b] ($x10^5$)	($\bar{M}_w/\bar{M}_n$)[b]
1. RD6 rice starch[a]	2.08	NA	NA	NA
2 Jasmine rice starch[a]	15.14	1.8 ± 0.5	1.3 ± 0.3	1.4 ± 0.5
3. Commercial rice starch	21.21	2.8 ± 0.5	2.3 ± 0.4	1.2 ± 0.3
4. Supanburi 1 rice starch[a]	22.43	2.9 ± 0.2	2.4 ± 0.2	1.2 ± 0.4

[a] starches derived from unaged rice

[b] the values obtained from means of triplicates ± SD.

NA: not available

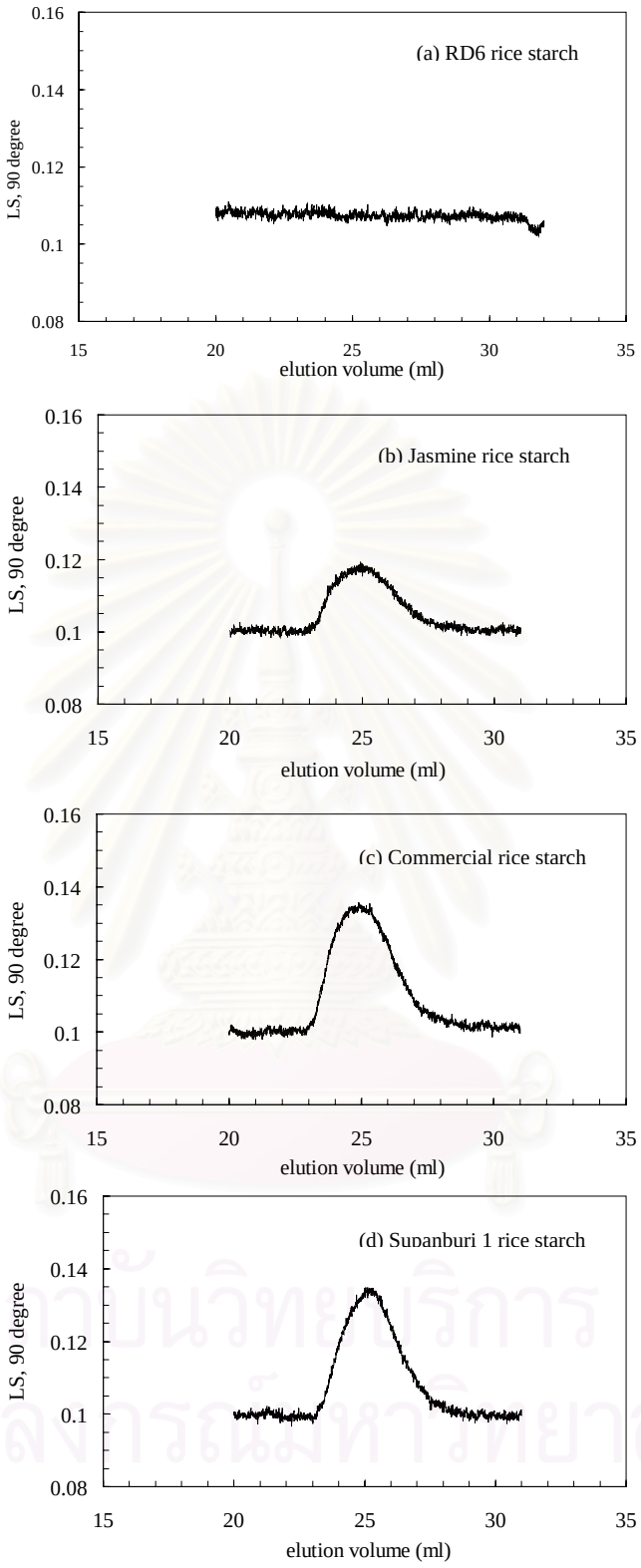

Figure 4.3 Amylose profiles of debranched rice starches obtained from Multi-angle Laser-Light-Scattering and Differential Refractometer (SEC-MALLS-RI). These starches (RD6, Jasmine and Supanburi 1) derived from unaged rice. The results shows the relative magnitude of the light scattering signal at an angle of 90^{0}.

4.1.3 Amylopectin chain length distribution

The amylopectin chain length distribution was dertermined since it is an important influences on functional properties such as texture of rice, gelatinization, retrogradation and pasting properties of starch (Juliano *et al*., 1987; Ong, 1994; Lu *et al*., 1997; and Jane *et al*., 1999).

The amylopectin fraction was assessed from HPAEC-PAD chromatograms as shown in Figure 4.4. This Figure shows that the amylopectin fraction was eluted over a broad range and was composed of multiple unresolved peaks, which indicates a high degree of branching with the branch having chain lengths that varied with the different rice varieties. The distribution profiles of amylopectin chain length of different rice starches (Figure 4.5) clearly shows that high amylose rice starches had fewer chains of $\bar{D}P_n$ 3-10 than low amylose and medium amylose rice starch, but the former contained more chains of DP_n 11-22 than the latter. However, there is no significant difference in long-chains of $\bar{D}P_n$ 23-40 among these starches. The area ratio under the curve for the chains of $\bar{D}P_n \leq 11$ to the chains of $\bar{D}P_n \leq 24$, which was referred as amylopectin chain ratio (ACR) was calculated and is shown in Table 4.4. The value of ACR was used to characterize the amylopectin fine structure of rice starches (Nakamura *et al*., 2002). These four Thai rice starches can be classified into two groups according to their ACR values as following:

- S-type amylopectin group having ACR value of 0.25: low amylose and medium amylose rice starch,
- L-type amylopectin group having ACR value of 0.19: high amylose rice starch

The results of this study and those reported by Nakamura *et al*. (2002) indicated that the structural character of starches from various rice varieties can be differentiated by the ACR value together with the amylose content. Therefore, the ACR value will be used to assess the functional properties of these Thai rice starches along with the amylose content.

This distribution curves of $\bar{D}P_n$ of amylopectin branch chain have shoulder around $\bar{D}P_n$ 18-21 for rice starches with low and medium amyloes content. According to Jane et al. (1999), this might indicate that these rice starches had high proportion of short chain ($\bar{D}P_n$ ~ 3-10) in the crystallite.

Table 4.4 Chain length distribution of amylopectin components for debranched rice starches

Starch source	Amylose content (%)	Area (%) for $\bar{D}P_n$			ACR	AP type
		3 - 11	12 - 24	25 - 40		
1. RD6 rice starch*	2.08	21.21	64.58	13.70	0.25	S
2. Jasmine rice starch*	15.14	21.38	64.18	11.44	0.25	S
3. Commercial rice starch	21.21	16.63	71.42	11.95	0.19	L
4. Supanburi 1rice starch*	22.43	16.38	72.01	11.61	0.19	L

* starches derived from unaged rice

ACR: area ratio under curve for the chains of $DP_n \leq 11$ to $DP_n \leq 24$

AP: amylopectin

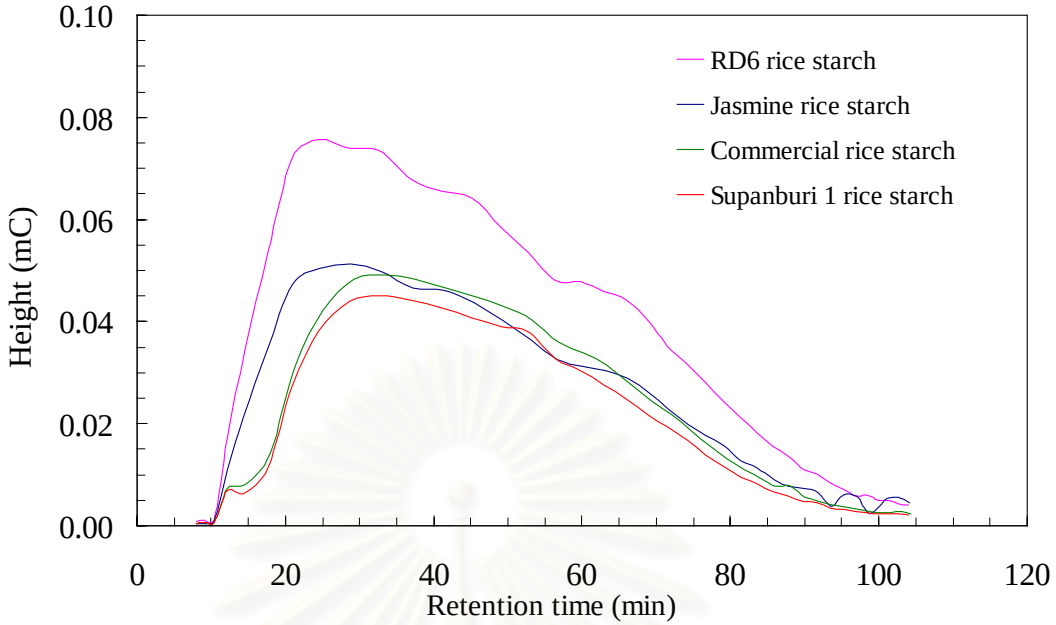

Figure 4.4 Chromatograms of amylopectin chain length distribution for debranched rice starches. These starches (RD6, Jasmine, and Supanburi 1) derived from unaged rice.

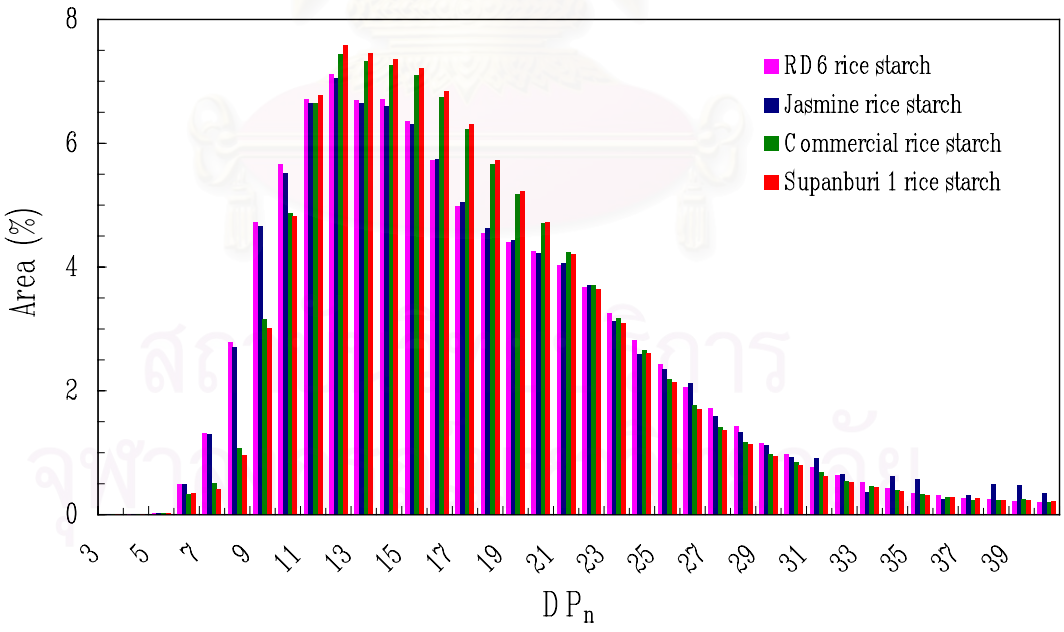

Figure 4.5 Distribution curve of $\bar{D}P_n$ of amylopectin chain length for debranched rice starches. These starches (RD6, Jasmine, and Supanburi 1) were derived from unaged rice.

4.1.4 Starch granule shape, size and size distribution

The polarised light microscope pictures (Figure 4.6) shows birefringence indicating that starch was not gelatinized during the extraction process (Thomas and Atwell, 1999). The SEM shows that Thai rice starches had common rice starch granule features of small, angular polyhedral shape (Figure 4.7). The large clusters of granules were found in the commercial waxy rice starch which may be caused by the steeping and/or drying condition used in manufacture (Fitt and Snyder, 1984). The granular surface of these Thai rice starches were rather smooth without other components. From these two optical techniques, there was no significant differences between these rice starches. Only starch from Jasmine rice of 5 months aging had some broken granules (Figure 4.7 d). This broken structure will affect its properties as will be seen in section 4.1.5, 4.2.2 and 4.2.3. Using the LALLS particle size analyser, the granule size and size distribution of these rice starches in Propan-2-ol (IPA) and water was determined. The granule size mean diameter of these Thai rice starches showed a common size of rice starch of 4 – 6 μm (Table 4.5). Figure 4.8 shows that these Thai rice starches showed the same pattern of bimodal distribution of size. The first group had a diameter range between 0.05 to 1.69 μm with the mean between 0.94 to 1.39 μm, and the second group had a diameter range between 1.69 to 17.61 μm with the mean between 5.45 to 6.63 μm. The area ratio of the first and the second group is between 0.21 to 0.37. For commercial waxy rice starch, the first distribution peak did not completely separate from the second one. It is due to the aggregation of the granules, which is consistent with the result obtained from SEM. Except starch from Jasmine of 5 months aging, there was no significant difference in granule size determined in both IPA and water indicating no damage of granules. In contrast, starch from Jasmine of 5 months aging swelled substantially in water that it

showed a greater ($P<0.01$) granules size mean diameter compared with the unaged Jasmine rice. This was due to water absorption of damaged starch granules.

Table 4.5 Granule size mean diameter for Thai rice starches

Starch source	Granule size mean diameter* (μm) determined in different dispersants	
	Propan-2-ol (IPA)	Water
1. RD6 rice		
- 0 month	5.17 ± 0.07	4.95 ± 0.01
- 5 months	5.38 ± 0.03	5.29 ± 0.03
2. Commercial waxy rice starch	4.16 ± 0.03	4.25 ± 0.04
3. Jasmine rice		
- 0 month	4.67 ± 0.09	4.55 ± 0.05
- 5 months	4.86 ± 0.06	5.80 ± 0.01
4. Commercial rice starch	5.12 ± 0.02	4.94 ± 0.08
5. Supanburi 1 rice		
- 0 month	5.72 ± 0.03	5.85 ± 0.05
- 5 months	5.83 ± 0.02	6.11 ± 0.06

* the values obtained from means of triplicates ± SD

Table 4.6 Diameter of starch granules and area ratio of the small granule group to the larger granule group determined in propan-2-ol (IPA)

Starch source	First group of size distribution		Second group of size distribution		Area ratio of the first and second group* (%)
	Granule size diameter range (μm)	Granule size mean diameter* (μm)	Granule size diameter range (μm)	Granule size mean diameter* (μm)	
1. RD6 rice					
- 0 month	0.05 to 1.69	0.94 ± 0.00	1.69 to 14.49	5.45 ± 0.00	0.37 ± 0.02
- 5 months	0.05 to 1.69	0.94 ± 0.00	1.69 to 14.49	5.45 ± 0.00	0.37 ± 0.01
2. Commercial waxy rice starch	0.05 to 1.69	1.39 ± 0.00	1.69 to 11.91	5.45 ± 0.00	0.28 ± 0.03
3. Jasmine rice					
- 0 month	0.05 to 1.69	1.14 ± 0.00	1.69 to 14.49	5.45 ± 0.00	0.34 ± 0.01
- 5 months	0.05 to 1.69	1.26 ± 0.17	1.69 to 14.49	5.45 ± 0.00	0.32 ± 0.03
4. Commercial rice starch	0.05 to 1.69	0.86 ± 0.12	1.69 to 14.49	5.45 ± 0.00	0.35 ± 0.01
5. Supanburi 1 rice					
- 0 month	0.05 to 1.69	1.04 ± 0.14	1.69 to 17.61	6.63 ± 0.00	0.22 ± 0.03
- 5 months	0.05 to 1.69	1.27 ± 0.18	1.69 to 17.61	6.63 ± 0.00	0.21 ± 0.02

* the values obtained from means of triplicates ± SD

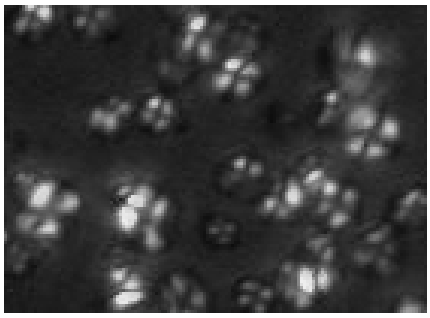

(a) unaged RD6 rice

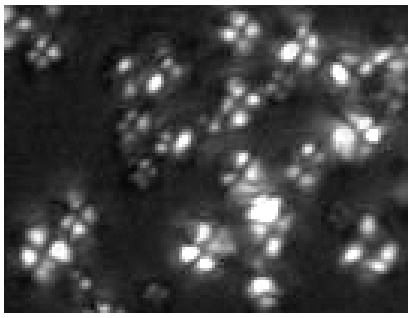

(b) 5 months aged RD6 rice

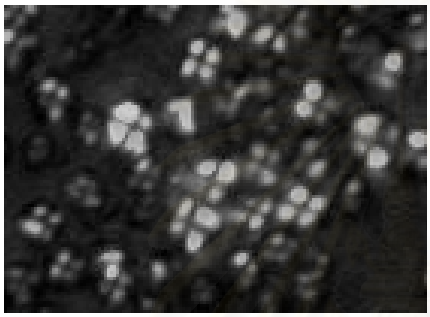

(c) unaged Jasmine rice

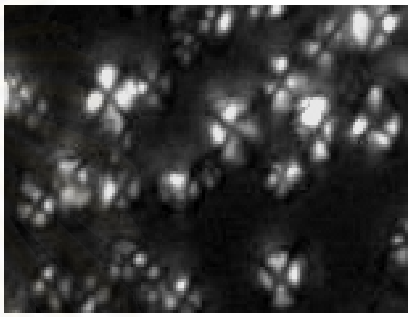

(d) 5 months aged Jasmine

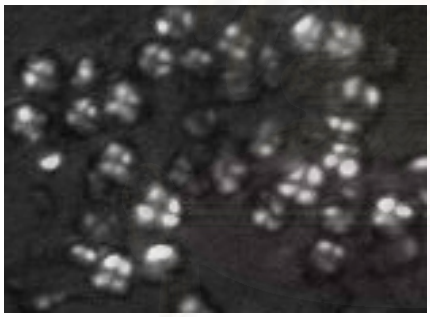

(e) unaged Supanburi 1 rice

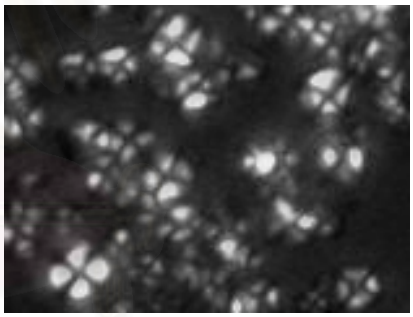

(f) 5 months aged Supanburi 1 rice

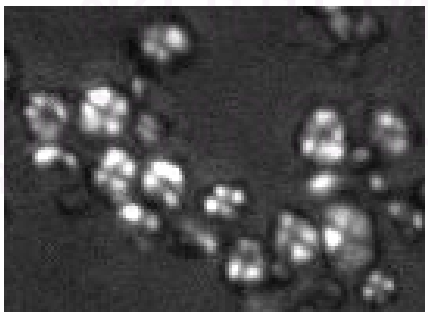

(g) commercial rice starch

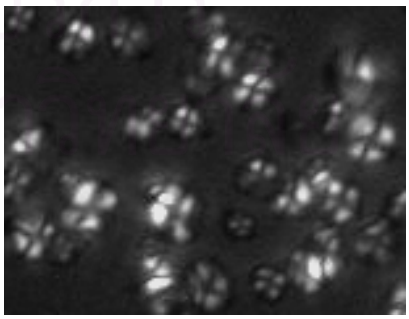

(h) commercial rice starch

Figure 4.6 Polarised light micrographs of rice starch granules.

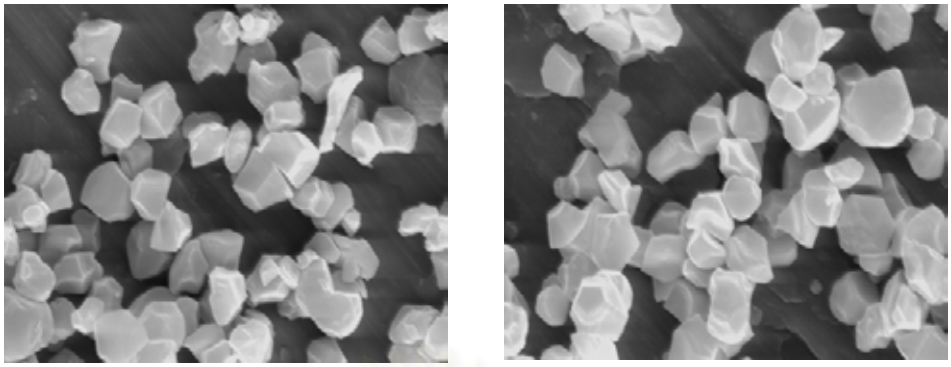

(a) unaged RD6 rice (b) 5 months aged RD6 rice

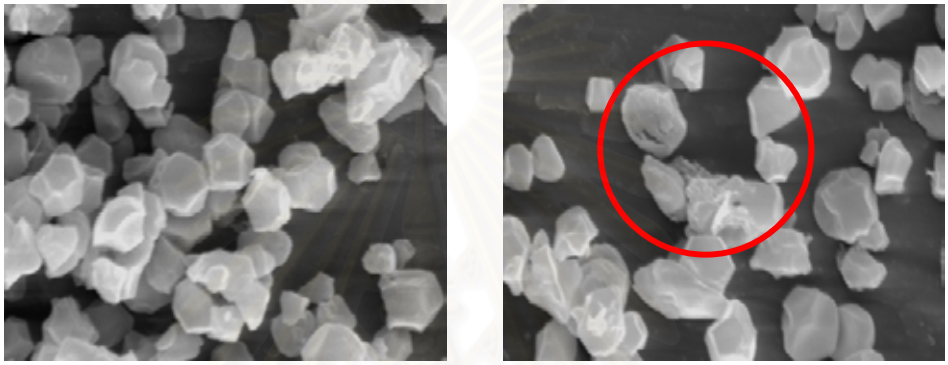

(c) unaged Jasmine rice (d) 5 months aged Jasmine

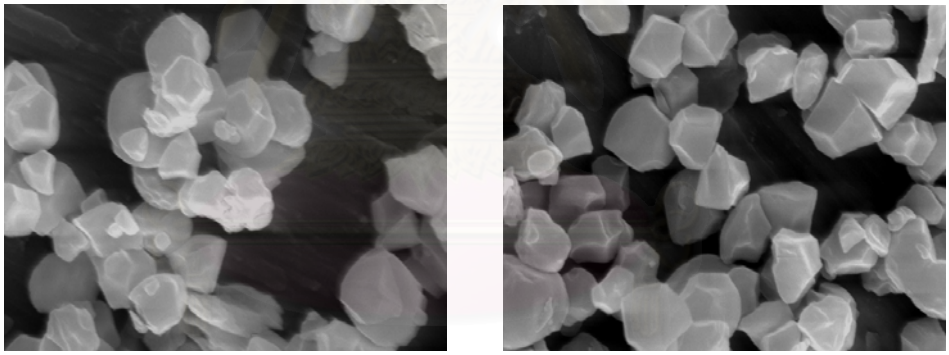

(e) unaged Supanburi 1 rice (f) 5 months aged Supanburi 1 rice

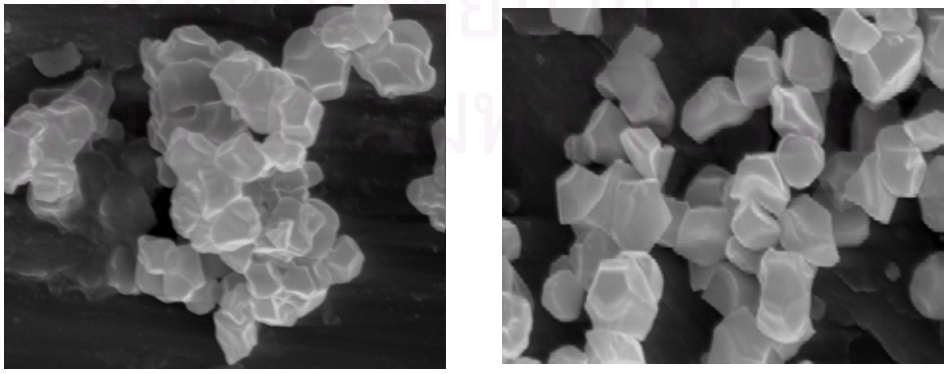

(g) commercial waxy rice starch (h) commercial rice starch

Figure 4.7 SEM micrographs (X2000) of rice starch granules. The granule in circled shows the some granule damage.

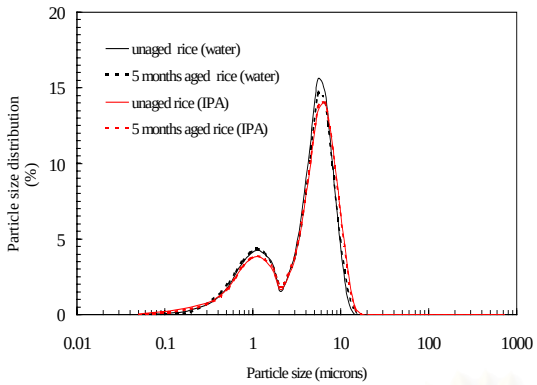

(a) RD6 rice starch

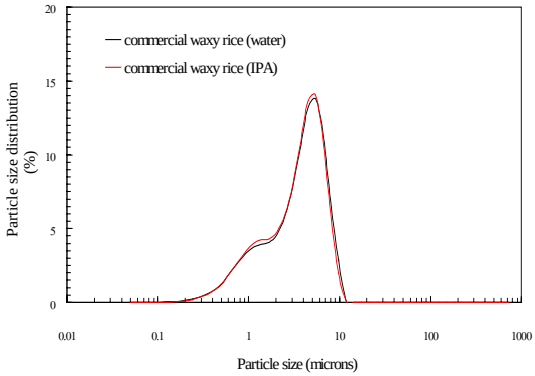

(b) commercial waxy rice starch

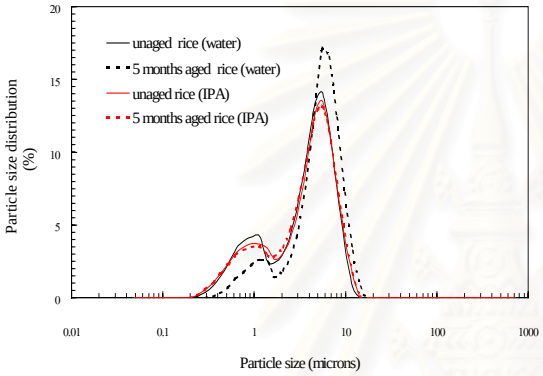

(c) Jasmine rice starch

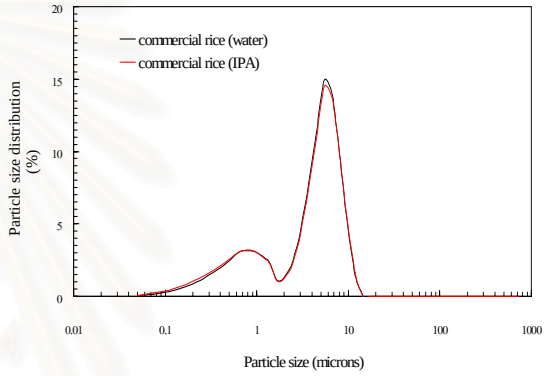

(d) commercial rice starch

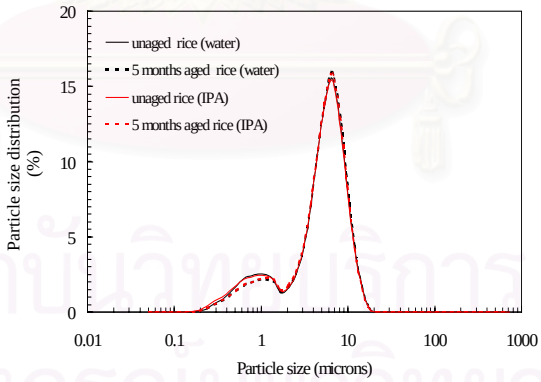

(e) Supanburi 1 rice starch

Figure 4.8 Particle size distribution of rice starch granules determined in propan-2-ol (IPA) and water.

4.1.5 Crystallinity and the ratio of short-range molecular order to amorphour region

Wide angle X-ray diffractograms show that all starches used in this study have an A-type crystallinity with unresolved peaks at ca. 17 and 18^0 2θ and two individual peaks at ca. 15 and 23 ^{0} 2θ (Figure 4.9). The calculated % crystallinity decreased linearly ($R^2 = 0.85$, $p < 0.01$) with increasing amylose content of rice starch (Figure 4.11). From FTIR specta (Figure 4.10), the ratio of short range molecular order to amorphous (RSA) was calculated from the ratio of relative absorbance of the wave number at 1047 to that of 1022 cm^{-1}. Figure 4.11 showed that the ratio of short-range molecular to amorphous decreased linearly with increasing amylose content of rice starches ($R^2 = 0.96$, $p < 0.01$). An increasing in % crystallinity and ratio of short-range molecular order to amorphous with amylopectin content was also expected, because it is recognized that crystallinity in native starches occurs in the amylopectin component. For native starches the major amount of helical order will exist within these crystalline amylopectin regions. Correlations between the ratio of short-range molecular order to amorphous and the % crystallinity have been previously reported by van Soest (1995).

The results from this also indicated that there is no significant difference in % crystallinity and the ratio of short-range molecular to amorphous due to aging of rice up to 5 months (Table 4.7). However the difference in crystallinity and the ratio of short-range molecular to amorphous of Jasmine rice starch obtained from fresh rice and 5 months aged rice may be due to the damaged of granules (as observed by SEM and LALLS in section 4.1.4) during extraction rather than an aging effect.

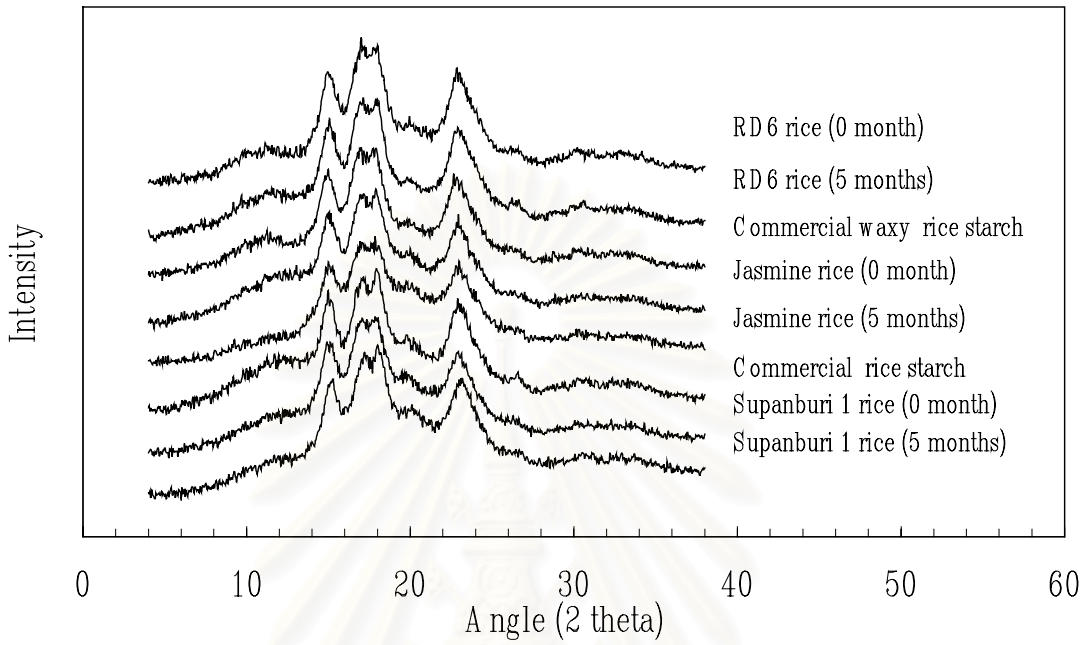

Figure 4.9 The crystalline patterns of Thai rice starches

Table 4.7 Crystallinity and the ratio of short-range molecular order to amorphous region for Thai rice starches

Starch source	Amylose content (%)	Crystallinity* (%)	RSA* (I1047/I1022)
1. RD6 rice			
- 0 month	2.08	34.62 ± 0.18	0.91 ± 0.04
- 5 months	1.70	34.44 ± 0.06	0.89 ± 0.03
2. Commercial waxy rice starch	2.39	33.58 ± 0.76	0.86 ± 0.03
3. Jasmine rice			
- 0 month	15.14	25.70 ± 0.10	0.81 ± 0.03
- 5 months	14.80	22.27 ± 0.45	0.75 ± 0.01
4. Commercial rice starch	21.21	28.94 ± 0.60	0.74 ± 0.02
5. Supanburi 1 rice			
- 0 month	22.43	23.00 ± 0.10	0.72 ± 0.05
- 5 months	22.70	24.50 ± 0.30	0.73 ± 0.04

* the values obtained from the means of triplicates ± SD

RSA: the ratio of short-range molecular order to amorphous region

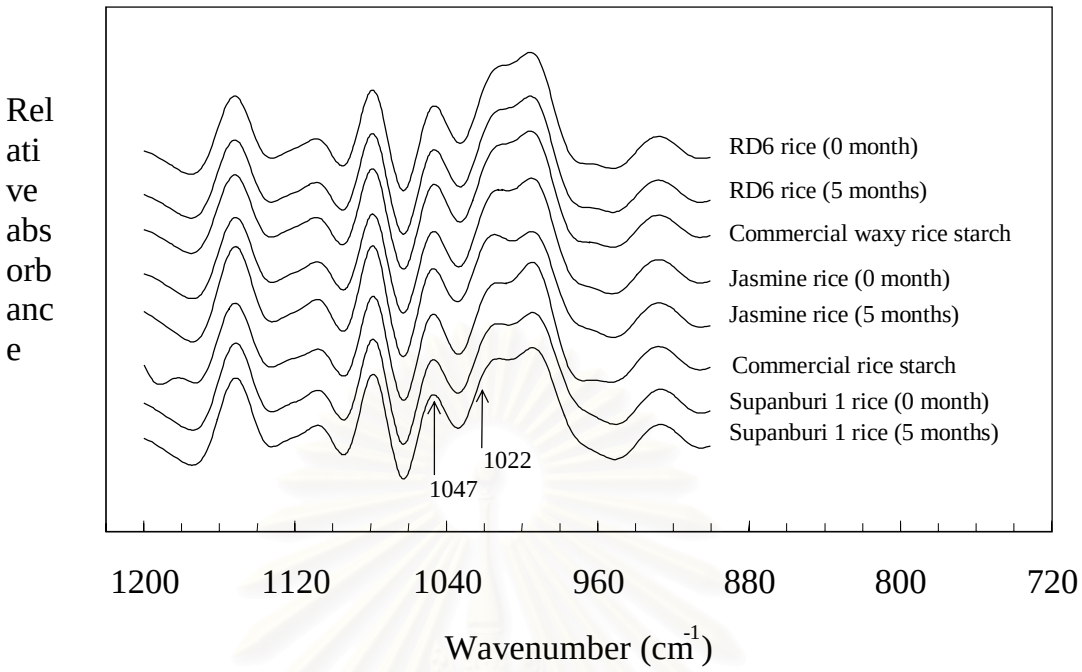

Figure 4.10 Deconvoluted and normalized FTIR spectra for Thai rice starches.

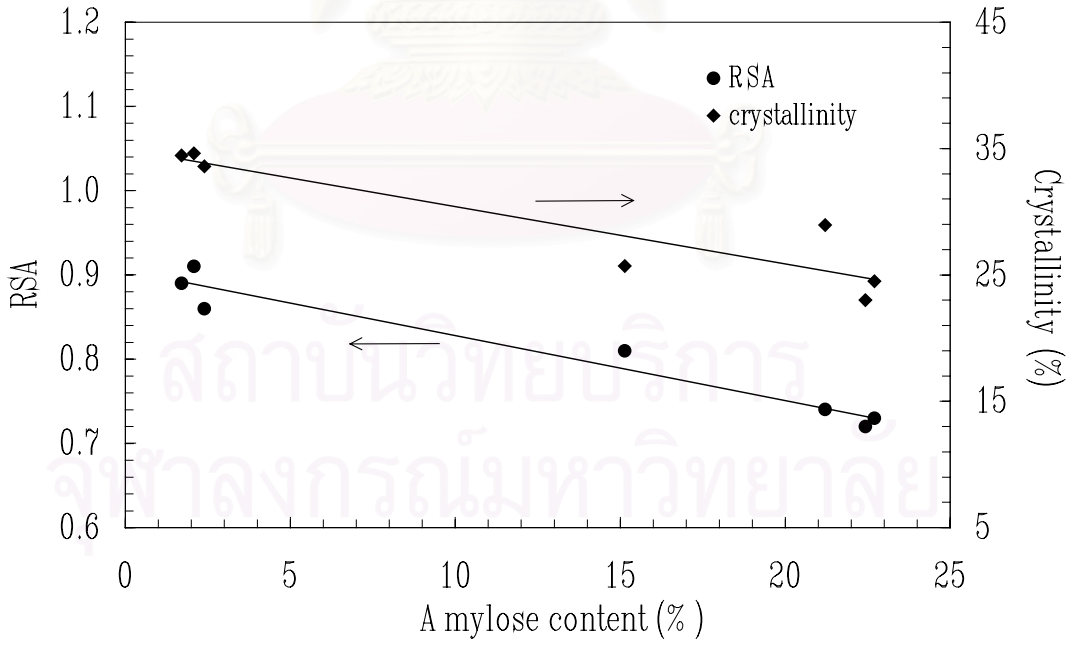

Figure 4.11 Relationship of the ratio of short-range molecular order to amorphous, RSA, and crystalllinity to amylose content for starches derived from unaged rice and 5 months aged rice, and from commercial waxy and commercial rice starch.

The relationship between the determined chemical composition (amylose content) and structural properties (average molecular of amylose, amylopectin chain length distribution, granule shape, size and size distribution, crystallinity and short-range molecular order) to the functional properties of rice starches was then investigated. These results will be discussed in section 4.2.

4.2 Functional properties of rice starches

In many applications, starches will be used generally in the gelatinised form obtained by heating starch in excess water. A combination of heat and water, however, causes starch granules to undergo unique and irreversible changes, the most dramatic of which are the disruption of the crystalline structure and granule swelling. These changes are governed by the chemical composition and structural properties, which affect directly the pasting behavior and rheological properties of starches. This will be discussed in this section.

4.2.1 Swelling power and water solubility index

As expected, low amylose RD6 and commercial waxy rice starches had the highest values of both swelling power (33.54 – 34.92) but the lowest values of water solubility index (6.00 – 8.50%) compared with medium amylose and high amylose rice starches. Figure 4.12 shows that the swelling power of these rice starches decreased linearly with increasing amylose content of rice starch (Equation 4.1, $R^2 = 0.97$, $p \leq 0.01$), while the water solubility index showed an inverse trend (Equation 4.2, $R^2 = 0.94$, $p \leq 0.01$).

$$Q = 36.30 - 0.94\,AM \quad (4.1)$$

$$WSI\ (\%) = 4.70 + 0.85AM \quad (4.2)$$

The swelling of these granules was due to the breaking of hydrogen bonds in the crystalline structure and the linkage of water molecules to the exposed hydroxyl groups of amylose and amylopectin (Hoover, 2001). The high leaches of amylose in

rice starches gives a strong interaction between starch chains within the granules (Sandhya Rani and Bhattacharya, 1989; Li and Yhe, 2001). This causes a decrease in the hydrogen bonding interaction between water molecules and the exposed hydroxyl groups of starch molecules inducing a low swelling of starch granules. However, a high amylose content in rice starch gives a high leaching out of amylose molecule into the continuous phase resulting in a high water soluble index. The results from this study also indicated that aging of rice up to 5 months did not affect either the swelling power or the water solubility index.

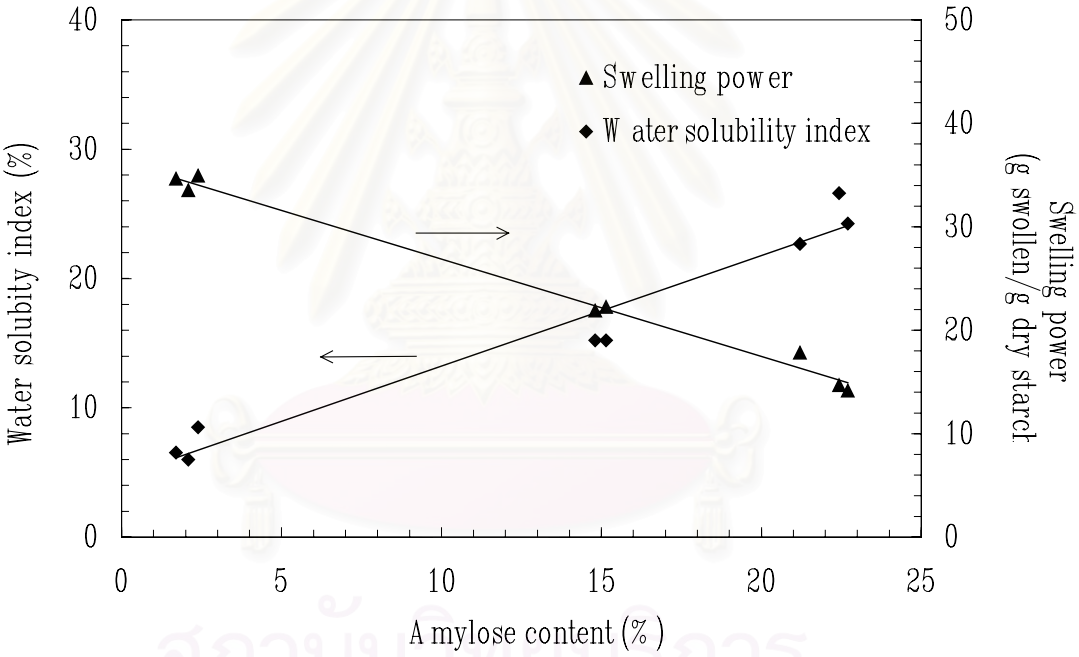

Figure 4.12 Relationship of water solubility index and swelling power to amylose content for starches derived from unaged rice and 5 months aged rice (RD6, Jasmine and Supanburi 1), and from commercial waxy rice and commercial rice starch. The values are obtained from mean of triplicate with a standard deviation in the range of 0.51-1.78.

4.2.2 Gelatinisation behaviour

Gelatinisation behavior of rice starches in excess water was measured by DSC. It was found that all rice starches gave the typical endotherm enthalpy peak showing a melting transition of the crystalline region of starch (Figure 4.13). The gelatinization parameters for these rice starches: onset temperature (T_0), peak temperature (T_p), end temperature (T_e) and enthalpy of gelatinization (ΔH) are shown in Table 4.8. These rice starches could be classified into two groups according to T_0 values, as follows

- low amylose and medium amylose rice starches having T_0 of 61-63 ^{0}C, and
- high amylose rice starches having T_0 of 72-73 ^{0}C.

This difference in T_0 values for these rice starches were influenced by the ACR values not by the amylose content. It was found that the T_0 values of L type amylopectin, high amylose rice starches, were markedly higher than those of S-type amylopectin, low amylose and medium amylose rice starch. These can be explained by the amylopectin structure having more long chains ($\bar{D}P_n$ 12-24), which are involved in more than one cluster, and may have less tendency to be dispersed because of entanglement with other amylopectin molecules (Han and Hamaker, 2001). Table 4.8 shows that there is no significant difference of ΔH among these rice starches, where the values are in the range of 11.52 - 14.48 (J/g).

The results from this study also indicated that aging of rice up to 5 months did not affect either the gelatinisation temperature or ΔH. However, the difference in ΔH of Jasmine rice starch derived from fresh rice and 5 months aged rice

may be due to the damage to the starch granules (as observed by SEM and LALLS in section 4.1.4) during extraction rather than an aging effect.

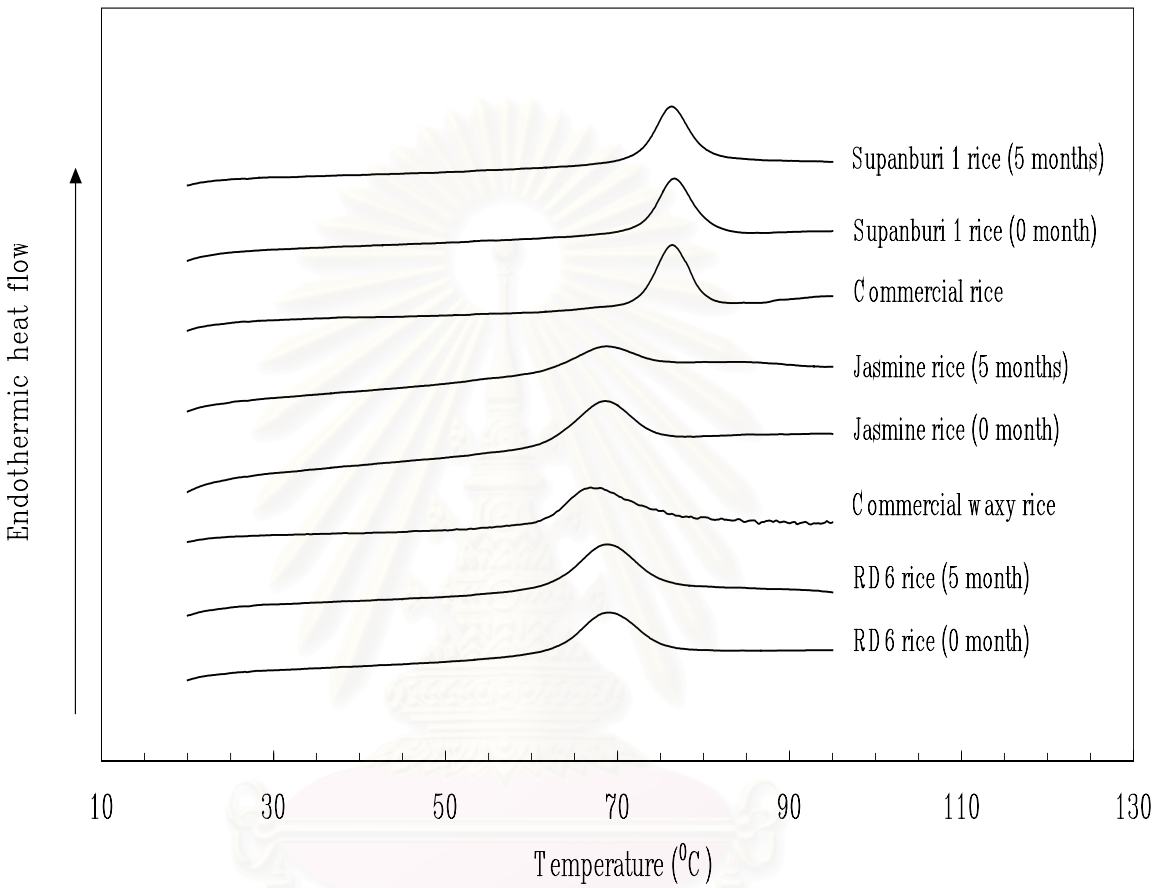

Figure 4.13 The DSC endotherms of Thai rice starches.

Table 4.8 Gelatinisation parameters of Thai rice starches

Starch source	Amylose content (%)	T_0^* (^{0}C)	T_P^* (^{0}C)	T_e^* (^{0}C)	ΔH^* (J/g)
1. RD6 rice					
- 0 month	2.08	62.68 ± 0.04	69.00 ± 0.17	75.21 ± 0.28	13.95 ± 0.46
- 5 months	1.70	62.14 ± 0.05	68.59 ± 0.09	74.05 ± 0.48	14.84 ± 0.27
2. Commercial waxy rice starch	2.39	61.93 ± 0.25	67.22 ± 0.52	76.55 ± 0.07	13.74 ± 0.24
3. Jasmine rice					
- 0 month	15.14	61.76 ± 0.47	68.53 ± 0.17	74.98 ± 0.31	12.66 ± 0.33
- 5 months	14.80	61.82 ± 0.52	68.50 ± 0.16	74.96± 0.40	9.40 ± 0.51
4. Commercial rice starch	21.21	72.49 ± 0.08	76.42 ± 0.09	80.52 ± 0.17	13.39 ± 0.31
5. Supanburi 1 rice					
- 0 month	22.43	72.50 ± 0.24	76.50 ± 0.09	80.76 ± 0.25	11.52 ± 0.41
- 5 months	22.70	72.12 ± 0.24	76.16 ± 0.16	80.50 ± 0.06	11.93 ± 0.16

* the values obtained from means of triplicates ± SD

T_0 : onset temperature, T_p : peak temperature, T_e : end temperature

ΔH: enthalpy of gelatinisation

4.2.3 Pasting behaviour

The pasting profiles of rice starches measured by the RVA (Figure 4.14) with respect to temperature, viscosity and time attributes demonstrated the phenomena occurring during the heating and cooling cycle. The pasting profiles of low amylose rice starches showed a sharper increase in viscosity over a narrow temperature range, which suggests a high degree of swelling. Table 4.9 showed that these rice starches could be classified into two groups according to breakdown viscosity and onset pasting temperature as following:

- low amylose and medium amylose rice starches having breakdown viscosity and onset pasting temperature in the range of 1839-2282 mPa.s and of 67-71^{0}C, respectively, and
- high amylose rice starches having breakdown viscosity of 1082-1148 mPa.s and onset pasting temperature of 77-80 ^{0}C, respectively.

This difference in breakdown viscosity and onset pasting temperature for these rice starches were governed by the ACR values and not by amylose content. It was found that breakdown viscosity decreased, while onset pasting temperature increased with increasing long chains amylopectin. This can be explained by the amylopectin structures having more long chains ($\bar{D}P_n$ 12-24), which are involved in more than one cluster and may have less tendency to be dispersed because of entanglement with other amylopectin molecules. Accordingly, higher proportion of short chains amylopectin ($\bar{D}P_n$ 3-11) for low amylose and medium amylose rice starch would result in high breakdown viscosity due to greater fragility of swollen granules (Han and Hamaker, 2001). Figure 4.15 shows that setback viscosity for these rice starches increased exponentially with increasing amylose content (Equation 4.3, R^2 = 0.96, $p \leq 0.01$), which suggests a major contribution of amylose association to viscosity

measured at 50 ^{O}C. Breakdown viscosity and onset pasting temperature are not affected by aging of rice up to 5 months (Table 4.9).

$$SV\ (mPa.s) = 299e^{0.09AM} \quad (4.3)$$

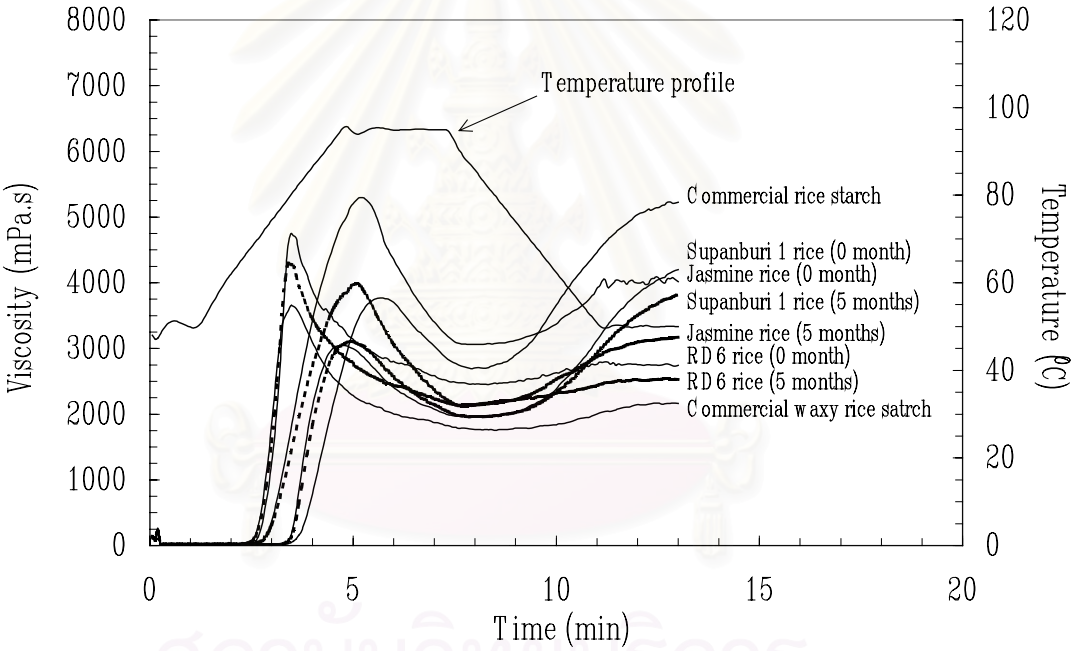

Figure 4.14 Pasting profiles of Thai rice starches.

Table 4.9 The RVA parameters of Thai rice starches

Starch source	Amylose content (%)	Pasting property		
		RVA viscosity* (mPa.s)		Onset pasting temperature (^{0}C)
		Break down	Setback	
1. RD6 rice				
- 0 month	2.08	2282 ± 13	300 ± 9	67.87 ± 0.03
- 5 months	1.70	2168 ± 6	397 ± 6	67.13 ± 0.03
2. Commercial waxy rice satrch	2.39	1864 ± 13	403 ± 4	68.08 ± 0.34
3. Jasmine rice				
- 0 month	15.14	2250 ± 12	1007 ± 13	70.25 ± 0.80
- 5 months	14.80	1839 ± 13	1051 ± 0	69.88 ± 0.38
4. Commercial rice starch	21.21	1082 ± 8	2526 ± 6	79.15 ± 0.05
5. Supanburi 1 rice				
- 0 month	22.43	1123 ± 14	2247 ± 10	77.88 ± 0.42
- 5 months	22.70	1148 ± 0.5	1848 ± 14	78.28 ± 0.07

* the values obtained from means of triplicates ± SD

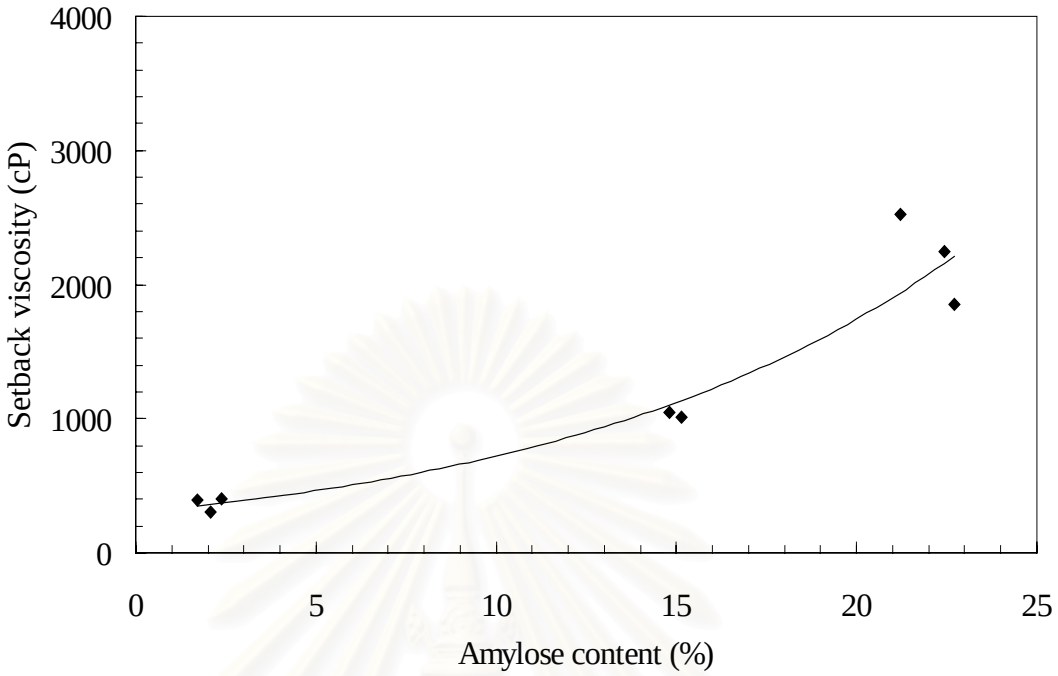

Figure 4.15 Relationship between setback viscosity and amylose content of Thai rice starches.

4.2.4 Rheological properties of rice starch paste

4.2.4 .1 Intrinsic viscosity

The intrinsic viscosity, [η], for these rice starches were calculated from the slope of plot between relative viscosity and concentration (Figure 4.16). This plot gave high correlation coefficient ($R^2 = 0.98$, $p \leq 0.01$). The [η] for each rice starches displayed in Table 4.10. The magnitudes of [η] for these rice starches correlated through a second order of polynomial ($R^2 = 0.92$, $p \leq 0.01$) with swelling power (Figure 4.17). However it decreased with increasing amylose content of rice starches. The lower hydrodynamic volume for the high amylose rice starches indicated the higher rigidity of polymer chains in the starch granule (Launay *et al*., 1986), which corresponded to a low swelling power for these rice starches. The [η] values for these rice starch polymers consisting of both amylose and amylopectin were in the range between those of indica rice amylopectin, 150-170 ml/g, (Takeda *et al*., 1987) and indica rice amylose, 180-249 ml/g, (Hizukuri *et al*., 1989). However, the [η] values of these rice starches were lower than that of potato starch (224 ml/g) and higher than that of wheat starch (137 ml/g) (Paterson *et al*., 1996). This suggested that the starch polymers within potato starch granules have a higher average molecular weight or a less rigid of polymers chain than these rice starches. In contrast wheat starch polymers had a long average molecular weight and greater rigidity than those of rice starches.

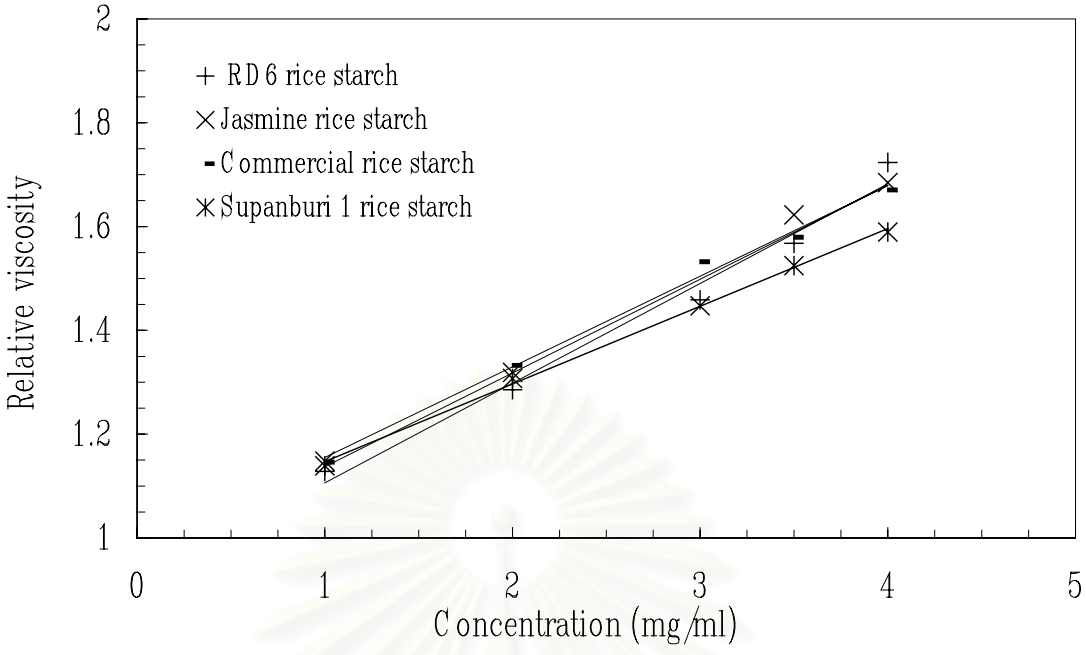

Figure 4.16 Relationship between relative viscosity and concentration for Thai rice starches.

Table 4.10 Intrinsic viscosity of Thai rice starches measured in 5 M KOH

Starch source	Amylose content (%)	Intrinsic viscosity* (ml/g)
1. RD6 rice (0 month)	2.56	192 ± 0
2. Jasmine rice (0 month)	15.12	185 ± 6
3. Commercial rice starch	21.97	171 ± 6
4. Supanburi 1 rice (0 month)	23.08	156 ± 7

* the values obtained from means of triplicates ± SD

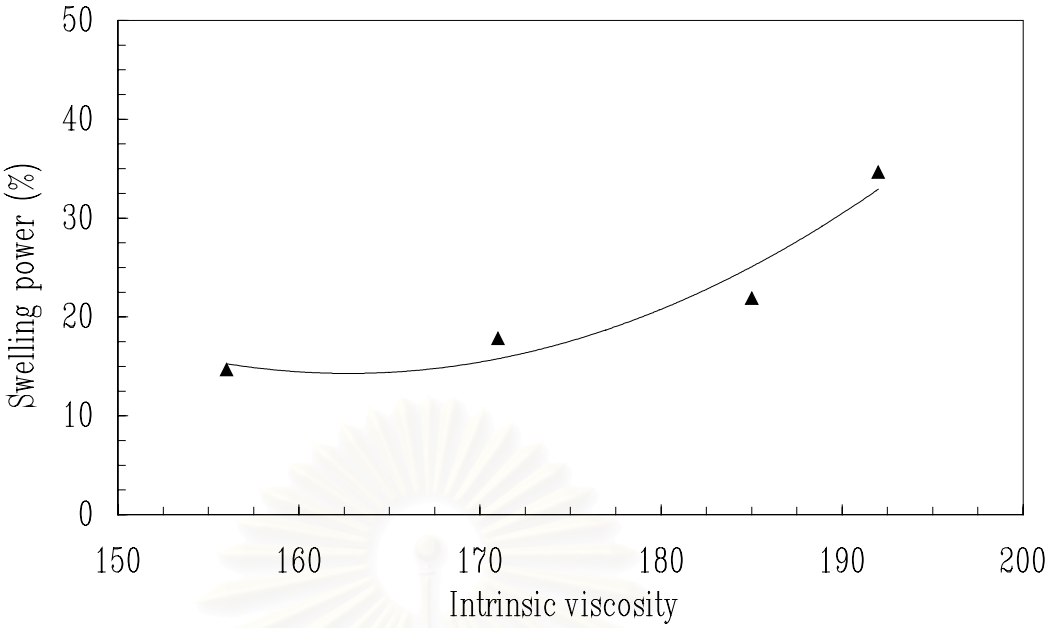

Figure 4.17 Relationship of swelling power to intrinsic viscosity in KOH of starches derived from unaged rice (RD6, Jasmine and Supanburi 1) and commercial rice starch.

4.2.4.2 Viscosity behavior

The relationship between shear rate and shear stress for rice starch at concentration of 2-8 %, in the shear rate range 50-1000 s^{-1} followed the power law equation (Equation 4.4) with a high correlation coefficient ($R^2 = 0.99$, $p \leq 0.01$). All of these rice starch pastes exhibited shear thinning behavior (Fig. 4.18).

$$\sigma = k\dot{\gamma}^n \qquad (4.4)$$

where σ is the shear stress (Pa), γ is the shear rate (s^{-1}), k is the consistency index ($Pa.s^n$), and n is the flow behavior index (dimensionless).

The viscosity decreased with shear rate, except for the high amylose Supanpuri 1 rice starch at 2%, which exhibited Newtonian behavior. This was due to the fact that the granules of high amylose rice starch were more rigid and swell less in dilute concentration.

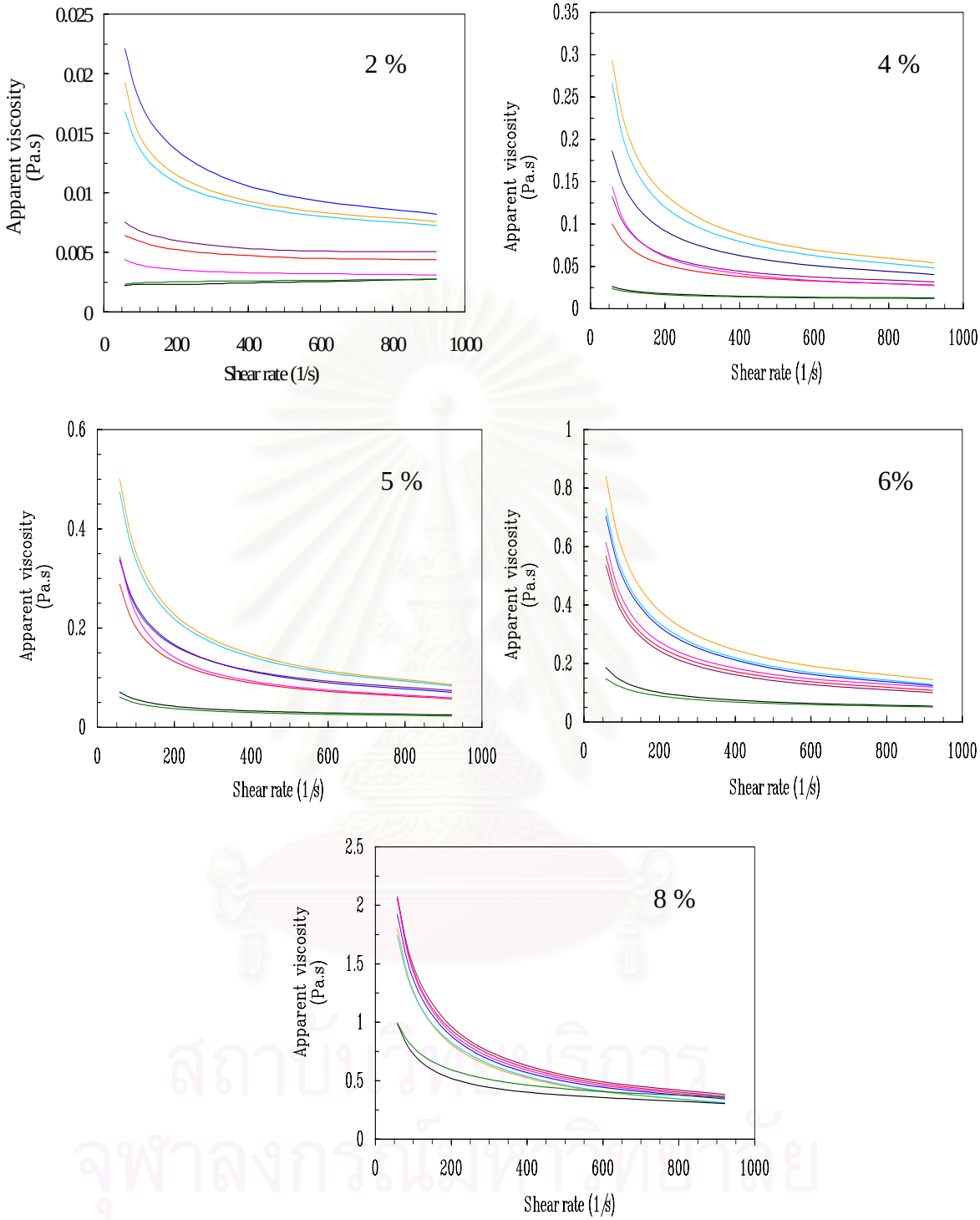

Figure 4.18 Relationship of apparent viscosity to shear rate for starch pastes at 60 ^{0}C over the shear rate range of 50-1000 s^{-1} determined by VOR. These starches derived from RD6 rice (0 month _, 5 months _), commercial waxy rice (_), Jasmine rice (0 month _ , 5 months _), commercial rice (_) and Supanburi 1 rice (0 month _, 5 months _).

The consistency index (k) was found to be starch concentration and amylose content dependence (Figure 4.19), which can be expressed by Equation 4.5 (Appendix C)

$$k = 0.01e^{-0.25AM} c^{3.85e^{0.021AM}} \quad (4.5)$$

The flow behavior index (n) was also found to be starch concentration and amylose content dependence in the starch concentration range of 2-5%, then it became constant (Figure 4.19). Equation 4.6 – 4.9 express the dependency of n on starch concentration and amylose content (Appendix C)

$$c = 2\text{-}5\%, \quad n = 0.72e^{0.04AM}c^{-[0.58+0.01AM)]} \quad (4.6)$$

c = 5-8%,

$$n = 0.36 \quad (AM = 1\text{-}3\%) \quad (4.7)$$

$$n = 0.40 \quad (AM = 14\text{-}21\%) \quad (4.8)$$

$$n = 0.60 \quad (AM = 22\text{-}23\%) \quad (4.9)$$

This suggested that for low amylose rice starches, the starch granules were more fragile and swelled more easily giving a high viscosity and more shear thinning behavior. In addition, the increase in k with concentration, which is due to an increase granule-granule interaction, is accompanied by a decrease in n indicating a greater degree of shear thinning.

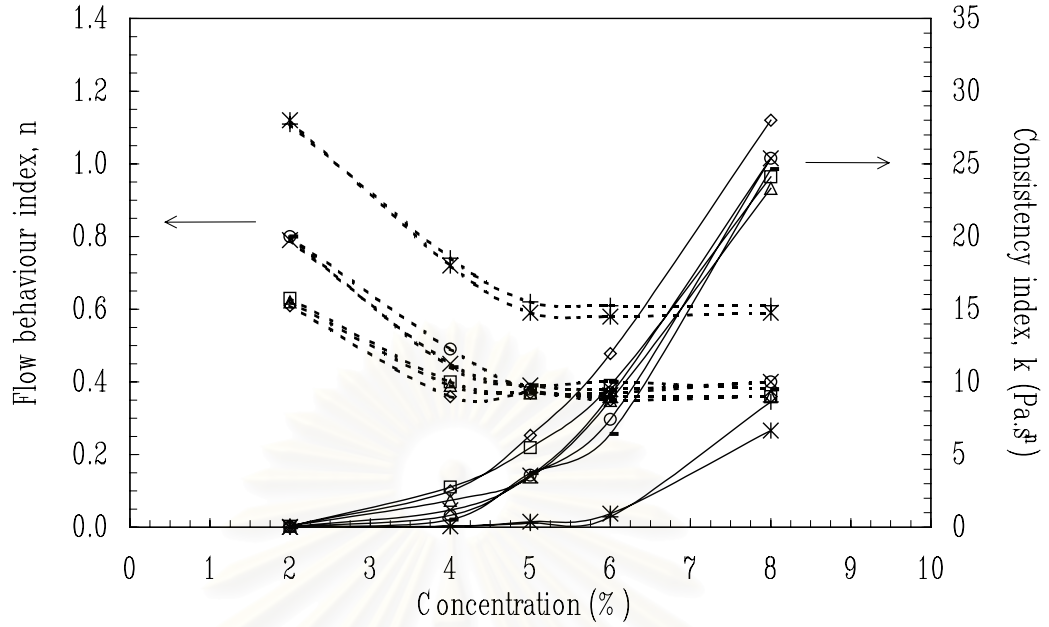

Figure 4.19 Relationship of flow behavior index (n) and consistency index (k) to concentration of starch pastes at 60 ^{0}C over the shear rate of 50-1000 s^{-1} determined by VOR. These starches were derived from RD6 rice (0 month [←] and 5 months aged [□]), commercial waxy rice [↖], Jasmine rice (0 month [×] and 5 months [○]), commercial rice [⇨], and Supanburi 1 rice (0 month [*] and 5 months [+]).

Figure 4.20 shows a plot of the consistency index k against the notional volume fraction parameter cQ. The low amylose starches show a much less severe dependence on cQ compared with the starches with a higher amylose content. This probably reflects the greater rigidity of the swollen granules from the higher amylose starches. At higher values of cQ when the swollen granules are closely packed, granule rigidity rather than extent of swelling starts to govern viscosity. Thus concentration viscosity relationships for different starches can cross

with high swelling starches giving higher viscosities at low concentrations and granules that swell to a smaller extent giving higher viscosities at high concentrations (Steeneken, 1989).

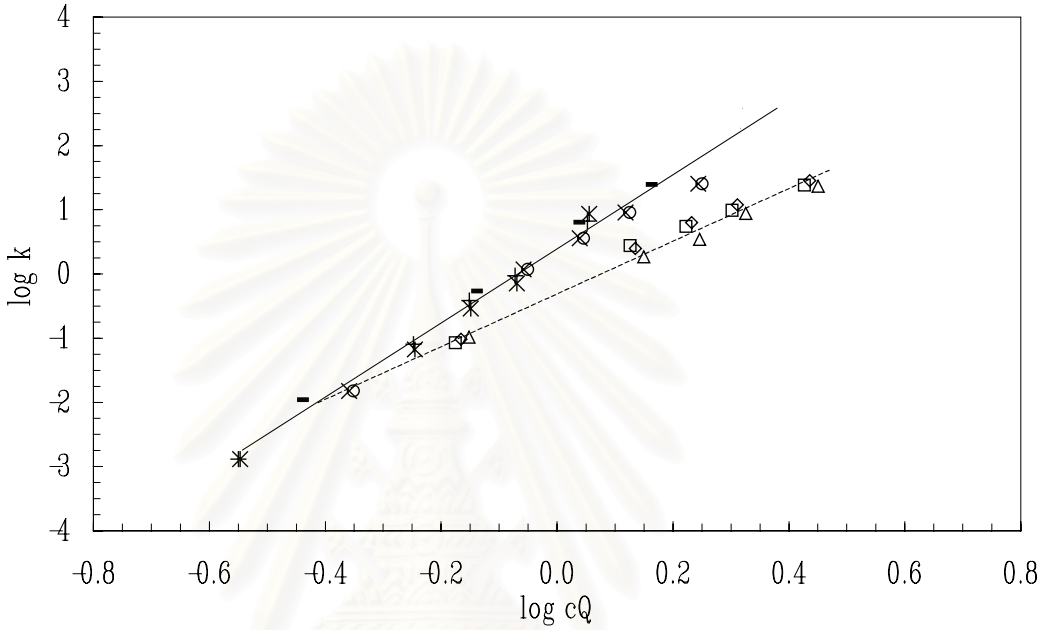

Figure 4.20 Relationship of log (k) and log (cQ) of starch pastes at 60 ^{0}C over the shear rate range 50-1000 s^{-1} measured by VOR. These starches derived from RD6 rice (0 month [←] and 5 months [□]), commercial waxy rice [↖], Jasmine rice (0 month [×] and 5 months [○]), commercial rice [⇨], and Supanburi 1 rice (0 month [*], 5 months [+]).

Increase in k with concentration is accompanied by a decrease in the flow behaviour index (n) indicating a greater degree of shear thinning. This is indicated in Figure 4.21 that displays the pseudoplasticity constant (m) that equals n-1, plotted against concentration. At low concentrations m extrapolates to 0, a value that corresponds to Newtonian behaviour whereas at high concentrations m reaches a constant (negative) value. One-way of obtaining onset concentration from

rheological data alone is to extrapolate to m=0. To do this Evans and Haisman (1979) linearised the data near onset concentration by plotting the reciprocal of m against $1/(c-c_0)$ (Equation 4.10) where c_0 (onset concentration) is an adjustable parameter that reflects the concentration at which the system tended to Newtonian behavior, and m_α and B are constants.

$$-\frac{1}{m} = -\frac{1}{m_\infty} + \frac{B}{c - c_0} \qquad (4.10)$$

The onset concentration measured by this procedure was consistent with the concentration in a sedimented suspension of gelatinised starch granules (Evans and Haisman, 1979).

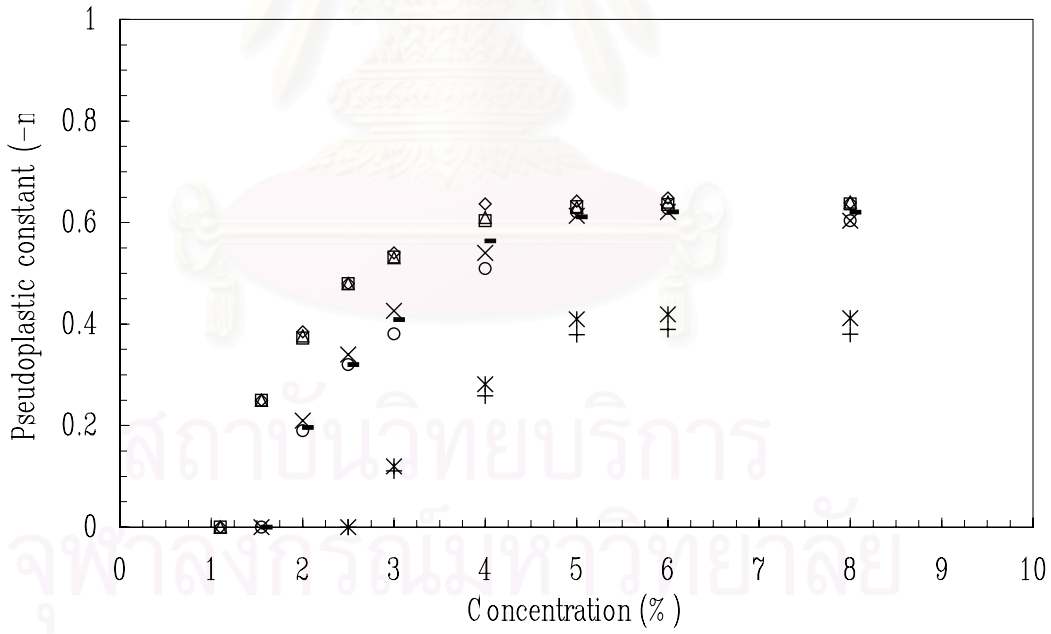

Figure 4.21 Relationship of Pseudoplastic constant (-m) and concentration of starch pastes at 60 ^{0}C over the shear rate range 50-1000 s^{-1} determined by VOR. These starches derived from RD6 rice (0 month [←] and 5 months [□]), commercial waxy rice [↖], Jasmine rice (0 month [×] and 5 months [○]), commercial rice [⇨], and Supanburi 1 rice (0 month [*], 5 months [+]).

Information on the concentration dependence of the viscosity can also be obtained from the RVA data where an apparent viscosity is obtained at the end of the preparation cycle. This is plotted against cQ in Figure 4.22. As found for the fundamental data the viscosity at high concentrations, for comparable values of cQ, is lower for the low amylose starches. It is interesting that the discontinuity in the slope of the log log plot is not seen for k obtained from fundamental measurements (Figure 4.21). This raises the possibility that "slip", due to the well know depletion effect of particles from a surface could be responsible for differences between measurements made with the propeller in the RVA and concentric cylinder geometry.

Table 4.11 The onset concentration (c_0) and the transition concentration (c*) of Thai rice starches

Starch source	Amylose content (%)	c_0 (%,w/w)	c^* (%,w/w)
1. RD6 rice			
- 0 month	2.08	1.1	2.6
- 5 months	1.70	1.1	2.7
2. Commercial waxy rice starch	2.39	1.1	2.6
3. Jasmine rice			
- 0 month	15.14	1.5	3.7
- 5 months	14.80	1.5	4.0
4. Commercial rice starch	21.21	1.5	4.0
5. Supanburi1 rice			
- 0 month	22.43	2.5	4.8
- 5 months	22.70	2.5	5.0

Table 4.11 compares the values for the c* parameter obtained from the change in slope of the plot in Figure 4.22 with the c_o values obtained from Equation (4.2). An interesting point is thet the c_o values and c* values for commercial high amylose rice are closer to the Jasmine rice than the high amylose Supanburi 1 rice extracted for this work. The different rheological behaviour between the two high amylose rice can be explained by the greater degree of swelling and lower degree of short range order after gelatinsation for the commercial high amylose rice compared with the Supanburi1 rice (Table 4.12). The residual order is related to helical content and after disruption of the amylopectin region this will be due to amylose lipid complexes that will probably not be disrupted by gelatinisation and also amylose association/retrogradation. Inverse correlations between the amount of lipid complexed amylose and granule swelling have previously been demonstrated (Morrison *et. al*, 1993). The higher degree of swelling and lower degree of short-range order after gelatinsation for the commercial high amylose will result in a less rigid granule. We suggest that this lower rigidity combined with greater swollen volume is the reason for the similar rheological behaviour of the commercial high amylose rice to the Jasmine rice. The short-range molecular order parameter after gelatinisation for the Jasmine and commercial high amylose rice are similar.

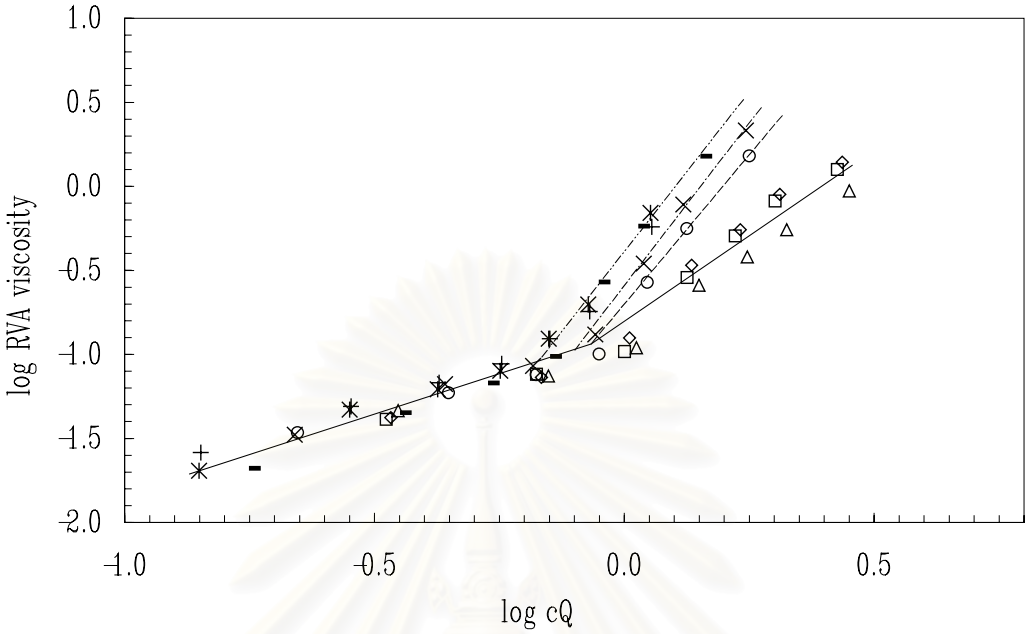

Figure 4.22 Relationship of log (RVA viscosity) and log (c) of starch pastes measured at 60 ^{0}C over the shear rate range 50-1000 s^{-1} determined by RVA. These starches derived from RD6 rice (0 month [←] and 5 months [□]), commercial waxy rice [↖], Jasmine rice (0 month [×] and 5 months [○]), commercial rice [⇨], and Supanburi 1 rice (0 month [*], 5 months [+]).

Table 4.12 The ratio of short-range molecular order to amorphous of native and gelatinized rice starches

Starch source	Amylose content (%)	Ratio of short-range molecular order to amorphous*		
		Native rice starch	Gelatinized rice starch	% of order loss after gelatinization
1. RD6 rice				
- 0 month	2.08	0.91 ± 0.04	0.28 ± 0.06	69.23±0.06
- 5 months	1.70	0.89 ± 0.03	0.27 ± 0.04	69.66±0.04
2. Commercial waxy rice starch	2.39	0.86 ± 0.03	0.25 ± 0.03	70.93±0.03
3. Jasmine rice				
- 0 month	15.14	0.81 ± 0.03	0.35 ± 0.01	56.79±0.01
- 5 months	14.80	0.75 ± 0.01	0.31 ± 0.01	58.67±0.01
4. Commercial rice starch	21.21	0.74 ± 0.02	0.32± 0.01	56.76±0.01
5. Supanburi1 rice				
- 0 month	22.43	0.72 ± 0.05	0.38± 0.01	47.76±0.01
- 5 months	22.70	0.73 ± 0.04	0.37 ± 0.02	49.32±0.02

* the values obtained from means of triplicates ± SD

4.2.4.3 Viscoelastic properties

The result of starch gelatinization is a composite product of dispersed phase (swollen starch granules) embedded in continuous phase (amylose/ amylopectin matrix). When the starch concentration is high enough, the corresponding high concentration of amylose or amylopectin in the continuous phase will allow interaction between the components and form a three-dimensional network gel upon cooling.

The rheological properties of this composite product will be influenced by (Eliasson, 1986; Biliaderis, 1992; and Rao, 1999):

- the nature of starch granules in the dispersed phase:
  - shape, size and size distribution
  - swelling pattern
  - rigidity and deformability
  - concentration
- continuous phase :
  - viscoelasticity of the phase
  - amount and type of leached amylose or amylopectin
  - entanglements
- interaction between the components or between phase :
  - granule-granule interactions
  - granule-amylose or amylopectin interaction
  - granule-amylose or amylopectin-granule interactions

To characterize this starch composite, both static and dynamic (in the linear region) viscoelastic properties were studied in the linear region and the results are discussed in this following section.

4.2.4.3.1 Dynamic viscoelastic properties of pastes and gels

Two sets of samples of 6-15 % w/w were used to evaluate for the effect of network development on starch structure after cooling. The first sample set (before cooling) was the 60 ^{0}C gelatinized starches prepared freshly by RVA and measured at 60 ^{0}C. Another set (after cooling) was the gelatinized starches which were stored at 6 ^{0}C for 12 h after preparation by RVA, and was measured at 25 ^{0}C. The dynamic viscoelastic properties were determined in the linear region at frequency range of 0.1-10 Hz and 2% strain (Figure 4.23 and 4.24, Figure 4.26 and 4.27). For overall results, storage modulus (G′) was higher than the loss modulus (G′′) for all samples, indicated the strong interactions between the components and between phases. The G′ for all samples increased exponentially with increasing amylose content (Equation 4.11, R^2 = 0.95 - 0.99, $p \leq 0.01$) as shown in Figure 4.25 and Figure 4.28, and it increased linearly with increasing starch concentration (R^2 = 0.95 - 0.99, $p \leq 0.01$).

$$G' \text{ (Pa)} = 40.69e^{0.11AM} \quad (4.11)$$

In concentrated starch pastes there is close contact between granules resulting in granule-granule interactions. The contact might also involve molecules, which has leached out from the granules. Furthermore, amylose molecules might have leached

out only partly. This situation permits interactions between starch granules and the continuous matrix, “granule-amylose or amylopectin interactions”, and also interactions between granules mediated by partly leached amylose molecules from different granules, “granule-amylose or amylopectin-granule interactions” (Eliasson, 1986; and Lii *et al*., 1995). For high amylose rice starches, greater amounts of leached-out components, amylose and long B-chains amylopectin are expected. This resulted in an increase the extent of interactions between components or between phases (Biliaderis and Juliano, 1993; Lii *et al*., 1995; and Tsai *et al*., 1997).

For the low amylose rice starch, G′ was frequency dependence and ranged from 20-110 Pa indicating weak gel behavior, while for medium amylose and high amylose rice starch, G′ was frequency independence behaving as rubber-like material, which is an important characteristic of strong gels (Ward, 1990; and Rao, 1999). It can be concluded that the amylose content of rice starch is a major factor influencing gel formation. The effect of cooling on G′, G″, G^* (complex modulus) and η^* (complex viscosity) of starch pastes was found only in high amylose rice starch (Figure 4.26 and Figure 4.27). Hence, an increase in G′ for high amylose rice starch after cooling could be attributed to the development of a three dimensional network between leached-out components, and the interactions between granule and leached-out components.

There was a linear relationship ($R^2 = 0.99$, $p < 0.01$) between the cQ and the complex viscosity (η^*) of starch pastes of 6-15% w/w before cooling (Figure 4.29). At a given value of CQ, the higher the amylose content amylose rice starches, the higher η^*. This probably reflects the greater rigidity of the swollen granules of the higher amylose starch. The effect of amylose content on viscoelastic behavior was observed over the whole volume fraction parameter cQ

studied, while this effect was not clearly shown for the lower values of cQ as studied in section 4.2.4.2 (Figure 4.20). This suggested that the higher starch concentration, the greater the dominant effect of interaction between granules or between phase on the viscosity behavior of starch pastes.

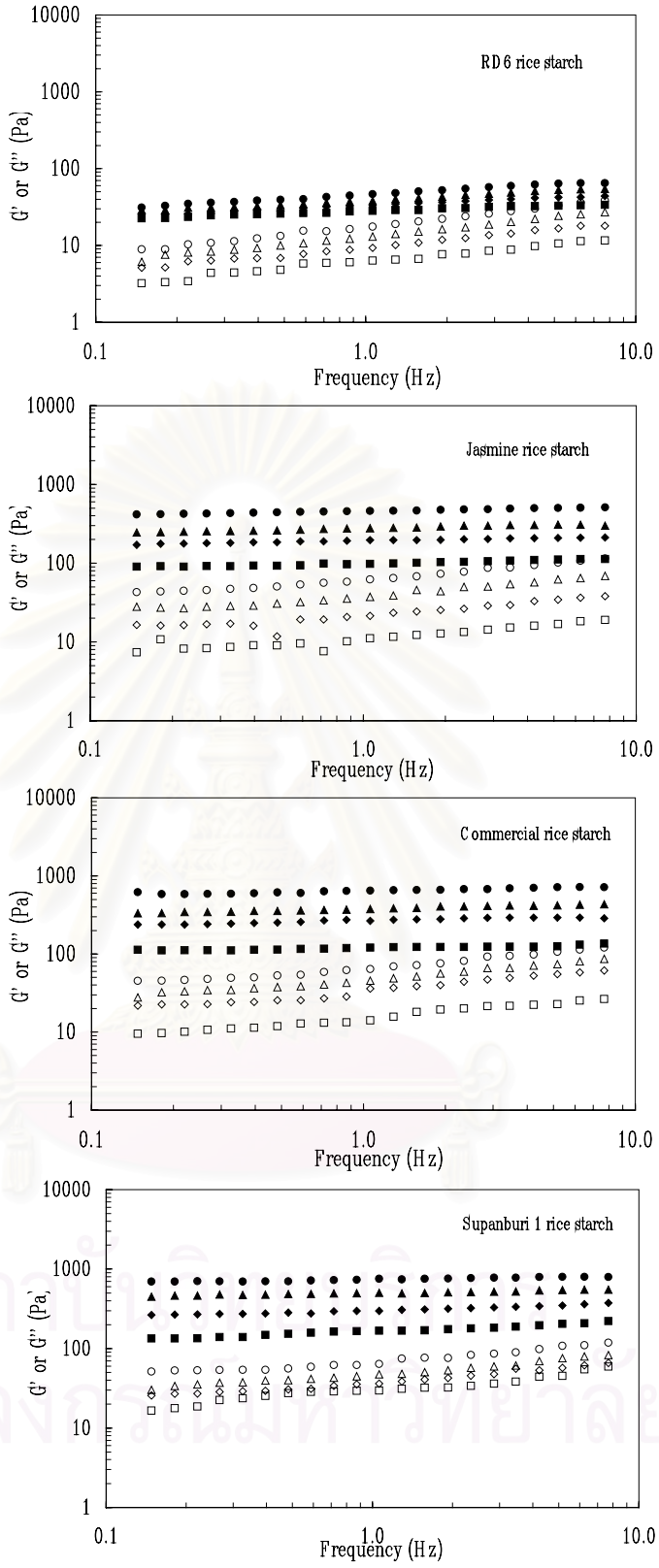

Figure 4.23 Effect of frequency on G′ (full symbol) and G″ (open symbol) for various concentrations (6% [□], 9% [◊], 12% [Δ] and 15% [o]) of rice starch pastes before cooling. All samples were measured at 60 ^{0}C and at 0.1-10 Hz.

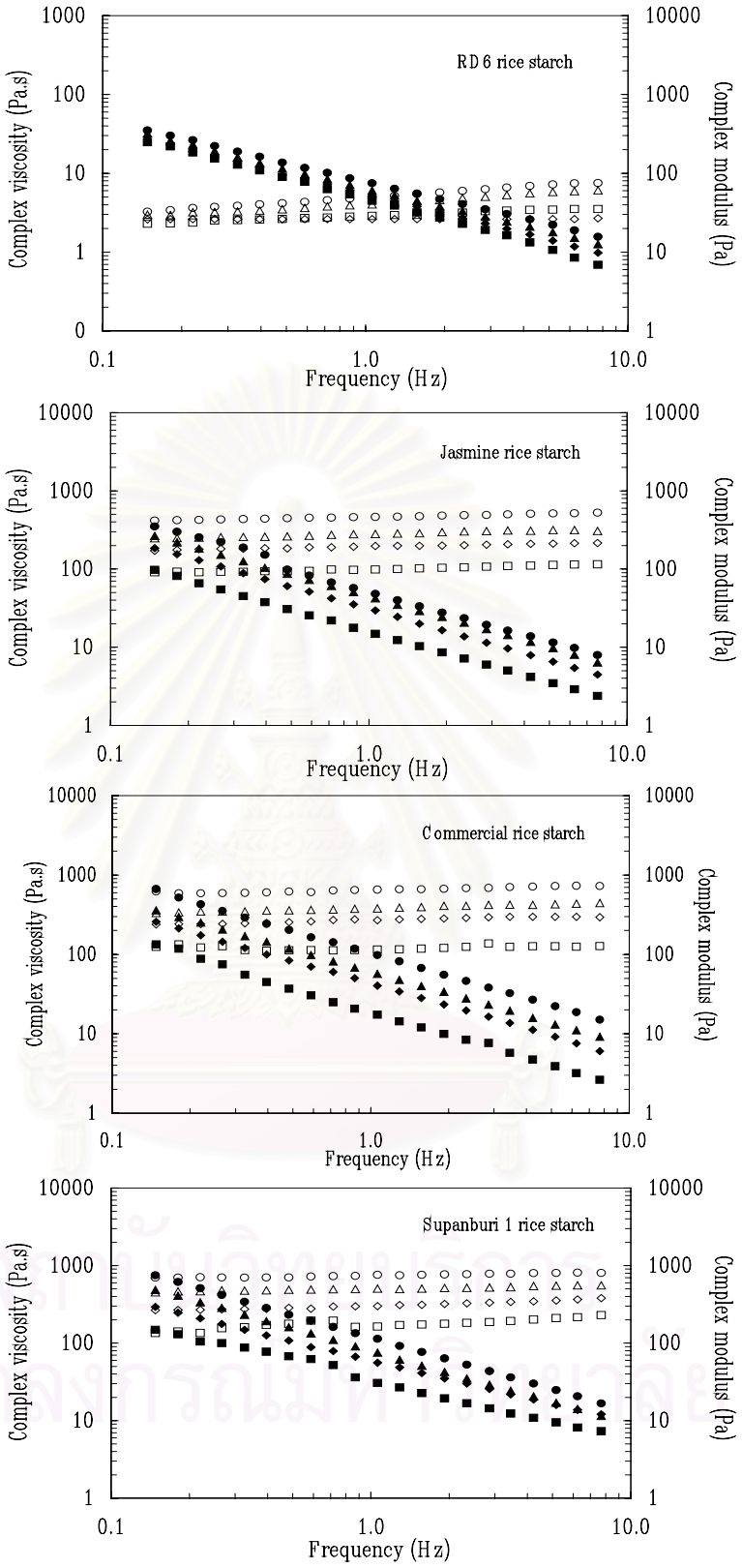

Figure 4.24 Effect of frequency on complex viscosity (full symbol) and complex modulus (open symbol) for various concentrations (6% [□], 9% [◊], 12% [Δ] and 15% [o]) of rice starch pastes before cooling. All samples were measured at 60 ^{0}C and at 0.1-10 Hz.

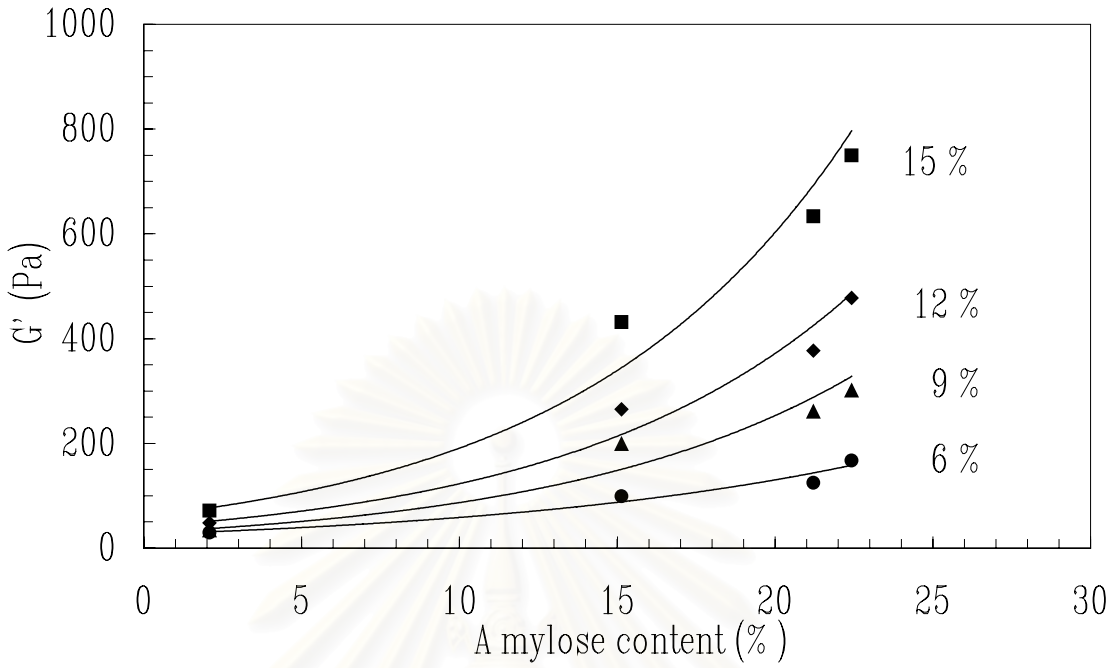

Figure 4.25 The relationship between G′ and amylose content for various concentrations of starch pastes before cooling measured at 60 ^{0}C and 1 Hz. These starch pastes were derived from unaged rice and 5 months aged rice (RD6, Jasmine, and Supanburi 1), and from commercial rice starch.

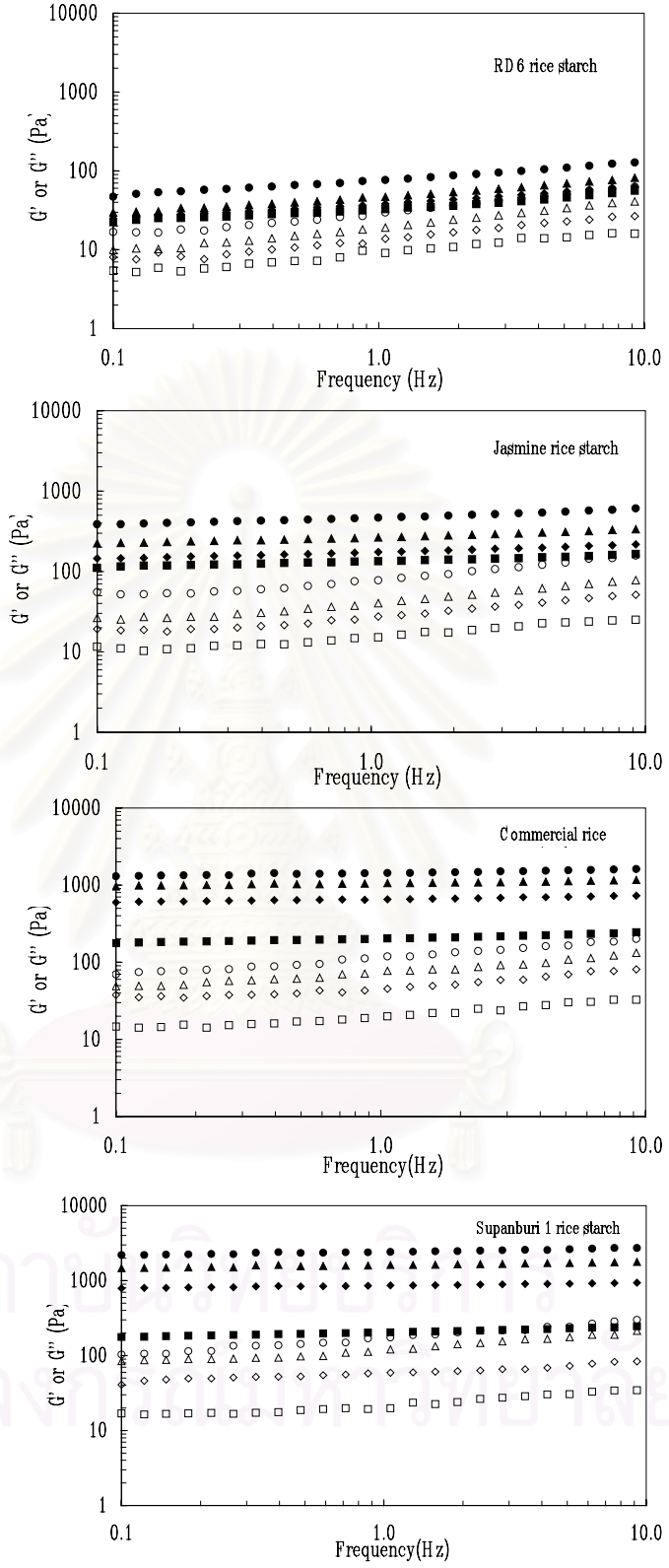

Figure 4.26 Effect of frequency on G′ (full symbol) and G″ (open symbol) for various concentrations (6% [□], 9% [◊], 12% [Δ] and 15% [o]) of rice starch pastes after cooling. All samples were measured at 25 ^{0}C and at 0.1-10 Hz.

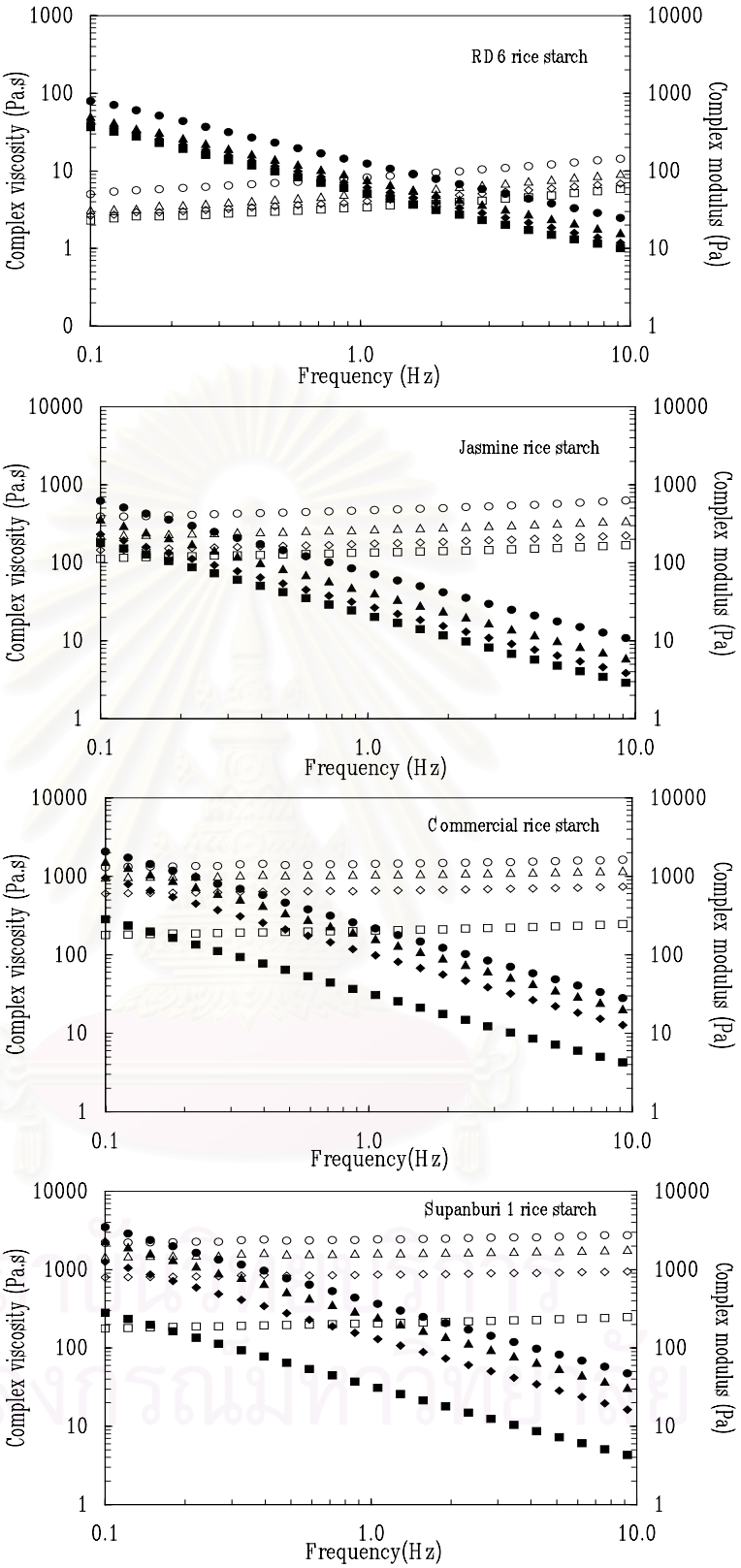

Figure 4.27 Effect of frequency on complex viscosity (full symbol) and complex modulus (open symbol) for various concentrations (6% [□], 9% [◊], 12% [Δ] and 15% [o]) of rice starch pastes after cooling. All samples were measured at 25 ^{0}C and at 0.1-10 Hz

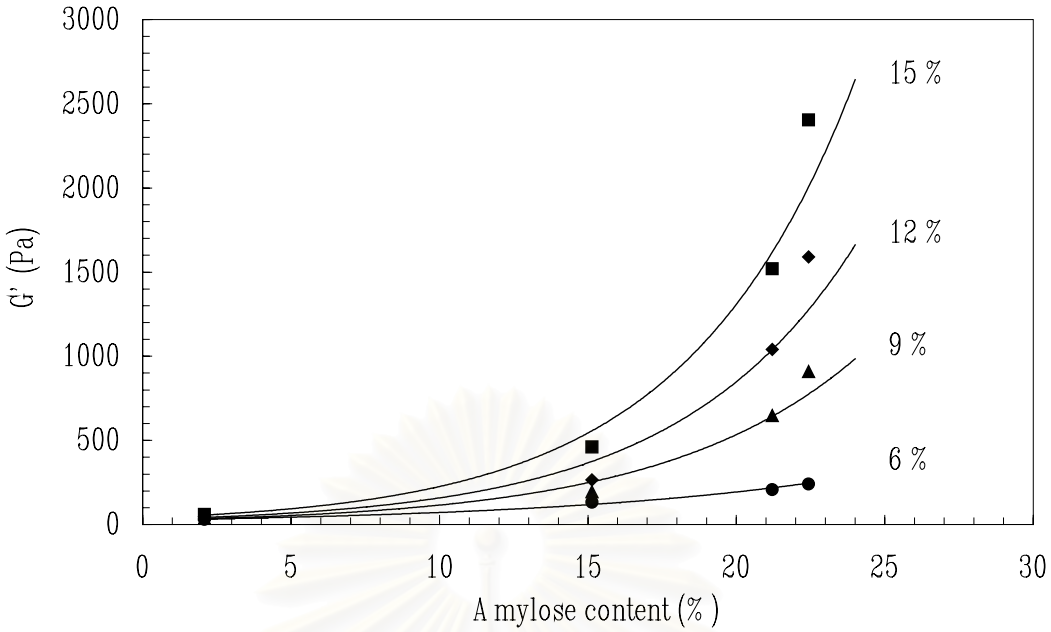

Figure 4.28 The relationship between G′ and amylose content for various concentrations of rice starch pastes after cooling measured at 25 ^{0}C and 1 Hz. These starch pastes derived from unaged rice and 5 months aged rice (RD6, Jasmine, and Supanburi 1), and from commercial rice starch.

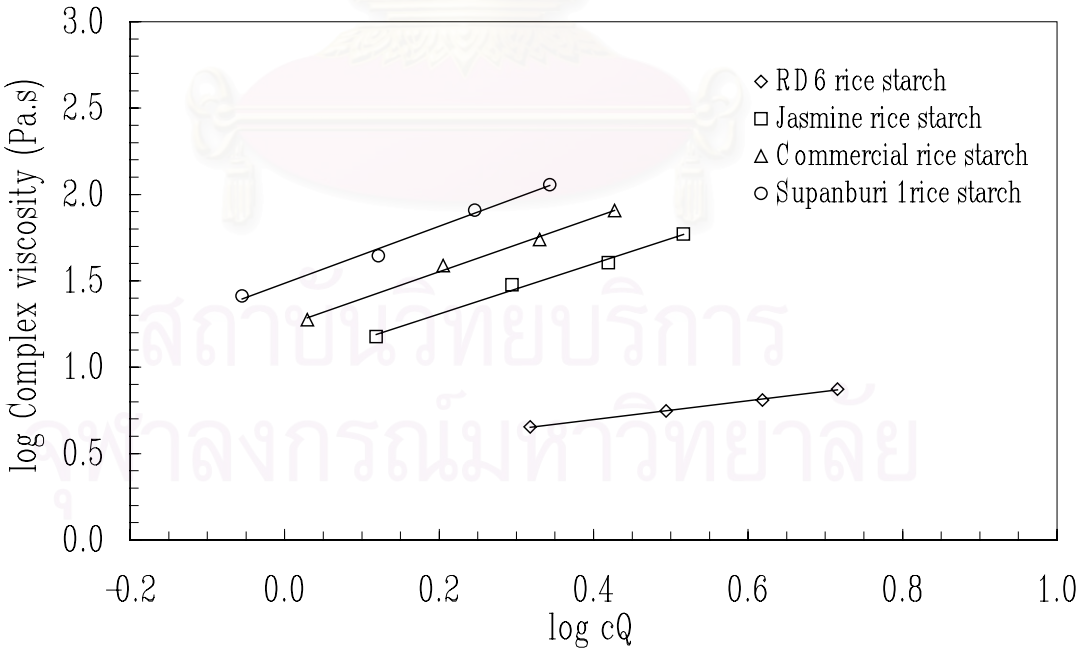

Figure 4.29 The relationship between log complex viscosity and log cQ for rice starch pastes before cooling. All samples were measured at 60 ^{0}C and 1 Hz.

4.2.4.3.2 Creep study for pastes and gels

The creep of all rice starch pastes (6-15 % concentration) after cooling and aging were also measured at shear stress of 10 Pa and temperature 25 ^{0}C (Figure 4.30). The creep compliance curve of 6% concentration of RD6 exhibited flow behavior with Newtonian viscosity of 16.4 Pa.s. While, the others exhibited a response, which could be fitted by 4-element Burger model (Equation 4.12).

$$J(t) = J_0 + J_1(1 - \lambda^{-t/\tau_1}) + \frac{t}{\eta_N} \qquad (4.12)$$

where J(t) = the measured compliance (1/Pa)

J_0 = the instantaneous elastic compliance (1/Pa)

= $1/G_0$

J_1 = the retarded elastic compliance (1/Pa)

= $1/G_1$

η_1 = the retarded viscosity (Pa.s)

η_N = the terminalviscosity (Pa.s)

τ_1 = the retardation time (s)

= $J_1 . \eta_1$

The static viscoelastic properties, instantaneous elastic modulus (G_0), retarded elastic modulus (G_1), η_1 and η_N calculated by the Equation (4.3) using the graphical method of Inokuchi (1955) are displayed in Table 4.13. G_0 ,G_1, η_1 and η_N increased with increasing amylose content and starch

concentration of rice starches, which is consistent with the dynamic viscoelastic test. It implied that the rigidity of starch granules and the increasing in granule-granule interaction inducrd gel structure strengthening. The retardation time (τ_1) of low amylose and medium amylose rice starch were similar, while that of for high amylose rice starches was noticeably lower. This again was due to the effect of granule rigidity.

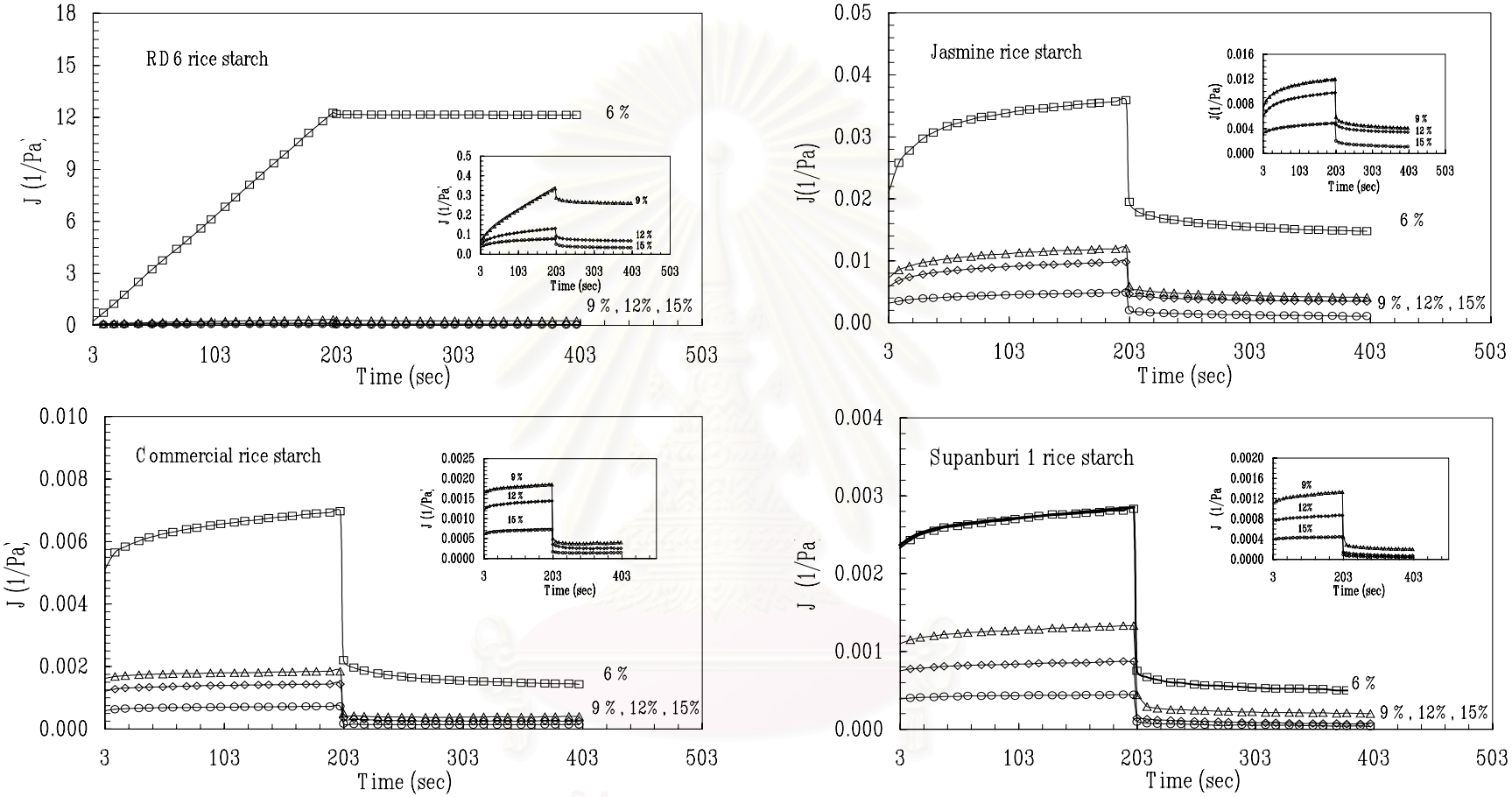

Figure 4.30 Creep compliance and creep recovery for various concentrations of rice starch gels after cooling measured at 25 ^{0}C and 10 Pa. These starch gels derived from unaged rice (RD6, Jasmine and Supanburi 1) and from commercial rice starch. The lines represent the 4-element Burger model fitting.

Table 4.13 The creep parameters for rice starches gels at various concentrations measured at 25 ^{0}C and 10 Pa

Starch gel derived from	Concentration (%, w/w)	Instantaneous modulus	Voigt element parameters			Terminal viscosity
		G_0 (Pa)*	G_1 (Pa)*	η_1 (Pa.s)*	τ_1 (sec)*	η_N (Pa.s)*
RD6 rice (0 month aged)	6	0	0	0	0	(1.64 ± 0.02) x 10
	9	18 ± 0.7	18 ± 0.7	(3.93 ± 0.16) x 10^2	22 ± 0.9	(8.66 ± 0.35) x 10^2
	12	21 ± 0.8	25 ± 1	(6.71 ± 0.27) x 10^2	27 ± 1.0	(4.58 ± 0.18) x 10^3
	15	31 ± 0.9	35 ± 1	(1.02 ± 0.03)x 10^3	29 ± 0.9	(1.16 ± 0.03) x 10^4
Jasmine rice (0 month aged)	6	48 ± 1	93 ± 3	(2.22 ± 0.07) x 10^3	24 ± 0.7	(5.00 ± 0.15) x 10^4
	9	132 ± 4	439 ± 13	(1.11 ± 0.02) x 10^4	25 ± 0.7	(1.43 ± 0.04) x 10^5
	12	172 ± 3	396 ± 8	(1.01 ± 0.02) x 10^4	26 ± 0.5	(1.33 ± 0.03) x 10^5
	15	318 ± 6	1023 ± 20	(2.92 ± 0.06) x 10^4	29 ± 0.6	(2.56 ± 0.05) x 10^5
Commercial rice	6	196 ± 4	1001 ± 20	(2.00 ± 0.04) x 10^4	20 ± 0.4	(2.32 ± 0.05) x 10^5
	9	617 ± 6	8201 ± 82	(1.21 ± 0.01) x 10^5	15 ± 0.1	(1.67 ± 0.02) x 10^6
	12	833 ± 8	7458 ± 74	(1.06 ± 0.01) x 10^5	14 ± 0.1	(1.78 ± 0.02) x 10^6
	15	1718 ± 17	9073 ± 73	(1.07 ± 0.01) x 10^5	12 ± 0.1	(3.31 ± 0.03) x 10^6
Supanburi 1 rice (0 month aged)	6	429 ± 9	4123 ± 82	(7.37 ± 0.15) x 10^4	18 ± 0.4	(7.14 ± 0.14) x 10^5
	9	909 ± 9	9358 ± 94	(1.61 ± 0.02) x 10^5	17 ± 0.2	(1.49 ± 0.01) x 10^6
	12	1330 ± 13	18657 ±187	(3.16 ± 0.03) x 10^5	16 ± 0.2	(2.17 ± 0.02) x 10^6
	15	2584 ± 26	29407 ± 294	(3.50 ± 0.04) x 10^5	12 ± 0.1	(6.74 ± 0.07) x 10^6

* the values obtained from the means of triplicates ± SD

4.2.5 Retrogradation of rice starch gels

During cooling and storage of gelatinised starch, amylose and amylopectin reassociate leading to a more ordered structure that may develop into crystalline forms (Tomas and Atwell, 1999). In this study, the change in degree of crystallinity during retrogradation at 25 ^{0}C was followed by the changes in G′ (Figure 4.31), the ratio of short range molecular order to amorphous (Figure 4.32) and the crystallinity index (Figure 4.35) using rotational rheometer, FTIR and X-ray diffraction, respectively. There were no changes of G′ and the ratio of short-range molecular order to amorphous for low amylose and medium amylose rice starch over storage time of 70 hours. This can be accounted for by the fact that a low amount of amylose and proportion of amylopectin chain length of $\overline{DP}_n$ 12-24 for low amylose and medium amylose rice starch could not contribute to the reassociation of starch molecules and the development of a three-dimensional network. In addition, these low amylose and medium amylose rice starches also had a high proportion of short chain amylopectin of $\overline{DP}_n$ 3-11, which could inhibit or retard retrogradation of starch gels (Levine and Slade, 1986). In contrast, for high amylose rice starch gels (Supanburi 1 and commercial rice starch), the changes of G′ and the ratio of short-range molecular order to amorphous with storage time were obviously observed and revealed three stages over storage time of 100 hours. Stage 1 is an initial fast changes for the first 24 hours (Supanburi 1 rice starch) and 20 hours (commercial rice starch). For this stage, G′ and the ratio of short range molecular order to amorphous increased rapidly at the rate of 0.57 kPa/h and 0.002 h^{-1}, respectively for Supanburi 1 and 0.44 kPa/h and 0.001 h^{-1} for commercial rice starch (Figure 4.31 and Figure 4.32). This was described as the fast formation of double helices of amylose and in the

amylopectin branch chains within a single polymer molecule, which leaded to the creation of three-dimension network of starch gels (Bulkin and Kwak, 1987; Goodfellow and Wilson, 1990; van Soest, 1994; and Hoover, 2001). These initial fast changes for amylose and amylopectin were not observed by X-ray diffraction since the X-ray diffraction can monitor only crystallinity not the double helix formations. Stage 2 is slow process, G′ and the ratio of short-range molecular order to amorphous increased slowly with time. This stage was completed after 90 and 85 hours for Supanburi 1 and commercial rice starch, respectively. This represented a slow formation aggregate of amylopectin helices, which leads to crystallite formation (Bulkin and Kwak, 1987; Goodfellow and Wilson, 1990; van Soest, 1994; and Hoover, 2001). The appearance of diffraction at 17.2^0 (2θ) in the X-ray pattern after 24 hours (Figure 4.34) and an increase in crystallinity index (Figure 4.35) confirmed these crystallite formation. Stage 3 is a very slow process, G′ and the ratio of short-range molecular order to amorphous were very slow changes and then reached a constant value represented by the propagation and perfection step for crystallite formation (Bulkin and Kwak, 1987; and Hoover, 2001). This was consistent with the constant values of the crystallinity index after 72 hours (Figure 3.45). The difference between two high amylose rice starches, the rate of changes in G′ and the ratio of short-range molecular order to amorphous region for Supanburi 1 rice starch were higher than those for commercial rice starch. This suggested that the higher amount of amylose and proportion of amylopectin chain length of $\bar{D}P_n$ 12-24, the higher the formation of helixes, aggregation and crystallization during the retrogradation process. However, the overall retrogradation rate calculated by the Avrami equation (Equation 2.4) for these two high amylose rice starches was not significantly different (Table 4.14).

The effect of starch concentration in the range of 20 - 40% on retrogradation at 25 ^{0}C was determined only for Supanburi 1 rice starch by following the ratio of short-range molecular order to amorphous region (Figure 4.33). Three stages: the formation of helixes, aggregation and crystallization, and perfection starch chains, were observed. The first stage of double helices formation completed within 10, 20, and 22 hours for 20, 30 and 40%, respectively. For this stage, the rate of changes in the ratio of short-range molecular order to amorphous were 0.001/h, 0.002/h, and 0.003/h for starch concentrations of 20, 30 and 40%, respectively. The final step of crystalline formation was observed after 55, 90, and 95 hours for starch concentration of 20, 30 and 40%, respectively. The rate of changes in the ratio of short-range molecular order to amorphous increased sharply with starch concentration, since an increase in starch concentration leaded to an increase in the total amount of amylose and proportion of amylopectin chain length of DP_n 12-24 in gel matrix, resulting in higher density of three-dimension network in starch gels during retrogradation. However, the overall retrogradation rate trended to increase with increasing water concentration (low starch concentration) in gelatinized starch (Table 4.14) due to an increase in the molecular mobility of starch molecules (Slade and Levine, 1987).

The effect of storage temperature at 5 ^{0}C and 25 ^{0}C on retrogrdation was also studied only for Supanburi 1 rice starch by following the changes of crystallinity index (Figure 4.36 and Figure 4.37). The crystallinity index increased with decreasing storage temperature due to an increase in the rate of the crystallite formation for low storage temperature (Biliaderis and Zawistowski, 1990; and Farhat, 1996).

The X-ray diffraction study also showed that the retrogradation for all gelatinized starches stored at both 5 ^{0}C and 25 ^{0}C had a B-type crystalline structure although the native starches had an A-type crystallite. This shift in the crystalline pattern from A to B type depended strongly on water content and storage temperature, A type crystal was observed at high temperature and/or low water contents, while the B type crystal was observed at low temperature and high water contents (Marsh, 1986).

The relative extent of retrogradation (% retrogradation) obtained from FTIR and rheological technique had a similar pattern (Figure 4.38 and Figure 4.39), where it increased sharply at the beginning then leveled off and reached a constant value. However, the relative extent of retrogradation obtained from X-ray diffraction technique was lower than the values obtained from FTIR and rheological techniques, since X-ray diffraction can monitor only long range molecular order (crystallinity) not short-range molecular order (double helices formation) occurring at the initial stage of retrogradation (Bulkin and Kwak, 1987).

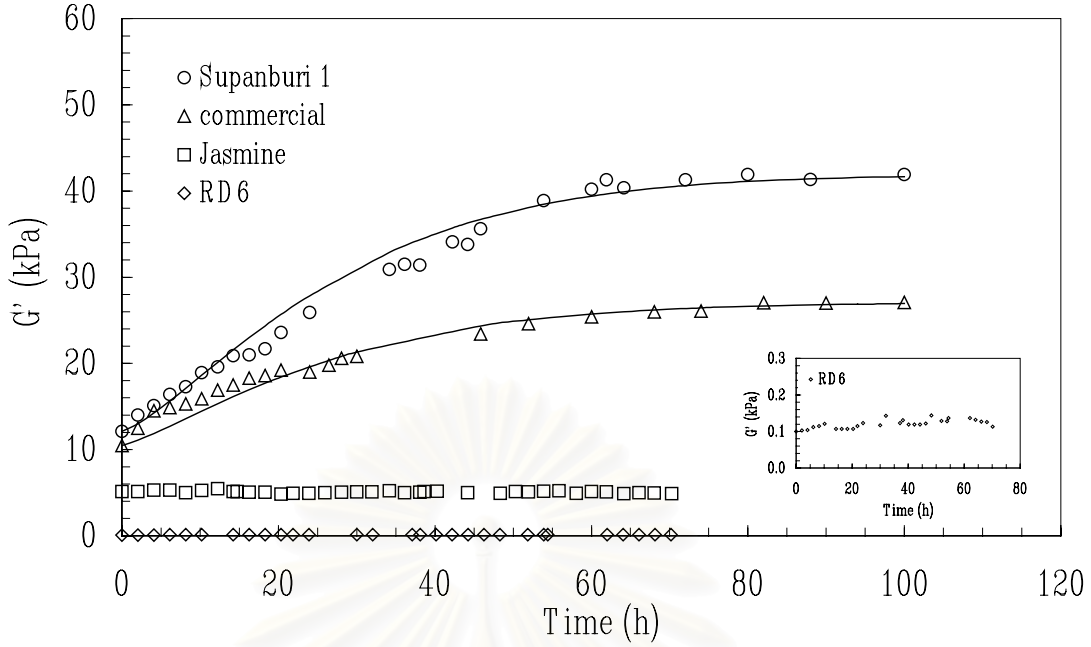

Figure 4.31 The changes of storage modulus (G′) of rice starch gels (30%, w/w) during storage at 25 ^{0}C. The lines represent the Avrami equation.

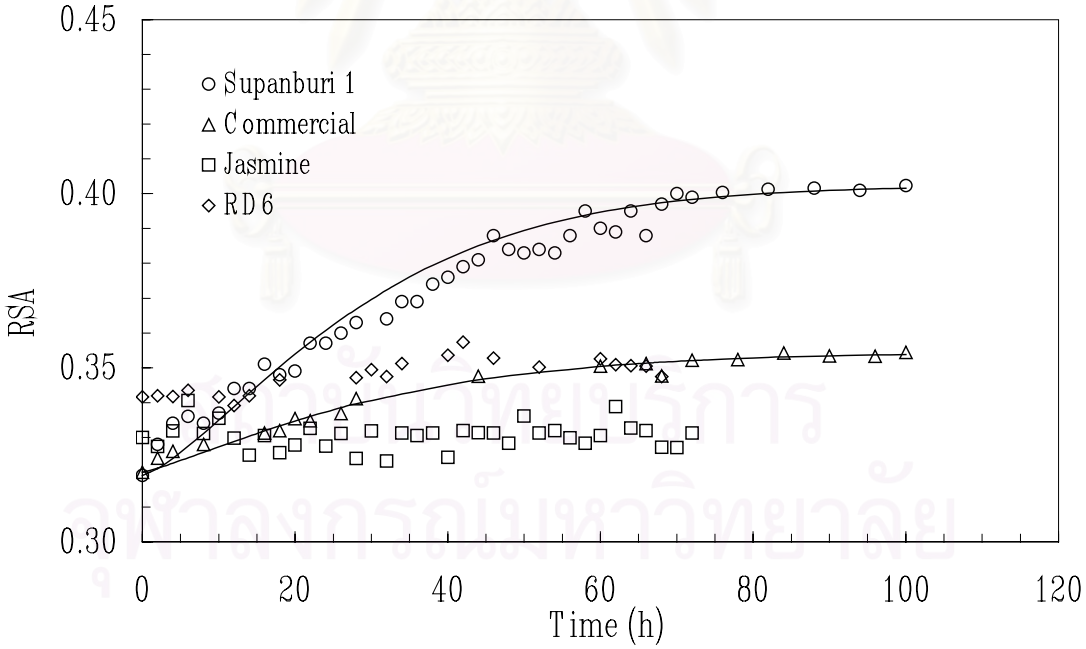

Figure 4.32 The changes for the ratio of short-range molecular order to amorphous region (RSA) of rice starch gels (30%, w/w) during storage at 25 ^{0}C. The lines represent the Avrami equation.

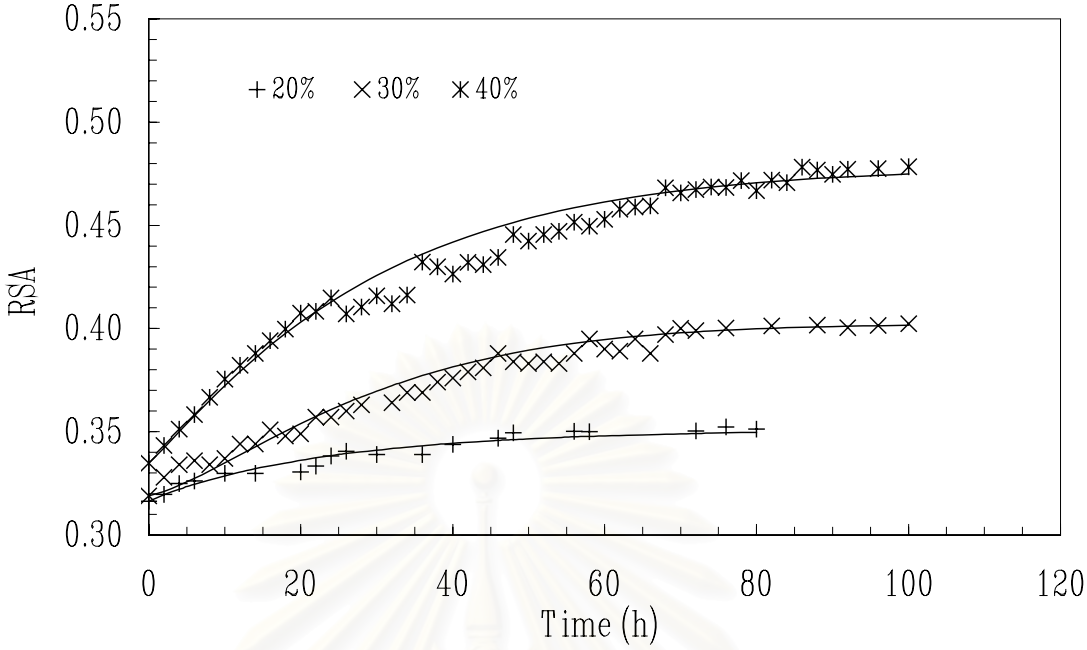

Figure 4.33 The change in the ratio of short-range molecular order to amorphous (RSA) of Supanburi 1 rice starch gels during storage at 25 ^{0}C. The lines represent the Avrami equation.

Table 4.14 The retrogradation rates at 25 ^{0}C of rice starches gels calculated by the Avrami equation

Data analysed from	Retrogradation rate (x10^{-5} s^{-1})			
	Commercial rice starch (30%)	Supanburi 1 rice starch		
		20%	30%	40%
The ratio of short-range molecular order to amorphous region*	0.88	1.17	0.86	0.83
Elastic Modulus (G′)	0.97	-	0.93	-

* ratio of absorbance at wave number 1047 to 1022

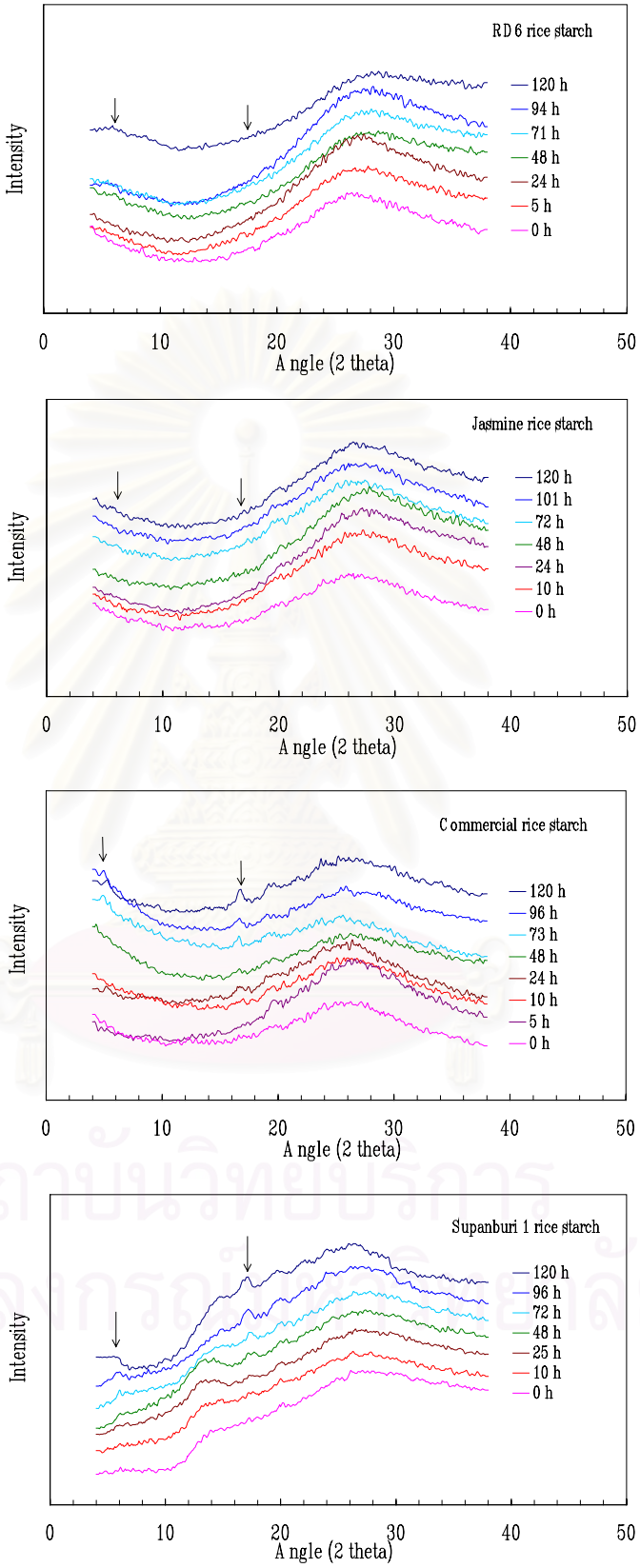

Figure 4.34 Crystallinity development in rice starch gels during storage at 25 ^{0}C for 120 hours.

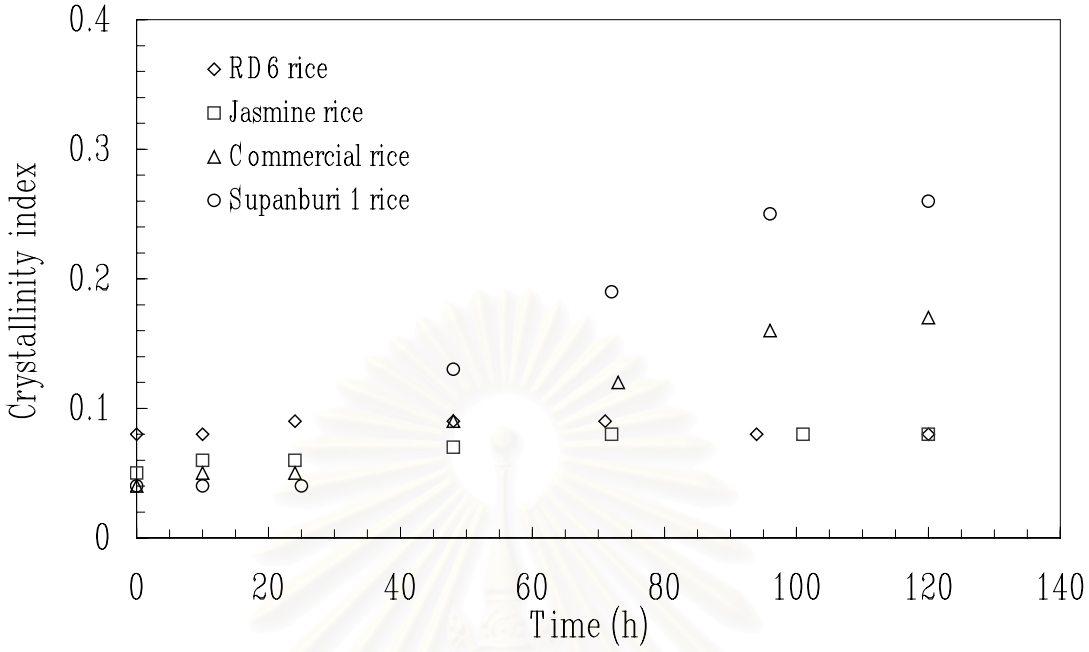

Figure 4.35 The changes of crystallinity index of rice starches gels (30%, w/w) during storage at 25 ^{0}C.

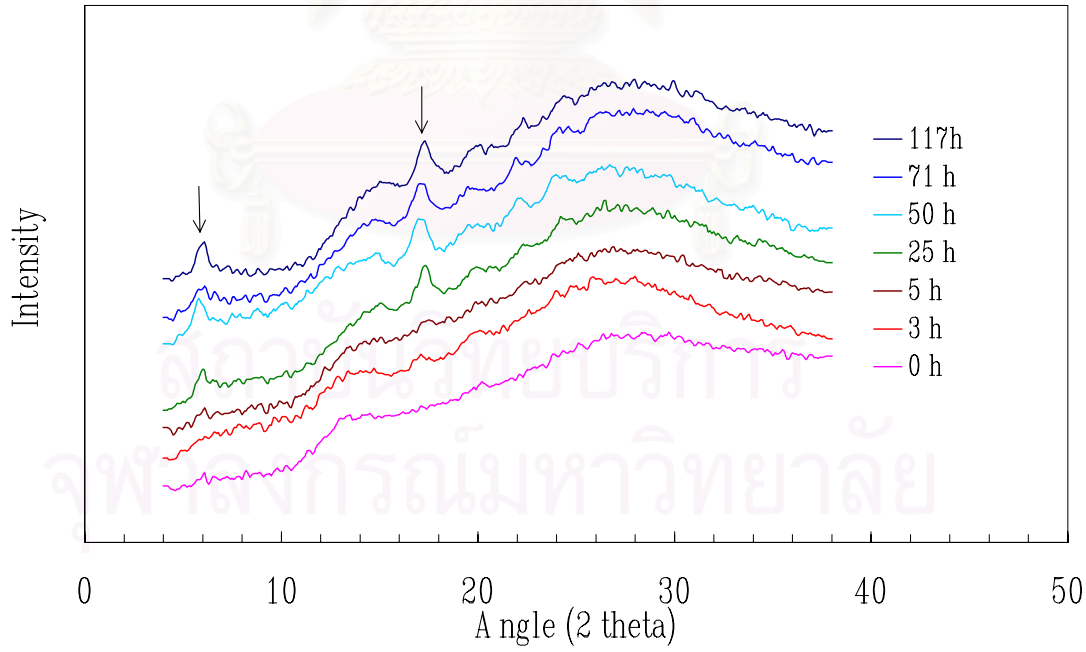

Figure 4.36 Crystallinity development in Supanburi 1 rice starch gel during storage at 5 ^{0}C for 117 hours.

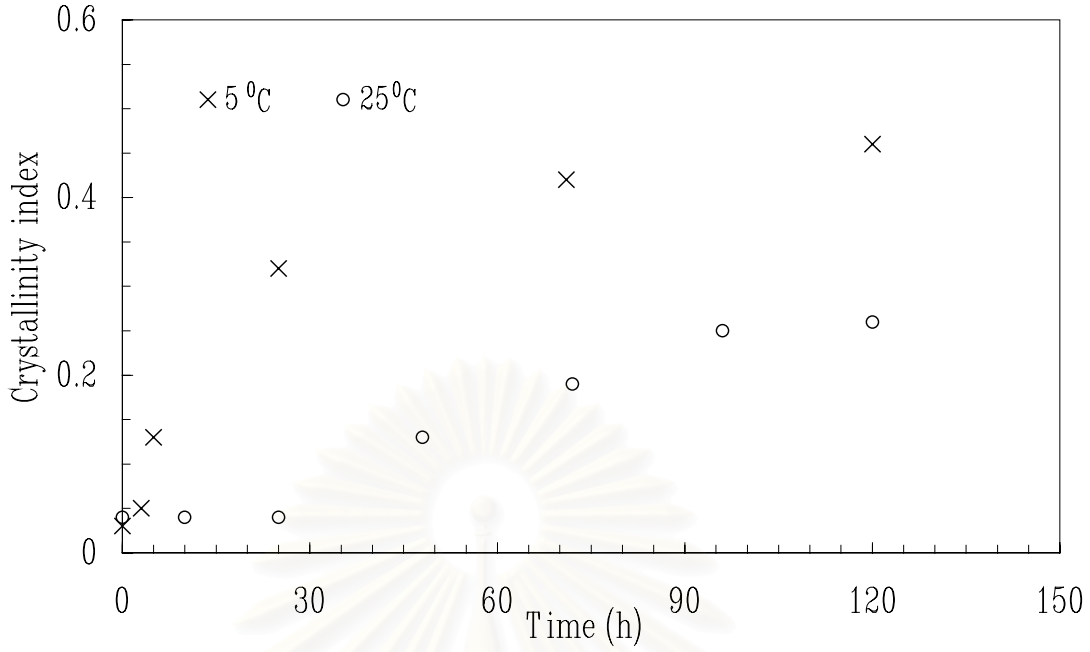

Figure 4.37 The changes of crystallinity index of Supanburi 1 gels (30%, w/w) during storage at 25 ^{0}C and 5 ^{0}C.

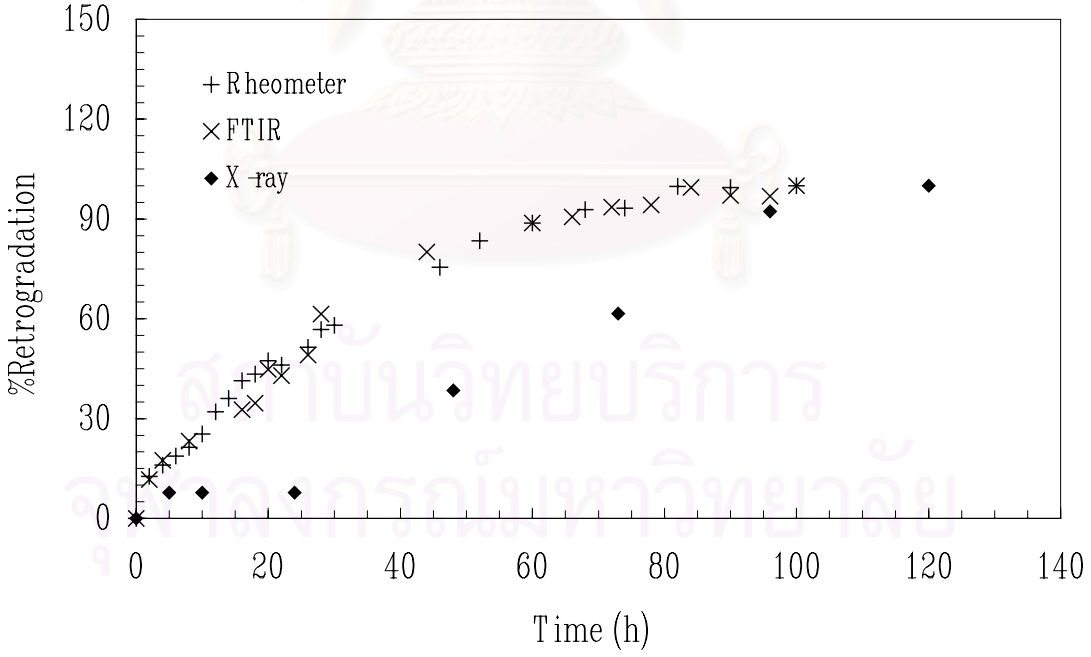

Figure 4.38 Comparison of the relative extent of the retrogradation at 25 ^{0}C for commercial rice starch as measured by the three techniques (rheometer, FTIR, and X-ray diffraction).

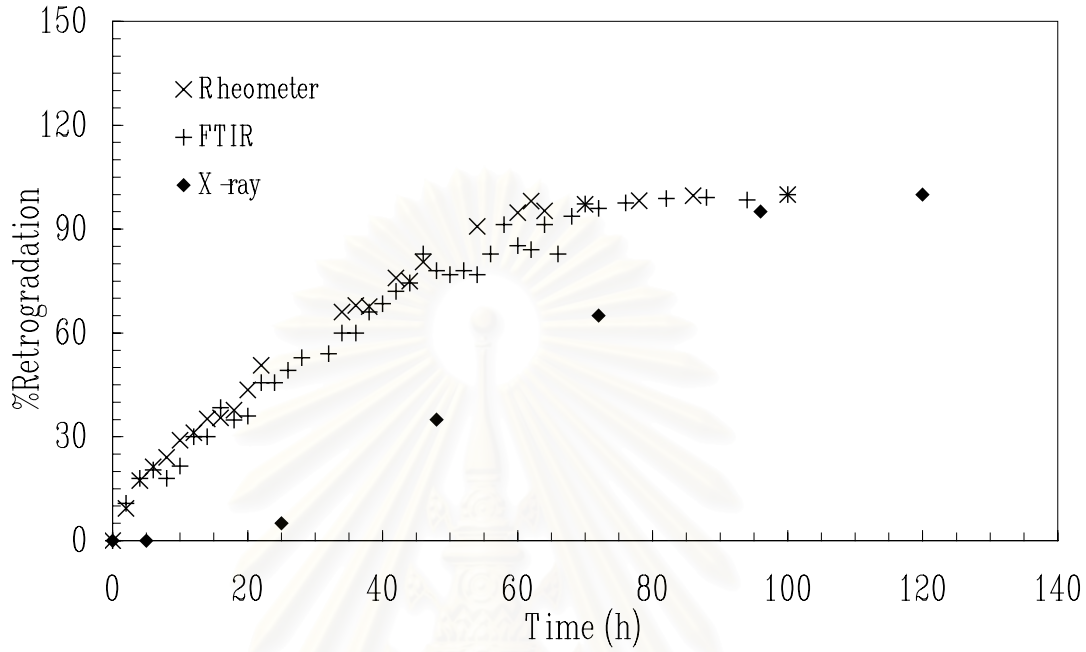

Figure 4.39 Comparison of the relative extent of the retrogradation at 25 ^{0}C for Supanburi 1 rice starch as measured by the three techniques (rheometer, FTIR, and X-ray diffraction).

CHAPTER V

CONCLUSIONS

Five Thai rice starches used in this study can be classified by amylose content into 3 classes :

- low amylose content, 1-3%, in RD6 and commercial waxy rice starches,
- medium amylose content, 14-15%, in Jasmine rice starch, and
- high amylose content, 21-23%, in Supanburi1 and commercial rice starches.

Furthermore, the characteristics of these five types of Thai rice, were found to be as follow :

- Amylose weight average molecular weight of in these rice starches was within 10^5 order of magnitude, and with the higher amylose content, the higher the weight average molecular weight.
- Rice starches with amylose content equal or lower than 15% had the S-type amylopectin with ACR values of 0.25, while rice starch of high amylose content had the L-type amylopectin with ACR values of 0.19.
- From SEM pictures, these Thai rice starches had common features of rice starch granule which are small, angular polyhedral shape, variable granular size having the average granule size of 4 – 6 μm with bimodal size distribution.

- Their crystalline was an A-type crystalline, located in the amylopectin component. There is relationship between amylose content in rice starches and crystallinity as well as short-range molecular order; the higher the amylose content, the lower the crystallinity and the short-range molecular order.

The amylose content (AM, ranging between 1.70 % to 22.70 %) has significant affected ($p \leq 0.01$) on water solubility index (WSI), swelling power (Q), setback viscosity (SV), and storage modulus (G'). These effect can be expressed by the following mathematical models, which have the coefficient of determination higher than 0.94.

- WSI (%) = 4.70 + 0.85AM (5.1)
- Q = 36.30 - 0.94 AM (5.2)
- SV (mPa.s) = $299e^{0.09AM}$ (5.3)
- for starch concentration of 12%, w/w, measured at 1 Hz and 60 ^{0}C

  G′ (Pa) = $40.69e^{0.11AM}$ (5.4)

The amylose content also affected intrinsic viscosity and flow behavior parameters of gelatinized rice starch suspension/ paste/ gel. Intrinsic viscosity of rice starches in KOH was 156-171, 185 and 192 ml/g for rice starch with amylose content of 21-23%, 14-15%, and 1-3%, respectively. Flow behavior properties of starch paste/ gel determined in the concentration range from 2% to 8% (w/w), at the shear rate range of 50 – 1000 s^{-1}, and at 60 ^{0}C gave:

- k can be expressed by following power law equation :

$$k = 0.01e^{-0.25AM} c^{3.85e^{0.021AM}}$$

- n can be expressed by following power law equation :
  - for the range of concentration of 2% to 5%

$$n = 0.72e^{0.04AM} c^{-[0.58+0.01AM)]}$$

  - for the range of concentration of 5% to 8%

    n = 0.36 (for amylose content of 1-3%)

    n = 0.40 (for amylose content of 14-21%)

    n = 0.60 (for amylose content of 22-23%)

- onset concentration was 1.1, 1.5, and 2.5 for rice starch with amylose content of 1-3%, 14-15%, and 21-23%, respectively

The viscoelastic properties for rice starch paste/gel were drawn from dynamic and creep study in the concentration range from 6% to 15% (w/w).

- Results of dynamic studied at 0.1-10 Hz, and 2% strain gave :
  - the G′ was higher than G″ for all rice starches
  - weak gel, frequency dependence of G′was found in rice starches with amylose content of 1- 3%
  - rubber-like gel, frequency independence of G′ was found for rice starches with amylose content lower than 23%

- Result of creep studied at shear stress of 10 Pa and at 25 ^{0}C gave :
    - only flow component existed in rice starch paste with amylose content of 1-3% at 6% concentration. The viscosity of this flow component were determined to be 16.4 Pa.s
    - viscoelastic behavior from rice starch gel, obtained from amylose content 1-3% in concentration range of 9–15%, and amylose content 14-23% in concentration range of 6-15%, exhibited viscoelastic properties, which could be represented by the 4-element Burger model :

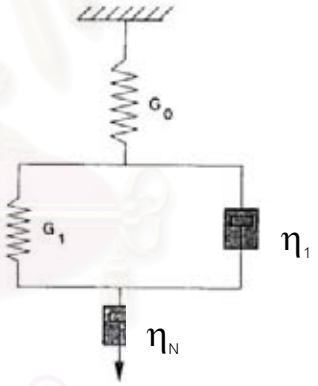

$$J(t) = J_0 + J_1(1 - \lambda^{-t/\tau_1}) + \frac{t}{\eta_N}$$

The parameters of 4-element Burger model were found to be affected by amylose content and starch concentration. The increase of amylose and starch concentration resulted in the increase of G_0, G_1, η_1, and η_N. The range of G_0, G_1, η_1, and η_N determined in this study were 18 – 2584 (Pa),

18 – 29407 (Pa), 393 – 3.5 x 10^5 (Pa.s) and 866 – 6.74x 10^6 (Pa.s), respectively.

The amylose content dependency of retrogradation behavior was found by storage rice starch gel of 30% starch concentration at 25 ^{0}C for 100 hours.

- No retrogradation occurred (no changes of G′ and RSA) for rice starch gel in amylose content equal or lower than 15%.
- The retrogradation occurred when there is an increase of G′, RSA, and crystallinity index for rice starch gel with amylose content of 21-23%. For rice starch gel of 30% amylose content, retrogradation started after storage for 1 h as indicated by increase of G′ and RSA. Three stages of retrogradation behavior were observed as :
  - the first stage occurred within the first 24 hours due to the fast formation of amylose double helixes. The characteristics of this stage were described by increase rate of G′ and RSA (dG′/dt and d(RSA)/dt), and these two characteristics were :
    - for commercial rice starch, dG′/dt and d(RSA)/dt were 0.44 (kPa/h) and 0.001 (h^{-1}), respectively
    - for Supanburi 1 rice starch, dG′/dt and d(RSA)/dt were 0.57 (kPa/h) and 0.002 (h^{-1}), respectively
  - the second stage occurred during 24-72th hour due to the slow formation of amylopectin helix crystalline
  - the third stage occurred indicating that no further retrogradation occurred after storage for 72 hour

- The effect of starch concentration (20-40%, w/w) on retrogradation of 30% amylose content of rice starch gel with amylose content of 21-23% was described through RSA and increasing rate of RSA in the first stage.
    - Increase in starch concentration resulted in increase of RSA and increasing rate of RSA in the first stage.
    - The increasing rates of RSA in the first stage were 0.001, 0.002, and 0.003 (h^{-1}) for rice starch gels at the concentration of 20%, 30%, and 40%, respectively
- Retrogradation of rice starch gel (amylose content of 21-23% and concentration of 30%) at 5 ^{0}C is higher than at 25 ^{0}C as indicated by an increasing in the crystallinity index.

Type of amylopectin controlled breakdown viscosity, onset of pasting temperature and gelatinization temperature. L-type amylopectin resulted in lower breakdown viscosity but higher onset of pasting and gelatinization temperatures than S-type.

No significant effect on composition, structure and properties were found in these starches in aging rice upto 5 months.

REFERENCES

American Association of Cereal Chemists (AACC). 2000. Approved Methods of the AACC. 10th ed. Washington, DC.: American Association of Cereal Chemists.

Association of Official Analytical Chemists (AOAC). 1995. Official Method of analysis. 16 th ed. Washington, DC.: Association of Official Analytical Chemists.

Asaoka, M., Okuno, K., Konishi, Y., and Fuwa, H. 1987. The effects of endotherm mutations and environmental temperature during development on the distribution of molecular weight of amylose in rice endosperms. Agric. Biol. Chem. 51(2): 3451-3453.

Atwell. W. A., Hood, L. F., Lineback, D. R., Varriano-Marston, E., and Zobel, H. F. 1988. The terminology and methodology associated with basic starch phenomena. Cereal Food World. 33: 306.

Avrami, M. 1941. Granulation, phase change, and microstructure, kinetics of phase change. III. J. Chem. Phys. 9: 177-184.

Bagley, E. B., and Christianson, D. D. 1982. Swelling capacity of starch and its relationship to suspension viscosity effect of cooking time, temperature and concentration. J. Texture Studies. 13: 115-126.

Banks, W., and Greenwood, C. T. 1975. Starch and its Components. Edinburgh: Edinburgh University Press.

Barber, S. 1972. Milled rice and changes during aging. In D. Houston (ed.). pp. 215-263. Rice: Chemistry and Technology. St. Paul, American Association of Cereal Chem.

Barnes, H. A., Hutton, J. F., and Walters, K. 1989. An Introduction to Rheology. New York: Elsevier Science Publishing Company, Inc.

Bertoft, E., and Koch, K. 2000. Composition of chains in waxy-rice starch and its structural units. Carbohydr. Polym. 41: 121-132.

Bhattacharya, K. R., Sombhagya, C. M., and Indudhara Swamy, Y. M. 1972. Interrelationship between certain physicochemical properties of rice. J. Food Sci. 37: 733-735.

Bhattacharya, K. R., Sombhagya, C. M., and Indudhara Swamy, Y. M. 1982. Quality profile of rice: A tentative scheme for classification. J. Food Sci. 47: 564-569.

Bhattacharjee, P., Singhal, R. S., and Kulkarni, P. R. 2002. Basmati rice: A review. Int. J. Food Sci Tech. 37: 1-12.

Bietz, J. A. 1982. Cereal prolamin evolution and homology revealed by sequence analysis. Biochem. Genetics. 20: 1039-1053.

Biliaderis, C. G. 1992. Characterization of starch networks by small strain dynamic rheometry. In R. J. Alexander and H. F. Zobel (ed.), Developments in Carbohydrate Chemistry, pp. 87-135. Minnesota: American Association of Cereal Chemists.

Biliaderis, C. G., and Zawistowski, J. 1990. Viscoelastic behavior of aging starch gels: Effect of concentration, temperature, and starch hydrolyzates on network properties. Cereal Chem. 67: 240-246.

Biliaderis, C. G. and Juliano, B. O. 1993. Thermal and mechanical-properties of concentrated rice starch gels of varying composition. Food Chem. 48: 243-250.

Blennow, A., Engelsen, S. B., Munck, L., and Moller, B. L. 2000. Starch molecular structure and phosphorylation investigated by a combined chromatographic and chemometric approach. Carbohydr. Polym. 41(2): 163-174.

Bolling, H., Hampel, G., and El Baya, A. W. 1978. Studies on storage of milled rice for a long period. Food Chem. 3: 7-22.

Buleon, A., Colonna, P., Planchot, V., and Ball, S. 1998. Starch granules: structure and biosynthesis. Int. J. Biol. Macromol. 23: 85-112.

Bulkin, B., and Kwak, Y. 1987. Retrogradation kinetics of waxy-corn and potato starches; A rapid, Raman-spectroscopy study. Carbohydr. Res. 160: 95-112.

Champagne, E. T. 1996. Rice starch composition and characteristics. Cereal Foods World. 41(11): 833-838.

Chang, T. T. 1976. Rice. In N. W. Simmonds (ed.), Evolution of Crop Plants, pp. 98-104. London: Longman.

Chrastil, J. 1990. Chemical and physicochemical changes of rice during storage at different temperature. J. Cereal Sci. 11: 71-85.

Chrastil, J. 1992. Correlations between the physicochemical and functional properties of rice. J. Agric. Food Chem. 40: 1683-1686.

Christianson, D. D., and Bagley, E. B. 1983. Apparent viscosities of dispersions of swollen corn starch granules. Cereal Chem. 60: 116-121.

Colas, B. 1986. Flow behavior of crosslinked corn starches. Lebensmittel Wissenschaft u. Technol. 19: 308-311.

Colonna, P., Bitobn, V., and Mercier, C. 1985. Interaction of concanavalin A with α-D-glucans. Carbohydr. Res. 137: 151-166.

Colwell, K. H., Axford, D. W. E., Chamberlain, N., and Elton, G.S.H. 1969. Effect of storage temperature on the aging of concentrated wheat starch gels. J. Sci. Food Agric. 20: 550-555.

Cooke, D., and Gidley, M. J. 1992. Loss of crystalline and molecular order during starch gelatinization: Origin of the enthalpic transition. Carbohydr. Res. 227: 103-112.

Dhaliwai, Y. S., Sekhon, K. S., and Nagi, H. P. S. 1991. Enzymatic activities and rheological properties of storage rice. Cereal Chem. 68(1): 18-21.

Donovan, J. W. 1979. Phase transitions of the starch-water system. Biopolymers. 18: 163.

Doublier, J. L. 1981. Rheological studies on starch: Flow behavior of wheat starch pastes. Starch. 33: 415-420.

Doublier, J. L. 1990. Rheological properties of Cereal Carbohydrate. In J. M. F. Hamed Faridi, Dough Rheology and Baked Product Texture, pp.111-156. New York: Van Nostrand Reinhold.

Efferson, J. N. 1985. Rice quality in world markets. In Rice Grain Quality and Marketing. IRIR, The Philippines.

Eliasson, A.-C. 1980. Effect of water content on the gelatinization of wheat starch. Starch. 32: 270.

Eliasson, A.-C., and Bohlin, L. 1982. Rheological properties of concentrated wheat starch gels. Starch. 34: 231-235.

Eliasson, A.-C. 1983. Differential scanning calorimetry studies on wheat starch-gluten mixtures. II. Effect of gluten and sodium stearoyl lactylate on starch crystallization during aging of wheat starch gels. J. Cereal Sci. 1: 2.7-213.

Eliasson, A.-C. 1985a. Retrogradation of starch as measured by differential scanning calorimetry. In R. D. Hill, and L. Munck (ed.), New Approaches to Research on Cereal Carbohydrates. pp. 93-98. Amsterdam: Elsevier Science Publishers

Eliasson, A. C. 1985b. Starch gelatinization in the presence of emulsifiers: A morphological study of wheat starch. Starch. 37(12): 411-415.

Eliasson, A.-C. 1986. Viscoelastic behavior during the gelatinization of starch. I. Comparison of wheat, maize, potato and waxy-barlay starches. J. Texture Stud. 17: 253-255.

Eliasson, A.-C. 1996. Starch: Physicochemical and Functional Aspects. In A.-C. Eliasson, Carbohydrates in Food, pp.440-449. New York: Marcel Dekker, Inc.

Ellis, H. S., Ring, S. G., and Whittam, M. A. 1989. A comparison of the viscous behavior of wheat and maize starch pastes. J. Cereal Sci. 10: 33-44.

Evans, I. D., and Haisman, D. R. 1979. Rheology of gelatinised starch suspensions. J. Texture Stud. 10: 347-370.

Evans, I. D. and Lips, A. 1992. Viscoelasticity of gelatinized starch dispersions. J. Texture Stud. 23(1): 69-86.

Farhat, I. A. 1996. Molecular mobility and interactions in biopolymer-sugar-water systems. Doctoral dissertation, Division of Food Sciences, School of Biological Sciences, The University of Nottingham.

Farhat, I. A., Blanshard, J. M. V., Mitchell, J. R. 2000. The retrogradation of waxy maize starch extrudates: Effect of storage temperature and water content. Biopolymers. 53: 411-422.

Ferry, J. D. 1980. Viscoelastic Properties of Polymers. New York: John Wiley and Sons.

Fitt, L. E., and Snyder, E. M. 1984. Photomicrographs of starches. In R. R. Whistler, BeMiller, J. N., and Paschall, E. F. (ed.), Starch Chemistry and Technology, pp. 675. Orlando: Academic Press.

French, D. 1973. Fine structure of starch and its relation to the organizaton of starch granules. Denpun Kagaku. 19: 8.

Ganashan, P. 1974. Genetics investigations of rice. Doctoral dissertation, Division of Plant Sciences, School of Biological Sciences, The University of Nottingham.

Gernat, C., Radosta, S., Anger, H., and Damaschun, G. 1993. Crystalline parts of three different conformations detected in native and enzymatically degraded starches. Starch. 45: 309-314.

Giboreau, A., Cuvelier, G., and Launay, B. 1994. Rheological behavior of three biopolymer/water systems with emphasis on yield stress and viscoelastic properties. J. Texture Stud. 25: 119-137.

Gibson, T. S., Solah, V. A., and McCleary, B. V. 1997. A Procedure to Measure Amylose in Cereal Starches and Flours with Concanavalin A. J. Cereal Sci. 5(2): 111-119.

Gidley, M. J., and Bociek, S. M. 1985. Molecular organization in starches: A C-CP/MAS NMR study. J. Am. Chem. Soc. 107: 7040-7044.

Gidley, M. J. 1987. Factors affecting the crystalline type (A-C) of native starches and model compounds: A rationalization of observed effects in terms of polymorphic structures. Carbohydr. Res. 161: 301-304.

Gidley, M. J., and Bulpin, P. V. 1987. Crystallization of malto-oligosaccharides as models of the crystalline forms of starch: Minimum chain-length requirement of the formation of double helices. Carbohydr. Res. 161: 291-300.

Godet, M. C., Tran, V., and Delagw, M. M. 1993. Molecular modelling of specific interactions in amylose complexation by fatty acids. Int. J. Biol Macromolecules. 15: 11-16.

Goodfellow, B., and Wilson, R. H. 1990. A Fourier transform IR study of the gelation of amylose and amylopectin. Biopolymers. 30: 1183-1189.

Greenwood, C. T. , and Thomson, J. A. 1959. A comparison of the starches from barley and malted barley. J. Institute Brewing. 65: 346-353.

Gudmundsson, M., and Eliasson, A. -C. 1993. Comparison of thermal and viscoelastic properties of four waxy starches and the effect of added surfactant. Starch. 45: 379-385.

Gudmundsson, M. 1994. Retrogradation of starch and the role of its components. Thermochimica Acta. 246: 329-341.

Han, Xian-Zhong, and Hamaker, B. R. 2001. Amylopectin fine structure and rice starch paste breakdown. J. Cereal Sci. 34: 279-284.

Harding, S. E. 1997. The intrinsic viscosity of biological macromolecules progess in measurement, interpretation and application to structure in dilute solution. Progess in Biophysical Molecular Biology. 68: 207-262.

Hensen, L. M., Hoseney, R. C., and Faubion, J. M. 1990. Oscillatory probe rheometry as a tool for determinng the rheological properties of starch-water systems. J. Texture Stud. 21: 213-224.

Hermans, P. H., and Weidinger, A. 1948. Quantitative X-Ray investigations on the crystallinity of cellulose fibers. A background analysis. J. Am. Chem. Soc. 19: 491-506.

Hizukuri, S., Takeda, Y., Maruta, N., and Suzuri, A. 1981. Multibranched nature of amylose and the action of debranching enzymes. Carbohydr. Res. 94: 205-213.

Hizukuri, S. 1986. Polymodal distribution of the chain lengths of amylopectins. Carbohydr. Res. 147: 342-347.

Hizukuri, S. 1985. Relationship between the distribution of the chain length of amylopectin and crystalline structure of starch granules. Carbohydr. Res. 141: 295-306.

Hizukuri, S. 1988. Recent advances in molecular structure of starch. J. Jpn. Soc. Starch Sci. 31: 185.

Hizukuri, S. 1993. Towards an understanding of the fine structure of starch molecules. Denpun Kagaku. 40(2): 133-144.

Hizukuri, S. 1996. Starch: Analytical Aspects. In A.-C. Eliasson, Carbohydrates in Food, pp.347-429. New York: Marcel Dekker, Inc.

Hoover, P. 2001. Composition, molecular structure, and physicochemical properties of tuber and root starches: A review. Carbohydr. Polym. 45: 253-267.

Imberty, A., and Perez, S. 1988. A revisit to the three-dimensional structure of B-type starch. Biopolymers. 27: 1205-1221.

Imberty, A., Chanzy, H., Perez, S., Buleon, A., and Tran, V. 1988. The double helical nature of the crystalline part of A-starch. J. Molecular Biol. 201: 365-378.

Imberty, A., Buleon, A., Tran, V., and Nantes, S. P. 1991. Recent advances in knowledge of starch structure. Starch. 43(10): 375-384.

Indudhara Swamy, Y. M., Sowbhagya, C. M., and Bhattacharya, K. R. 1978. Changes in the physicochemical properties of rice with aging. J. Sci. Food Agric. 29: 627-639.

Jane, L.-J., Wong, K. -S., and MacPherson, A. E. 1997. Branch structure difference in starches of A- and B-type X-ray patterns revealed by their Naegeli dextrin. Carbohydr. Res. 300: 219-227.

Jane, J., Chen, Y. Y., Lee, L. F., McPherson, A. E., Wong, K. S, Radosavljevic, M. and Kasemsuwan, T. 1999. Effects of amylopectin branch chain length and amylose content on the gelatinization and pasting properties of starch. Cereal Chem. 76(5): 629-637.

Jenkins, P. J. 1994. X-ray and neutron scattering studies of starch granule structure. Doctoral dissertation, Robinson College, The University of Cambridge.

Juliano, B. O. 1982. An Interational Survey of Methods Used for the Cooking and Eating Qualities of Milled Rice. IRRI, The Philippines.

Juliano, B. O. 1984a. Rice starch: Production, properties, and uses. In R. L. Whistler, BeMiller, J. N. and Paschall, E. F. (ed.), Starch: Chemistry and Technology, pp 516. New York: Academic Press, Inc.

Juliano, B. O. 1984b. Rice starch: Production, properties, and uses. In R. L. Whistler, J. N. BeMiller, and E. F. Paschall (ed.), pp. 507-528. Starch: Chemistry and Technology. New York: Academic Press, Inc.

Juliano, B. O. 1985a. Production and utilization of rice. In B. O. Juliano (ed.), Rice: Chemistry and Technology, pp. 1-16. Minnesota: The American Association of Cereal and Chemists:

Juliano, B. O. 1985b. Polysaccharides, proteins, and lipids of rice. In B. O. Juliano (ed.), Rice: Chemistry and Technology, pp. 59-174. Minnesota: The American Association of Cereal and Chemists.

Juliano, B. O., Villareal, R. M., Perez, C. M., Villareal, C. P., Laguna, L. B., Takeda, Y., and Hizukuri, S. 1987. Varietal differences in properties among high amylose rice starches. Starch. 39: 390-393.

Juliano, B. O. 1992. Structure, chemistry, and function of rice grain and its fractions. Cereal Food World. 37(10): 772-779.

Kalichevsky, M. T., Orfords, P. D., and Ring, S. G. 1990. The retrogradation aggelation of amylopectins from various botanical sources. Carbohydr. Res. 198: 49-55.

Kim, S. K., Ciacco, C. F., and D'Appolonia, B. L. 1976. Kinetic study of retrogradation of cassava starch gels. J. Food Sci. 41: 1249-1250.

Kumar, K. R., and Ali, S. Z. 1991. Properties of rice starch from paddy stored in cold and at room temperature. Starch. 43(5): 165-168.

Lai, K. P., Steffe, J. F., and Ng, P. K. W. 2000. Average shear rate in the rapid visco analyser (RVA) mixing system. Cereal Chem. 77(6): 714-716.

Launay, B., Doublier, J. L., and Cuvelier, G. 1986. Flow properties of aqueous solutions and dispersions of polysaccharides. In J. R. Mitchell, and D. A. Ledward (ed.), Functional Properties of Food, pp. 1-78. London: Applied Science.

Leloup, V. M., Colonna, P., Ring, S. G., Roberts, K., and Wells, B. 1992. Microstructure of amylose gels. Carbohydr. Polym. 18: 189-197.

Levine, H., and Slade, L. 1986. A polymer physicochemical approach to the study of commercial starch hydrolysis products (SHPs). Carbohydr. Polym. 6: 213-244.

Li, J.-Y., and Yhe, An-I. 2001. Relationships between thermal, rheological characteristics and swelling power for various starches. J. Food Eng. 50: 141-148.

Lii, C. Y., Shao, Y. Y., and Tseng, K. H. 1995. Gelation mechanism and rheological properties of rice rtarch. Cereal Chem. 72(4): 393-400.

Lii, C.-Y., Tsai, M. -L., and Tseng, K. -H. 1996. Effect of amylose content on the rheological properties of rice starch. Cereal Chem. 73(4): 415-420.

Liu, H., Arntfield, S. D., Holley, R. A., and Aime, D. B. 1997. Amylose-lipid complex formation in acetylated pea starch-lipid systems. Cereal Chem. 74: 159-162.

Longton, J., and LeGrys, G. A. 1981. Differential scanning calorimetry studies on the crystallinity of aging wheat starch gels. Starch. 33: 410-414.

Lopes da Silva, J. A. L., and Rao, M. A. 1992. Viscoelastin properties of food gum dispersions. In M. A. Rao, and J. F. Steffe (ed.), Viscoelastic Properties of Food, pp. 285-316. London: Elsevier Applied Science.

Lu, S., Chen, L.-N., and Lii, C.-Y. 1997. Correlations between the fine structure, physicochemical properties, and retrogradation of amylopectins from Taiwan rice varieties. Cereal Chem. 74(1): 34-39.

Lui, H., Lelievre, J., and Ayoung-Chee, W. 1991. A study of starch gelatinization using differential scanning calorimetry, X-ray, and birefringence measurements. Carbohydr. Res. 210: 79.

Mandelkern, L. 1964. Crystallization of polymers. New York: McGraw-Hill.

Manners, D., and Matheson, N. K. 1981. The fine structure of amylopectin. Carbohydr. Res. 90: 99-110.

Manners, D. J. 1985. Some aspects of the structure of starch. Cereal Food World. 30(10): 722-727.

Marsh, R. D. L. 1986. A study of the retrogradation of wheat starch systems using X-ray diffraction. Doctoral dissertation, Division of Food Sciences, School of Biological Sciences, The University of Nottingham.

Matheson, N. K., and Welsh, L. A. 1988. Estimation and fraction of the essential unbranched (amylose) and branched (amylopectin) components of starches with concanavalin A. Carbohydr. Res. 180: 301-313.

Matheson, N. K. 1990. A comparison of the structures of the fractions of normal and high-amylose pea-seed starches prepared by precipitation with concanavalin A. Carbohydr. Res. 199: 195-205.

Miles, M. J., Morris, V. J., Orford, P. D., and Ring, S. G. 1985a. The roles of amylose and amylopectin in gelation and retrogradation of starch. Carbohydr. Res. 135: 271-281.

Miles, M. J., Morris, V. J., and Ring, S. G. 1985b. Gelation of amylose. Carbohydr. Res. 135: 257-269.

Mita, T. 1992. Structure of potato starch pastes in the aging process by the measurement of their dynamic moduli. Carbohydr. Polym. 17: 269-276.

Mod, R. R., Conkerton, E. J., Chapital, D. C., and Yatsu, L. Y. 1983. Rice phenolic acids and their changes with aging. Cereal Food World. 28: 560.

Moritaka, S., and Yasumatsu, K. 1972. Studies on cereals. X. The effect of sulfhydryl groups on storage deterioraton of milled rice. Eiyo To Shokuryo. 25: 59-62.

Morris, E. R., and Ross-Murphy, B. 1981. Chain flexibility of polysaccharides and glycoproteins from viscosity measurements. In D. H. Northcote (ed.), Techniques in Carbohydrate Metabolism. pp. 310. Amsterdam: Elsevier Science.

Morris, V. J. 1990. Starch gelation and retrogradation. Trends Food Sci. Technol July: 2-6.

Morrison, W. R., Tester, R. F., Snape, C. E. Law, R. and Gidley, M. J. 1993. Swelling and gelatinization of cereal starches. IV. Effect of lipid-complexed amylose and free amylose in waxy and normal barley starches. Cereal Chem. 70(4): 385-391.

Morrison, W. R. 1995. Starch lipids and how they relate to starch granule structure and functionality. Cereal Chem. 40: 107-109.

Moss, G. E. 1976. The microscopy of starch. In J. A. Radley (ed.), Examination and Annalysis of Starch and Starch Products, pp. 1. London: Applied Science Publishers.

Nakamura, Y., Sakura, A., Inaba, Y., Kimura, K., Iwasawa, N., and Nagamine, T. 2002. The Fine structure of amylopectin in endosperm from asian cultivated rice can be largely classified into two classes. Starch. 54: 117-131.

Nara, S., Mori, A., and Komiya, T. 1978. Study on relative crystallinity of moist potato starch. Starch. 30(4): 111-114.

Nikuni, Z. 1969. Starch. Tampakushitsu Kakusan Koso. 14: 943.

Noda, T. T., Y., Sato, T., Ikoma, H., and Mochida, H. 1996. Physicochemical properties of starches from purple and orange fleshed sweet potato roots at two levels of fertilizer. Starch. 48: 359-399.

Noel, T. R., Ring, S. G., and Whittam, M. A. 1993. Physical properties of starch products. Structure and function. In E. Dickinson, and P. Walstra (ed.), Food Colloids and Polymers: Stability and Mechanical Properties, pp.126-135. Cambridge: Royal Society of Chemistry.

Okabe, M. 1979. Texture measurement of cooked rice and its relationship to the eating quality. J. Texture Stud. 10: 131-152.

Okechukwu, P. E. and M. A. Rao. 1995. Influence of granule size on viscosity of cornstarch suspension. J. Texture Stud. 26(5): 501-516.

Okechukwu, P. E., and Rao, M. A. 1998. Rheological of structured polysaccharide food system starch and pectin. In R. H. Walter (ed.), Polysaccharide Association Structures in Food, pp. 289-328. New York: Marcel Dekker, Inc.

Ong, M. H. 1994. Factor affecting the molecular properties of starch and their relation to the texture of cooked rice. Doctoral dissertation, Division of Food Sciences, School of Biological Sciences, The University of Nottingham.

Orford, P. D., Ring, S. G., Carroll, V., Miles, M. J., and Morris, V. J. 1987. The effect of concentration and botanical source on the gelation and retrogradation of starch. J. Sci. Agric. 39: 169-177.

Paterson, L., Mitchell, J. R., Sandra, E. H., Blanshard, J. M. V. 1996. Evidence for sulfite induced oxidative reductive depolymerisation of starch polysaccharides. Carbohydr. Res. 292: 143-151.

Quemada, D., Fland, P., and Jezequel, P. H. 1985. Rheological properties and flow of concentrated disperse media. Chem. Eng. Comm. 32: 61-83.

Ramesh, M., Mitchell, J. R., Jumel, K., and Harding, S. E. 1999. Amylose content of rice starch. Starch. 8-9: 311-313.

Ramesh, M., Bhattacharya, K. R., and Mitchell, J. R. 2000. Developments in understanding the basis of cooked-rice texture. Crit. Rev. Food Sci. Nutr. 40 (6): 449-460.

Reddy, R. K., Zakiuddin, S., and Bhattacharya, K. R. 1993. The fine structure of rice-starch amylopectin and its relation to the texture of cooked rice. Carbohydr. Polym. 22: 267-275.

Reddy, K. R., Subramanian, R., Ali, S. Z., and Bhattacharya, K. R. 1994. Viscoelastic properties of rice-flour pastes and their relationship to amylose content and rice quality. Cereal Chem. 71(6): 548-552.

Remsen, C. H., and Clark, J. P. 1978. A viscosity model for a cooking dough. J. Food Process Eng. 2: 39.

Ring, S. G. 1985. Some studies on starch gelation. Starch. 37(3): 80-83.

Ring, S. G., Colonna, P.,I'Anson, K. J., Kalichevsky, M. T., Miles, M. J. Morris, V. J., and Orford, P. D. 1987. The gelation and crystallization of amylopectin. Carbohydr. Res. 162: 277-293.

Robin, J. P., Mercier, C., Charbonniere, R., and Guilbotm, A. 1974. Gel filtration and enzymic studies of insoluble residue from prolonged acid treatment of potato starch. Cereal Chem. 51: 389-406.

Russell, P. L. 1983. A kinetic study of bread staling by DSC and compressibility measurements. The effect of added monoglycerides. J. Cereal Sci. 1: 297-303.

Sanders, E. B., Thompson, D. B., and Boyer, C. D. 1990. Thermal behavior during gelatinization and amylopectin fine structure for selected maize genotype as expressd in four inbred lines. Cereal Chem. 67: 594-602.

Sandhya Rani, M. R., and Bhattacharya, K. R. 1989. Rheology of rice-flour pastes: Effect of varieties, concentration and temperature and time of cooking. J. Texture Stud. 20: 127-137.

Sandhya Rani, M. R., and Bhattacharya, K. R. 1985. Rheolgical properties of rice flour slurries and pastes. J. Food Sci. Technol. 22: 322-326.

Schoch, T. J. 1964. Swelling power and solubility of granular starch. In R. L. Whistler (ed.), Methods in Carbohydrate Chemistry, pp. 106-108. New York: Academic Press.

Shanthy, A. P., Sowbhagya, C. M. and Bhattacharya, K. R. 1980. Simplified determination of water-insoluble amylose content of rice. Starch. 12: 409-411.

Shama, F., and Sherman, P. 1966. The texture of ice cream. 2. Rheological properties of frozen ice cream. J. Food Sci. 31: 699-706.

Sharp, R. N. 1990. Rice: Production, processing and utilization. In K. J. Lorenz, and Kulp, K (ed.), Handbook of Cereal Science and Technology, pp. 301-329. New York: Marcel Dekker.

Sherman, P. 1966. The texture of ice cream. 3. Rheological properties of mix and melted ice cream. J. Food Sci. 31: 707-716.

Sherman, P. 1970. Industrial Rheology with Particular Reference to Foods, Phamaceutical, and Cosmetics. London: Academic Press.

Shi, Y.-C., and Paul, A. S. 1992. The structure of four waxy starches related to gelatinization and retrogradation. Carbohydr. Polym. 227: 131-145.

Slade, L., and Levine, H. 1987. Recent advances in starch retrogradation. In S. S. Stivala, V. Crecenzi, and I. C. M. Dea (ed.), Industrial Polysaccharides: The Impact of Biotechnology and Advanced Methodologies, pp. 387-430. New York: Gorndon and Breach Science Publishers.

Sombhagya, C. M., Ramesh, B. S. and Bhattacharya, K. R. 1987. The relationship between cooked-rice texture and the physicochemical characteristics of rice. J. Cereal Sci. 5: 287-297.

Sowbhagya, C. M., and Bhattacharya, K. R. 2001. Changes in pasting behavior of rice during aging. J. Cereal Sci. 34: 115-124.

Sowbhagya, C. M. and Bhattacharya, K. R. 1979. Simplified determination of amylose in milled rice. Starch. 31(5): 159-163.

Steeneken, P. A. M. 1989. Rheological properties of aqueous suspensions of swollen starch granules. Carbohydr.Polym. 11(1): 23-42.

Steffe, J. F. 1996. Rheological Methods in Food Process Engineering. East Lansing: Freeman Press.

Svnsson, E., and Eliasson, A. -C. 1995. Crystalline changes of native wheat and potato starches at intermediate water levels during gelatinization. Carbohydr. Polym. 26: 171.

Swamy, Y. M. I., Sombhagya, C. M., and Bhattacharya, K. R. 1978. Changes in the physicochemical properties of rice with aging. J. Sci. Food Agric. 29: 627-639.

Swinkels, J. J. M. 1985. Source of starch, its chemical and physics. In G. M. A. van Beynum, and J. A. Roels (ed), Starch Conversion Technology, pp. 15-45. New York: Marcel Dekker, Inc.

Takeda, Y., and Hizukuri, S. 1986. Purification and structure of amylose from rice starch. Carbohydr. Res. 148: 299-308.

Takeda, Y., Hizukuri, S., and Juliano, B. O. 1987. Structures of Rice Amylopectins with low and high affinities for iodine. Carbohydr. Res. 168(1): 79-88.

Takeda, Y., Hizukuri, S., Takeda, C., and Suzuki, A. 1987. Structures of branched molecules of amylose of various origins and the molar fractions of branched and unbranched molecules. Carbohydr. Res. 165: 139-145.

Takeda, Y., Maruta, N., Hizukuri, S., and Juliano, B. O. 1989. Structures of indica rice starches (IR48 and IR64) having intermediate affinities for iodine. Carbohydr. Res. 187(2): 287-294.

Tanglertpaibul, T., and Rao, M. A. 1987. Intrinsic viscosity of tomato serum as affected by methods of determination and methods of processing concentration. J. Food Sci. 52(6): 1642-1645, 1688.

Tester, R. F., and Morrison, W. R. 1990. Swelling and gelatinization of cereal starches. I. Effect of amylopectin, amylose and lipids. Cereal Chem. 67: 551-559.

Thomas, D. J., and Atwell, W. A. 1999. Starches. Minnesota: The American Association of Cereal Chemists.

Tongdang, T. 2001. Molecular structure of native and processed rices. Doctoral dissertation, Division of Food Sciences, School of Biological Sciences, The University of Nottingham.

Tsai, M., Li, C., and Lii, C. 1997. Effect of granular structures on the pasting behaviors of starches. Cereal Chem. 74(6): 750-757.

Tsugita, T. 1986. Aroma of cooked rice. Food Rev. Int. 1(3): 497-520.

USDA. 1992. Rice, situation and outlook yearbook. In Economic Research Service, RS-64, July. Washington, D. C.

van Soest, J. J. G., Tournois, H. D., de Wit, J. F., and Vliegenthart, G. 1994. Retrogradation of potato starch as studied by Fourier-transform infrared-Spectroscopy. Starch. 46(12): 453-457.

Villareal, R. M., Resurreccion, A. P., Suzuki, L. B., and Juliano, B. O. 1976. Changes in physicochemical properties of rice during storagre. Starch. 28 (3): 88-94.

Wang, H. -H., and Sun, D. -W. 1999. Flow behavior and rheological models of rice flour pastes. J. Food Process Eng. 22: 191-200.

Ward, I. M. 1990. Mechanical Properties of Solid Polymer. New York: John Wiley & Sons.

Wilson, R. H., Kalichevski, M. T., Ring, S. G., and Belton, P. S. 1987. A Fourier-transform infrared study of the gelation and retrogradation of waxy-maize satrch. Carbohydr. Res. 166: 162-165.

Wong, R. B. K., and Lelievre, L. 1981. Viscoelastic behavior of wheat starch pastes. Rheological Acta. 20: 299-307.

Wong, R. B. K., and Lelievre, J. 1982. Effect of storage on dynamic rheological properties of wheat starch pastes. Starch. 34: 231-233.

Yamamoto, K., Sumie, S., and Toshio, O. 1973. Properties of rice starch prepared by alkali method with various conditions. Denpun Kagaku. 20: 99-102.

Yun, S.-H., and Matheson, N. K. 1990. Estimation of the amylose content of starches after precipitation of amylopectin by concanavalin A. Starch. 42.

Zeleznak, K. J., and Hoseney, R. C. 1986. The role of water in the retrogradation of wheat starch gels and bread crumb. Cereal Chem. 63: 407-411.

Zhou, Z., Robards, K., Helliwell, S., and Blanchard, C. 2002. Composition and functional properties of rice. J. Food Sci. Technol. 37: 849-868.

Zobel, H. F. 1964. X-ray analysis of starch granules. In R. L. Whistler, R. J. Smith, and J. N. BeMiller (ed.), Method in Carbohydrate Chemistry, pp. 109-113. New York: Academic Press.

Zobel, H. F. 1973. Review of bread staling. Baker's Digest. 47: 52-61.

Zobel, H. F. 1988. Molecules to granules: A comprehensive starch review. Starch. 40: 44-50.

Zobel, H. F., Young, S. N., and Rocca, L. A. 1988. Starch gelatinization: An X-ray diffraction study. Cereal Chem. 65: 443.

APPENDICES

APPENDIX A

LINEAR VISCOELASTIC

(STRAIN SWEEP TEST)

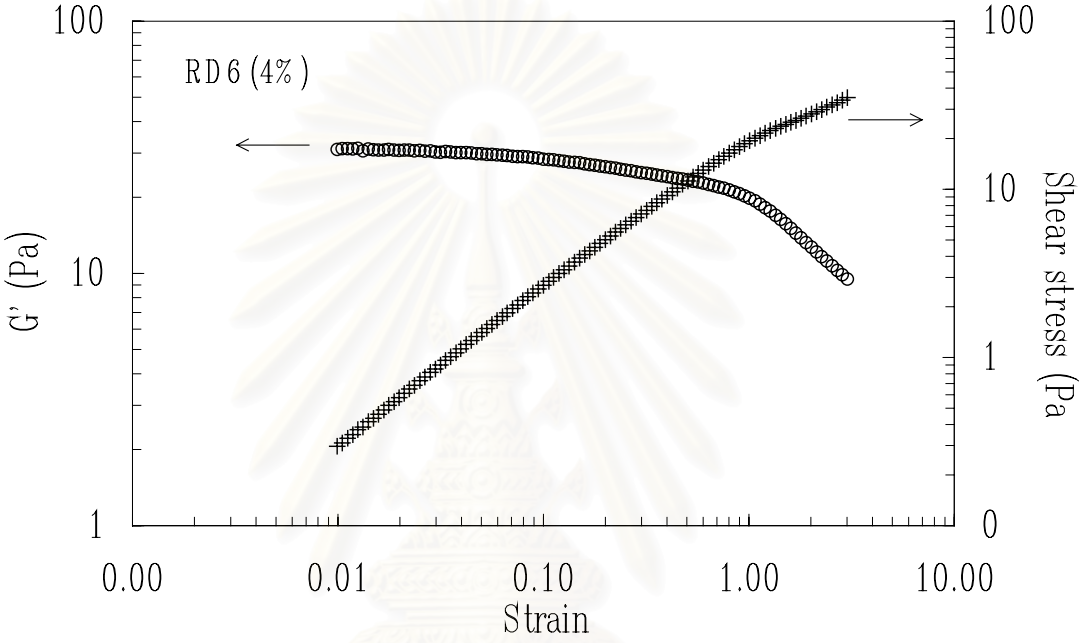

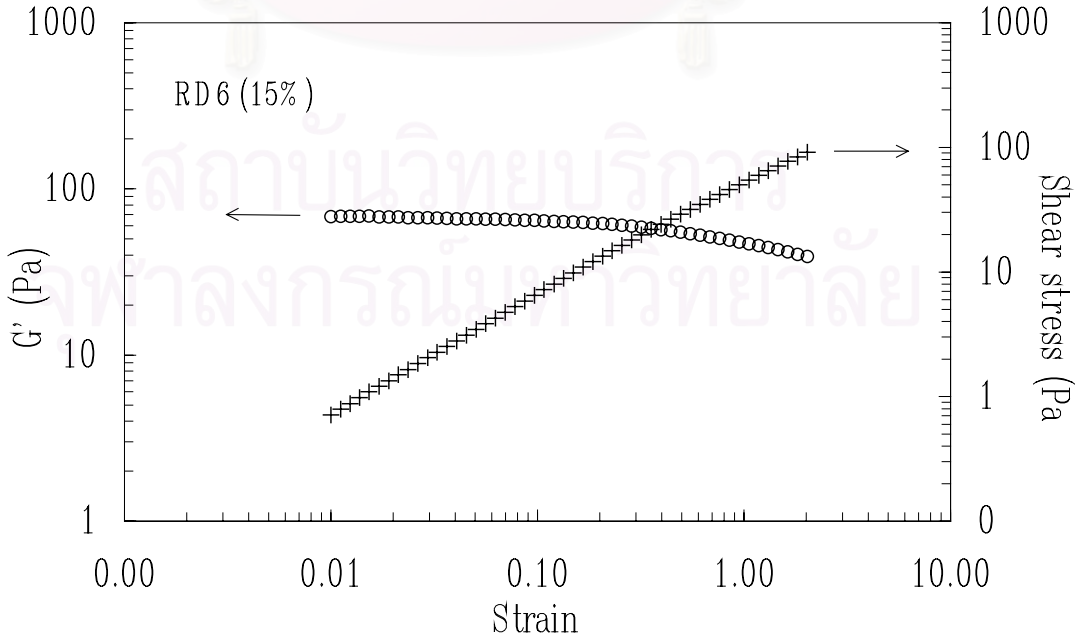

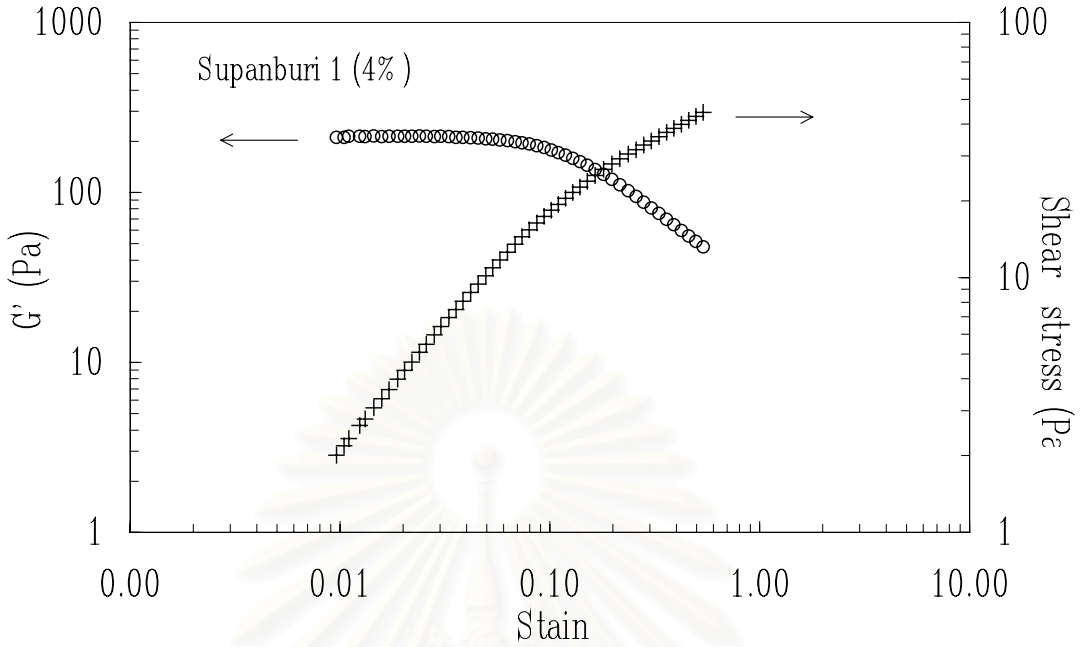

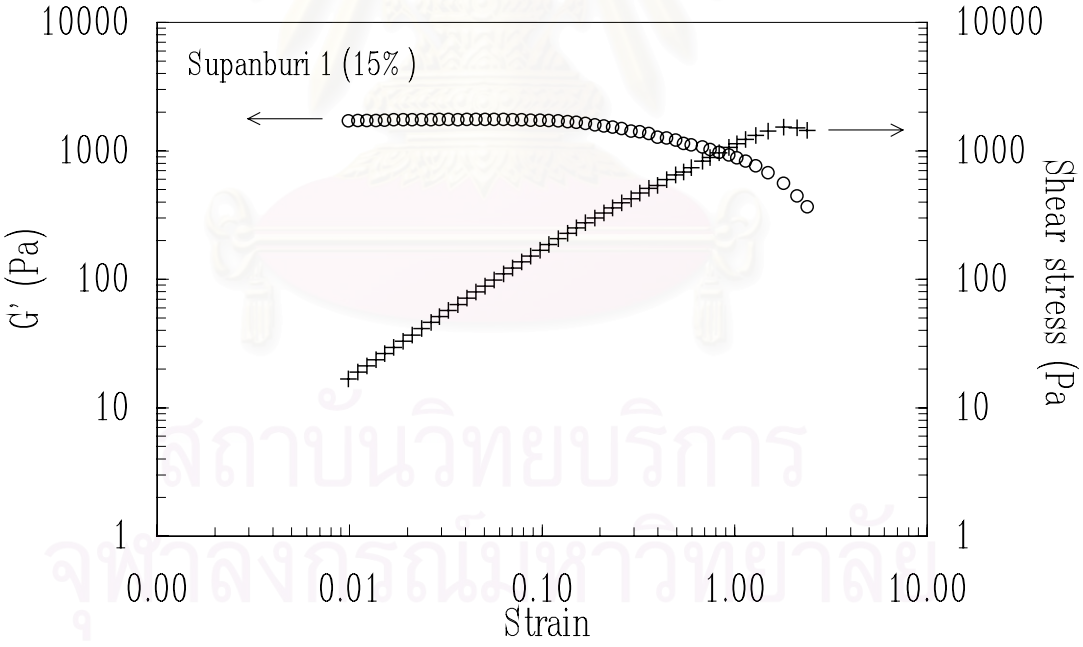

APPENDIX B

INOKUCHI GRAPHICAL PROCEDURE

The creep curve for viscoelastic materials has an overall compliance J(t) at any time t, where J is the ratio of strain $\gamma(t)$ to stress (σ).

The creep compliance curve can be subdivided into three distinct regions (Shama and Sherman, 1996, and Sherman, 1966):

a) A region of instantaneous elastic compliance, J_0, (in the region A-B of Figure 2.16) in which bonds are stretched elastically. If shear does not continue beyond this point the recovery is complete when stress is removed.

$$J_0 = \frac{1}{G_0} = \frac{\gamma_0(t)}{\sigma} \qquad (a)$$

b) A time-dependent retarded elastic compliance J_R (B-C), associated with a retarded elastic modulus, G_R, viscosity, η_R, and retard time,τ, ($=\eta_R/ G_R$) during which bonds break and reform. All bonds do not break and reform at the same rate, so that τ should be replaced by a spectrum of retardation times. Consequently, G and η_R should be replaced by a distribution spectrum of retarded elastic moduli G_1, G_2, G_3, ….G_i and viscosity η_1, η_2, η_3……η_i , assuming i components.

In its simplest form:

$$J_R = \frac{1}{G_R} = J_a(1 - e^{\frac{-t}{\tau}}) = \frac{\gamma_R(t)}{\sigma} \qquad (b)$$

where J_a is the average retarded elastic compliance.

In the expanded form:

$$J_R = \sum_{i=1}^{n} J_i(1 - e^{\frac{-t}{\tau_i}}) = \sum_{i=1}^{n} J_i(1 - e^{\frac{-t}{\eta_i J_i}}) \qquad (c)$$

where η_i is the number of viscosity components associated with retarded elastic compliance. Applying the graphical procedure of Inokuchi (1955) to Equation (c), let

$$Q = \sum_{i=1}^{n} J_i - \frac{\gamma_R(t)}{\sigma} \qquad (d)$$

This corresponsds to the distance between the extrapolated straight line DCP at ant time t, because of the exponential decay or relaxation of compliance. In addition, therefore,

$$Q = \sum_{i=1}^{n} J_i e^{\frac{-t}{\tau_i}} \qquad (e)$$

When In Q is plotted against t a straight line should be obtained at large values of t, from which a single retardation time (τ_1) and creep compliance (J_1) can be calculated. These values are inserted in Equation (b), and if it does not adequately define the form of the experimental curve, a second plot is required of ln ($Q - J_1e^{-t/\tau 1}$) against t to determine the magnitude of the second retardation time (τ_2) and the second creep compliance J_2. Equation (e) indicates that this second plot should also be linear at large values of t provided $\tau_1 > \tau_2$. Similarly, if it is necessary a third retardation time τ_3 can be determined by plotted ln ($Q - J_1e^{-t/\tau 1} - J_1e^{-t/\tau 2}$) against t. This procedure is repeated until such time that sufficient retardation times and compliances have been calculated for Equation (c) to represent adequately the form of the experimentally determined retarded elastic compliance.

c) A region of Newtonian flow (C-D) with compliance J_N. Once the bonds have ruptured, i. e. the time for them to reform is much longer than the test period, individual particles or units flow past one another.

Newtonian flow is proportional to the time of loading in this region of the curve, so that

$$J_N = \frac{\gamma_N(t)}{\sigma} = \frac{t}{\eta_N} \qquad (f)$$

where γ_N is the shear stain in the linear region of the creep curve. Thus, the gradient of this region equal $1/\eta_N$.

APPENDIX C

DEPENDENCY OF CONSISTENCY INDEX (k) AND FLOW BEHAVIOR INDEX (n) ON STARCH CONCENTRATION (c) AND AMYLOSE CONTENT (AM) AT $p \leq 0.01$

For c = 2-8%,

k	=	Ac^{B}	($R^2 = 0.99$)
A	=	$0.01e^{-0.25AM}$	($R^2 = 0.85$)
B	=	$3.85e^{0.021AM}$	($R^2 = 0.98$)

For c = 2-5%,

n	=	Dc^{E}	($R^2 = 0.99$)
D	=	$0.72e^{0.04AM}$	($R^2 = 0.86$)
E	=	-[0.58+0.01AM)]	($R^2 = 0.97$)

For c = 5-8%,

n	=	0.37	(AM = 1-3%)
n	=	0.40	(AM = 14-21%)
n	=	0.60	(AM = 22-23%)

APPENDIX D

THE CONSTANT VALUES

FOR EQUATION (4.10)

Starch source	m_∞	B
1. RD6 (0 month aged rice)	-0.83	1.27
2. RD6 (5 months aged rice)	-0.83	1.27
3. Commercial waxy rice starch	-0.83	1.27
4. Jasmine (0 month aged rice)	-0.84	1.75
5. Jasmine (5 months aged rice)	-0.84	1.75
6. Commercial rice starch	-0.84	1.75
7. SP1 (0 month aged rice0	-0.92	3.80
8. SP1 (5 months aged rice)	-0.92	3.80

VITA

Miss. Piyarat Noosuk was born on October 25, 1970 in Songkla, Thailand. She obtained a B.Sc. degree in Agro-Industry from Prince of Songkla University in 1992 and a M.Eng. degree in Food Engineering from King Monkut's Institute of Technology Thonburi in 1995. Since 1996, she has worked for the Department of Food Technology, Faculty of Agro-Industry, Prince of Singkla University. In 2000, she received a scholarship from the Royal Thai Government under the Agro-Industry PhD Program Consortium to further her PhD at the Department of Food Technology, Chulalongkorn University. After being finished her PhD degree, she will join the Department of Food Technology, Faculty of Agro-Industry at Prince of Songkla University.

Permanent mailing address:
81/61 Kanchanavanich Rd.,
Tambol Kao-Rhup-Chang, Ampher Maung,
Songkhla, 90000
THAILAND